Design and Synthesis of Photoswitchable Polymerization Catalysts

DISSERTATION

zur Erlangung des akademischen Grades
doctor rerum naturalium
(Dr. rer. nat.)
im Fach Chemie
eingereicht an der

Mathematisch-Naturwissenschaftlichen Fakultät
der Humboldt-Universität zu Berlin
von

Antti Alexander Senf, M. Sc.

Präsident der Humboldt-Universität zu Berlin
Prof. Dr. Jan-Hendrik Olbertz

Dekan der Mathematisch-Naturwissenschaftlichen Fakultät
Prof. Dr. Elmar Kulke

Gutachter/innen: 1. Prof. Stefan Hecht, Ph.D.
2. Prof. Dr. Christoph A. Schalley
3. Prof. Dr. Hans Börner

Tag der mündlichen Prüfung: 15.06.2016

Die vorliegende Arbeit wurde in der Zeit von Oktober 2012 bis Dezember 2015 am Institut für Chemie der Humboldt-Universität zu Berlin unter der Anleitung von Prof. Stefan Hecht, Ph.D. angefertigt.

Teile dieser Arbeit wurden bereits veröffentlicht in: / Parts of this work have already been published in:

[1] R. Göstl, A. Senf, S. Hecht, *Chem. Soc. Rev.* **2014**, *43*, 1982–1996.

Danksagung

An dieser Stelle möchte ich mich bei allen Bedanken die mir bei der Anfertigung meiner Dissertation geholfen haben.

Mein besonderer Dank geht an Prof. Stefan Hecht für das in mich gesetzte Vertrauen, die Möglichkeit mich in meiner Forschung frei zu entfalten, die überaus guten Arbeitsbedingungen und die zahlreichen fachliche Gespräche und Diskussionen.

Darüber hinaus möchte ich mich bei allen Mitgliedern der Arbeitsgruppe bedanken. Ein besonderer Dank geht an meine Laborkollegen Yves Garmshausen, Alexis Goulet-Hanssens und Philipp Viehmann für die stets gute Laboratmosphäre. Meiner studentischen Hilfskraft Kristine Klaue, meinen Bachelorstudenten Tom Kunde und Constantin Stuckhardt sowie meinen Forschungspraktikanten Lachezar Hristov und Jade Nguyen danke ich für die gute Zusammenarbeit, ihren großen Einsatz und die vielen fachlichen und nicht-fachlichen Diskussionen. Bei Yves Garmshausen und Alexis Goulet-Hanssens bedanke ich mich für die überaus engagierte Korrektur meines Manuskripts.

Darüber hinaus möchte ich bei Yves, Alex, Derk-Jan, Petr und Björn für die zahlreichen interessanten und lustigen Gespräche, die wir nach der Arbeit hatten, bedanken.

Mein größter Dank geht an Deborah Schmidt. Vielen Dank für deine Liebe, dein Vertrauen und die Kraft, die du mir immer gegeben hast.

Abschließend möchte ich mich bei meinen Eltern bedanken, die immer an mich geglaubt und mich unterstützt haben.

Abstract

Rapid developments in the field of controlled polymerization have led to numerous ways to produce well defined polymeric structures. This influence on the polymeric microstructure allowed a more efficient control over the macroscopic properties as well. Here, approaches are described to *in situ* control the polymerization outcome, which will eventually lead to a more defined manipulation of polymeric properties.

For this purpose well established organometallic catalyst were functionalized with azobenzene moieties to alter the catalysts geometry *in situ*. First a salen catalyst with an azobenzene in close proximity to the active site was synthesized. The catalyst showed promising photochemical behavior, but irradiation of the catalyst would interfere with the binding of the polymeric chain, due to excitation of the metal's LMCT band.

To overcome this challenge a dinuclear salen catalysts with a better separation of the bands was synthesized that would allow control over cooperative effects. This catalysts showed *trans* → *cis*-isomerization but no photochemical back-reaction, due to an overlap of the absorption bands of the *cis*-azobenzene with the metal moiety. Different approaches to change the azobenzene absorption were investigated, without finding a practical route.

Therefore, the absorption of the catalytically active moiety was altered by introducing a rigid fully conjugated salphen system as the ligand. Three systems were synthesized, of which an ethylene bridged ligand showed the best results. It allowed reversible switching between both states and showed an activity change in the polymerization of β-butyrolactone. The catalyst showed an increased activity by a factor of 2.4 in the *trans*-isomer compared to the photostationary state and it also allowed for an *in-situ* switching between both states without affecting the efficiency of the system.

Furthermore, it was shown that *ortho*-azobenzene functionalized Schiff-bases can be used to control the reactivity in dynamic covalent chemistry. An increased reactivity in the imine formation when comparing the *trans*-azobenzene and the reaction under constant irradiation by a factor of 2.2 was observed.

Zusammenfassung

Die andauernden Entwicklungen auf dem Gebiet der kontrollierten Polymerisation haben zu zahlreichen neuen Methoden geführt, um klar definierte Polymere zu synthetisieren. Die dabei entstehenden molekularen Strukturen haben einen großen Einfluss auf die makroskopischen Eigenschaften. Hier werden Ansätze beschrieben um Polymerisation *in situ* zu steuern, was zur besseren Kontrolle von Polymereigenschaften führen soll.

Zu diesem Zweck wurden etablierte organometallische Katalysatoren mit Azobenzolen funktionalisiert, um die Geometrie des Katalysators *in situ* zu ändern. Zuerst wurde ein Salen-Katalysator synthetisiert, der ein Azobenzol in der Nähe des aktiven Zentrums besitzt. Dieser zeigte vielversprechende photochemische Eigenschaften. Es wurde aber festgestellt, dass die Bestrahlung die LMCT Bande des Metalls anregt, was die Bindung des Polymers zum Katalysator beeinträchtigt.

Um dieses Problem zu umgehen wurde ein dinuklearer Salen-Katalysator, mit einer besseren Bandentrennung, synthetisiert. Dieser Katalysator zeigte eine *trans* → *cis*-Isomerisierung, konnte photochemisch aber nicht zurück geschaltet werden, da die Absorptionsbanden des Azobenzols mit denen des Metalls überlappten. Es wurden dann mehrere Ansätze verfolgt, um das Absorptionsverhalten des Azobenzols zu ändern, jedoch ohne eine praktikable Lösung zu finden.

Daher wurde das Absorptionsverhalten des katalytischen Zentrums durch die Einführung eines rigiden durchkonjugierten Salphen Liganden geändert. Drei Systeme wurden synthetisiert, wobei der Katalysator mit einer Ethylenbrücke zwischen dem Azobenzol und dem Metallzentrum die besten Ergebnisse zeigte. Dieser Katalysator konnte reversibel geschaltet werden und zeigte auch einen Aktivitätsunterschied in der Polymerisation von β-Butyrolacton. Es konnte gezeigt werden, dass die Aktivität des Katalysators um einen Faktor von 2,4 zwischen dem *trans*-Isomer und dem bestrahlten Reaktionsgesmisch erhöht werden konnte. Das gleiche Ergebnis wurde auch bei *in situ* Experimenten beobachtet.

Darüber hinaus konnte gezeigt werden, dass *ortho*-Azobenzol funktionalisierte Schiff Basen genutzt werden können, um die Reaktivität in dynamisch kombinatorischer Chemie zu steuern. Bei der Bildung von Iminen wurde die Reaktivität um einen Faktor von 2,2 zwischen dem *trans*-Azobenzol und dem bestrahlten Reaktionsgemisch gesteigert.

Table of Content

1. Introduction[a]

The creative force of chemistry is primarily evident through the emergence of new substances and materials with unprecedented functions. They are typically the result of designing and synthesizing new molecules that exhibit specific properties, ranging from biological activity (pharmaceuticals) all the way to device performance (materials). Therefore, the impact of chemistry on society largely depends on the success of making new molecules in an environmentally benign and sustainable manner. For this reason over the past decades, chemical research, has been primarily concerned with developing new synthetic methods and applying them to generate new drugs, scaffolds, and polymers. These accomplishments have recently been complemented by a surge to perform "green" chemical reactions,[1] which has led to better atom economy and energy efficiency. This is evident from the development of catalysts with boosted efficiency and selectivity[2-5] as well as advanced reaction engineering combined with improved purification methods.[6] Up to date the research in this field continues to thrive and there are many new tools available to the synthetic chemists. However, besides controlling *what* and *how* to make a molecule, it will become increasingly important for chemists to control *when* and *where* chemical reactions take place. The ultimate goal is to perform chemical processes with high temporal and spatial resolution, which would allow one to time reactions, for example in simple cascades or complex chemical networks, as it is evident in nature. Ideally, control over time and space of the chemical transformation of choice is provided by an entity, which upon the action of an external stimulus acts as a "remote control". Regarding the quest to attain the best possible control, the best spatial resolution is clearly provided by an STM tip, which can be used to induce chemical reactions on the nanoscale.[7-10] A clear drawback of using an STM is the slow speed, rather serial processing, and limited scale-up. Other stimuli such as temperature or mechanical forces suffer from poor spatial resolution besides other limitations and offer little parallelization capability.[11] It is generally accepted that light serves by far as the best stimulus to operate as the trigger. While the choice of the wavelength and intensity allows for precise control of a specific photoreaction, the exposure can be carried out using modern optics thereby enabling highly parallel processes. In addition to providing excellent temporal control over illumination, spatial resolution that is traditionally limited due to the law of diffraction has recently been improved significantly by super-resolution techniques[12] and two-photon processes.[13,14] To use light for controlling a chemical reaction, the gate entity can either

[a] Parts of the introduction have been published in R. Göstl, A. Senf, S. Hecht, *Chem. Soc. Rev.* **2014**, *43*, 1982–1996.

undergo an irreversible or a reversible photoreaction. While the first allows for a singular activation or de-activation event in a fuse-like fashion only, the latter provides the opportunity to toggle between two states multiple times allowing to switch the system and hence the entire chemical process. Therefore, only reversible photoreactions, which are typically associated with the phenomenon of photochromism, provide true "remote-control" over the chemical process by light.

One of the great challenges that chemists have to face in gaining control over *when* and *where* reactions are taking place is diffusion. The light source that one uses could be as well-defined as possible, yet it would still not be able to provide control when molecules diffuse away from the irradiated space. There are two ways how to overcome this problem. One is to immobilize the substrate on a surface and the other one is a fast switching catalyst in a living polymerization where substrates stick to the catalyst at all time.

The latter approach would allow temporal and spatial control over polymerization reactions which is an intriguing opportunity. Polymer chemistry is a field with an enormous impact on every-day life. Applications range from simple water bottles to more sophisticated polymers that are used in microelectronics or biotechnology. A major impact for this development was the introduction of controlled radical polymerization (CRP) which allowed the rational design of polymers with well-defined molecular weights and polydispersities. The advantage of CRP-polymerizations is the high tolerance towards functional groups which allowed an easy access to copolymers. This technique and others like ring-opening polymerization (ROP)[15], chain-walking coordination polymerization[16] and ring-opening metathesis polymerization (ROMP)[17] are well established procedures for the production of well-defined polymers with a high precision in the placement of functional groups. Furthermore the use of reliable methods for post functionalization like orthogonal click-chemistry[18] has further increased the variety of possible polymer architectures.

Looking at the near endless variety of different architectures as well as applications one can raise the question of which fundamental challenges are left to be addressed. The answer comes from a source of inspiration present in many fields: nature. The synthetic methods that are available to polymer chemists nowadays are still far from what ribosomes are able to do: synthesizing error-free, high molecular weight polymers that fold into a well-defined structure.[19] The even more impressive aspect behind this is the temporal and spatial control with which the body is able to control these polymerizations.

Mimicking the temporal and spatial control, that is reached by natural systems, is an enormous challenge for polymer chemists. But the potential that lies behind such a technology is worth it,

because it would ultimately allow to control the chemical structure of polymers and with that the macroscopic properties. One just has to look at the application of irreversible temporal control of polymerizations that has led to new industries in material science which range from coatings, duroplasts, foams and glues. Furthermore the technology was a milestone in the development of advanced materials like photohealable dental resins.

To gain reversible temporal control over polymerizations there are several different stimuli that have successfully been used: allosteric[20], chemical[21,22], electrochemical[23] and light[24].

Amongst the stimuli mentioned, light is the ideal stimulus for the control of polymerization. Nevertheless recent efforts in the field have the major drawback that the photocontrol is limited to the initiation step of polymerizations. Strategies to overcome this drawback are focusing on using light to activate monomers[25,26], the propagating chain-end[27] and the catalyst[24].

2. Theoretical Background

2.1. Azobenzene

Azobenzenes[28] are a class of compounds that can exist as two isomers (Scheme 1). The *trans* → *cis*-isomerization around the central N-N-double bond can be triggered electrochemically[29,30], thermally, using mechanical actuation[31] or by light[28]. For almost all azobenzenes the *trans*-form is thermodynamically stable, whereas the *cis*-form is metastable, and can undergo the *cis* → *trans*-isomerization thermally. Therefore azobenzenes are classified as T-type chromophores, whereas chromophores that have to thermally stable state are classified as P-type. The thermal half-life of the *cis*-form is usually long enough that both forms can be investigated, but can also be ranging from a half-life of milliseconds[32] to several years.[33]

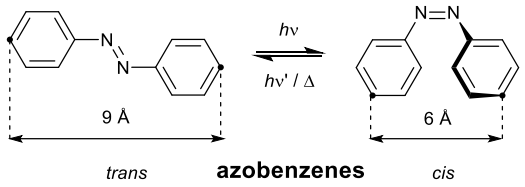

Scheme 1: Isomerization of azobenzene. *trans* → *cis*-isomerization occurs upon irradiation with light, *cis*-*trans* isomerization can occur either photochemically or thermally. The C-C' distance is 9 Å in the *trans* azobenzene and 6 Å in the *cis* azobenzene.

Azobenzene undergoes large geometrical changes due to the isomerization process. In the thermodynamically stable *trans*-form the molecule is planar and the distance between the 4 and 4' carbon atoms is ~9 Å. The *cis*-form on the other hand is twisted due to steric repulsion between the hydrogen atoms *ortho* to the N-N double bond. Furthermore the distance between the 4 and 4' carbon atom is significantly smaller with only ~6 Å of separation. This large geometrical change has led to a wide range of applications azobenzenes being used in. These include photoswitchable materials like polymers,[34,35] MOFs and functionalized surfaces,[36] photopharmacology,[37-39] molecular sensors and machines[40-43] and photoswitchable catalysts.[44-47]

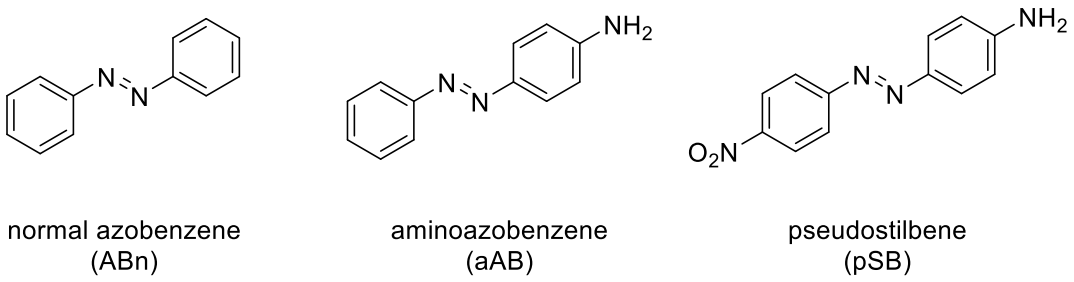

normal azobenzene (ABn) | aminoazobenzene (aAB) | pseudostilbene (pSB)

Scheme 2: Three different classes of azobenzene: normal azobenzene (ABn), aminoazobenzene (aAB) and pseudostilbene (pSB).

The photochromic properties of azobenzenes are highly dependent on the substitution pattern of the phenyl rings. These affect the spectral absorption, the thermal half-life as well as the isomerization mechanism. Azobenzenes are historically[48] classified depending on their absorption spectrum into three groups (Scheme 2): the normal azobenzenes (ABn), the aminoazobenzenes (aAB) and the pseudostilbenes (pSB). Even though this classification falls short to categorize new developments in the field[49] by Hecht[33] and Woolley[50] this overview will stick with it.

2.1.1 Normal Azobenzenes

The group of the normal azobenzenes (ABn) includes azobenzenes substituted with alkyl, aryl, halide, carbonyl, amide, nitrile, ester, nitro and carboxylic acids. The absorption spectra of these are very similar to unsubstituted azobenzenes. The spectrum of azobenzene (Fig. 1) shows two very well separated bands and a band in the UV region (ε_{320} = 22000 L mol^{-1}cm^{-1}) arising from the $\pi \rightarrow \pi^*$ transition, a band in the visible region (ε_{450} = 400 L mol^{-1}cm^{-1}). The latter is much weaker and arises from the symmetry forbidden $n \rightarrow \pi^*$ transition. The $\pi \rightarrow \pi^*$ transition for *cis*-azobenzene (ε_{270} = 5000 L mol^{-1}cm^{-1}) is weaker compared to *trans*-azobenzene, but the absorption of the $n \rightarrow \pi^*$ transition (ε_{450} = 1500 L mol^{-1}cm^{-1}) is stronger. This behavior can be explained by the twist of the molecule in the *cis*-state that results in a steric repulsion of the 2 and 2' substituents in the *cis*-azobenzene.[51,52]

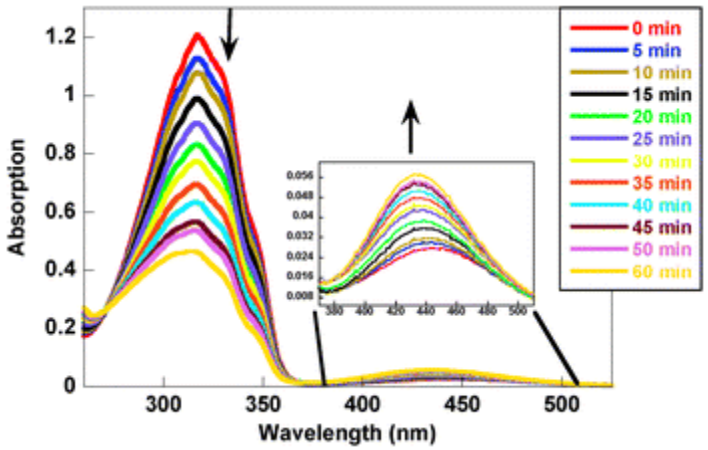

Fig. 1: Change in the absorption spectrum of azobenzene upon irradiation with light of a wavelength of 316 nm. The π → π* band at ~320 nm decreases and the n → π* band at ~440 nm increases. Reproduced by permission of The Royal Society of Chemistry[53]

Irradiation of azobenzene with light of a wavelength of 313 nm results in a photostationary state (PSS) of 80% *cis*-azobenzene, while irradiation with 436 nm results in a PSS of 10% *cis*-azobenzene.[54] The quantum yield for the isomerization is higher when it is excited into the S_1 state than when it is excited to the S_2 state, which is a violation of Kasha's rule.[55-57] The quantum yield for the isomerization is dependent on the temperature,[58] solvent polarity and viscosity.[55,59] The mechanism of the isomerization is despite many studies, still not fully understood in all cases. There are several isomerization pathways possible including the rotational, inversion and concerted inversion mechanism.

The requirement for the rotational mechanism depicted in Scheme 3 is a rupture of the N-N π-bond. This allows free rotation, which leads to a change in the C-N-N-C dihedral angle while the N-N-C angle of 120° stays the same.[60] The inversion mechanism includes an increase of one N=N-C bond angle above 180° while the C-N=N-C dihedral angle stays fixed at 0°. This results in an sp hybridized azo-nitrogen atom in the transition state.[61] In the concerted inversion mechanism both N=N-C bond angles increase to 180° to generate a linear transition state.

The transition state of the concerted inversion mechanism has no net dipole moment. All other mechanisms proceed via a polar transition state. The relaxation occurs close from the transition state and can either form *cis* or *trans* azobenzenes therefore all mechanisms predict photostationary states with both isomers present. To explain many experimental observations multiple isomerization pathways are used.[62]

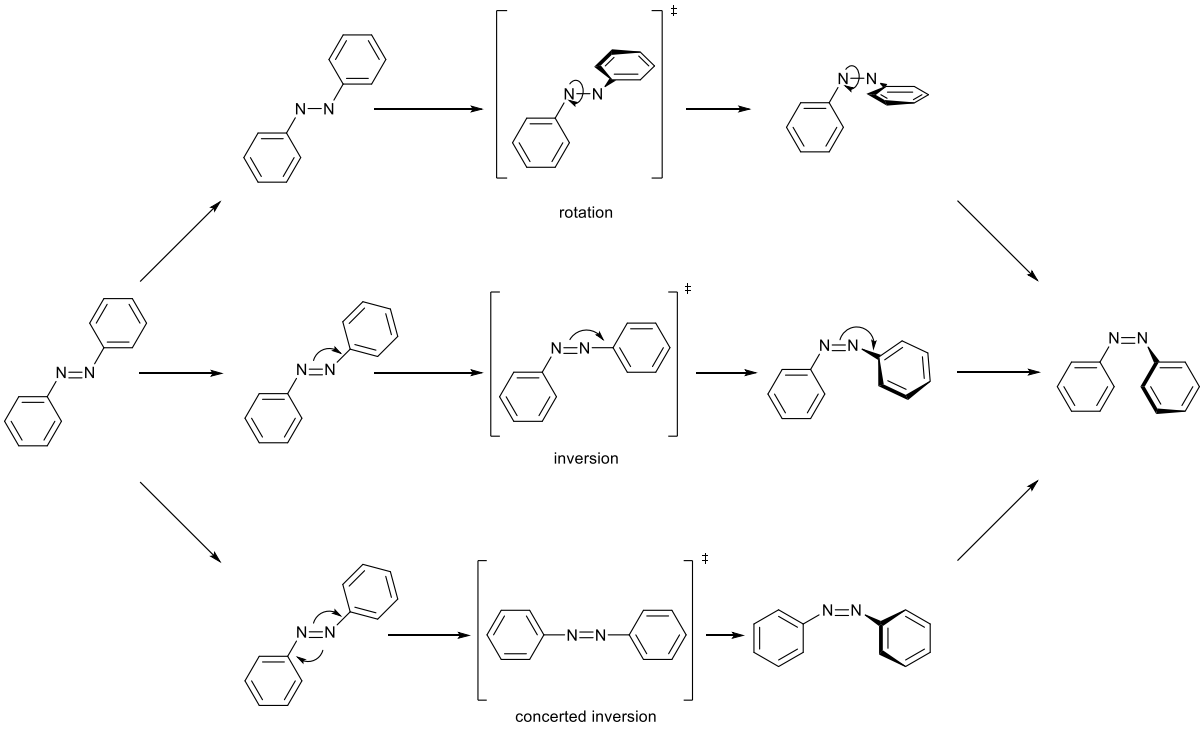

Scheme 3: Different possible isomerization mechanism for azobenzenes that are discussed in the literature.

Thermal isomerization occurs through multidimensional pathways that are dominated by concerted inversions.[63] The activation barrier for the thermal isomerization is usually decreased proportional to the number of substituents. Electron withdrawing substituents like -NO_2 and -CO_2H have a significant influence on the thermal stability, they decrease the energy barrier which leads to a fast thermal *cis* → *trans*-isomerization of these azobenzenes.

2.1.2 Aminoazobenzenes

Electron donating substituents have a small influence on the thermal isomerization. They increase the electron density in the π* orbital, which leads to faster thermal *cis* → *trans*-isomerization rates compared to normal azobenzenes.[64,65] The rates for these isomerizations are dependent on the solvent polarity but not the solvent viscosity.[66,67] In compounds such as **2HAB** where an intramolecular hydrogen-bond can be formed the thermal isomerization occurs on a scale of milliseconds to seconds.[64]

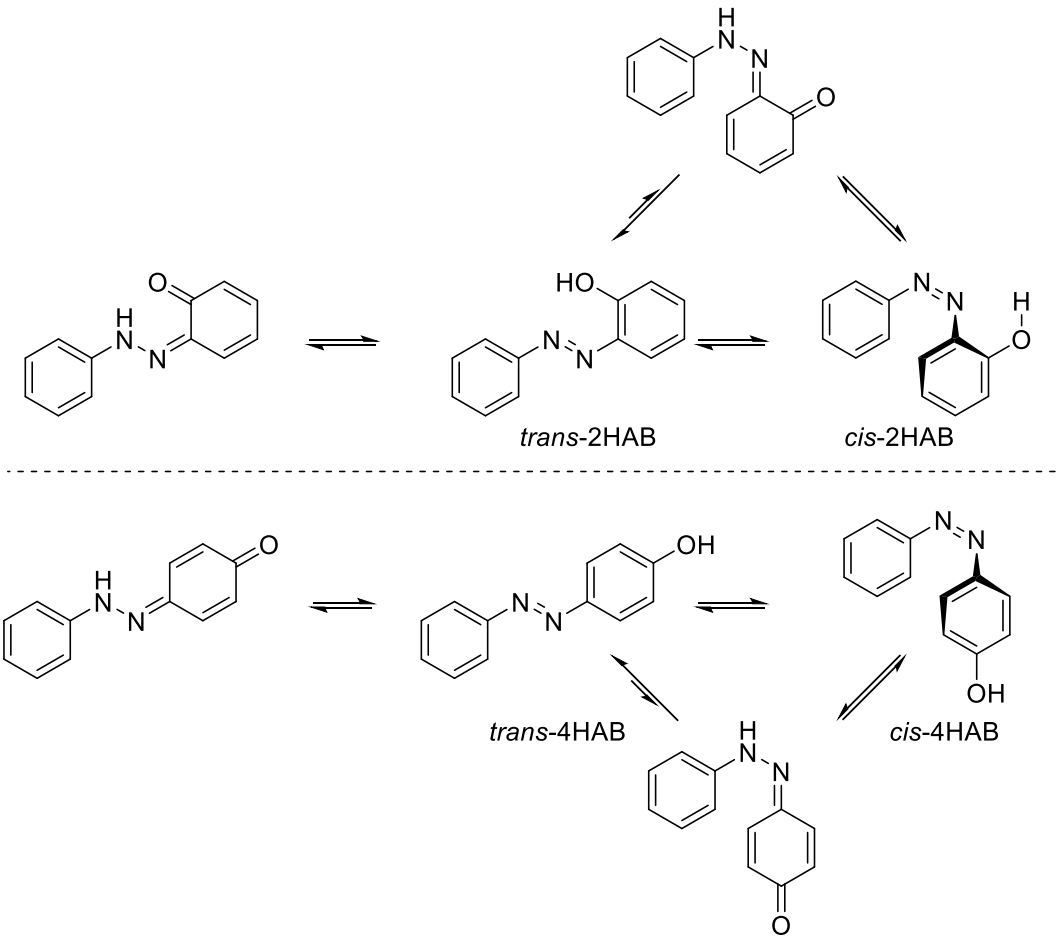

Scheme 4: Tautomerization that occurs in hydroxyazobenzenes and the influence on the isomerization behavior of azobenzenes.

For this reason hydroxyazobenzenes behave completely differently compared to other azobenzenes. A rapid thermal isomerization is caused by the hydrogen-bond in the 2-hydroxyazobenzene **2HAB** shown in Scheme 4.[68,69] Tautomerization can occur which leads to the formation of the corresponding phenylhydrazone. Irradiation can initiate the tautomerization, therefore 2-hydroxyazobenzenes show complex decay behavior after excitement with ultrafast pulses.[70] Tautomers of 2-hydroxyazobenzes have been observed, however the intramolecular hydrogen-bonds are rarely strong enough to prevent isomerization.[71]

4-Hydroxyazobenzenes **4HAB** (Scheme 4) undergo isomerization upon irradiation.[69,72-74] The thermal isomerization is highly dependent on the solvent, it proceeds very fast in polar and slow in non-polar solvents. This solvent dependence indicates a rotation-dominated process.[66,75] In acidic media hydroxyazobenzenes can tautomerize to the corresponding azoxybenzene[76] and in polar solvents it undergoes tautomerization via a solvent assisted proton transfer.[73,75,77] These

4-hydroxyazobenzenes can dimerize at low temperature and high concentration via intermolecular hydrogen-bonding as shown in Scheme 5.[73,78] Alkylation of the hydroxyl-group restores the usual azobenzene properties.[73,79]

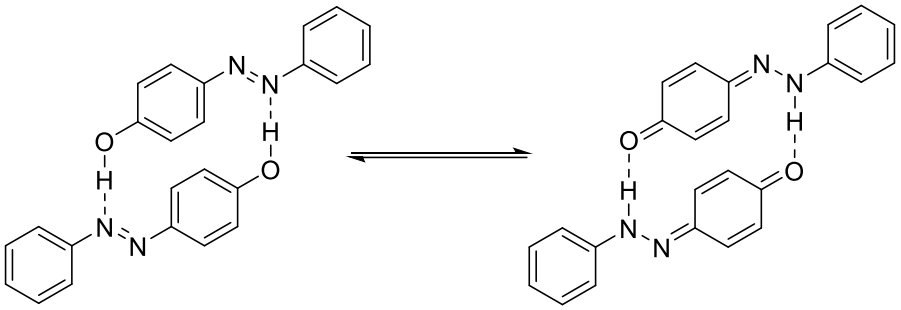

Scheme 5: Dimerization of 4-hydroxyazobenzene that can lead to protonation of the azo-bond.

2.1.3 Pseudostilbenes

Pseudostilbene (pSB) are divided into two classes: protonated azobenzenes and push-pull azobenzenes (ppAB). The $\pi \rightarrow \pi^*$ and $n \rightarrow \pi^*$ transitions occur in the visible region. ppABs have a strong electron acceptor and a strong electron donor in the 4 and 4'-positions of the azobenzene, lowering the energy of the $\pi \rightarrow \pi^*$ state. In addition to the transitions present in normal azobenzenes, ppABs exhibit additional intermolecular charge transfer bands that are due to electron-transfer between the donor and acceptor moieties.[80] Because of their fast thermal half-life, measuring quantum yields for ppABs is still complicated and ultra-fast spectrometry is needed. The *trans* → *cis*-isomerization quantum yield is significantly lower than for the *cis* → *trans*-isomerization.[73]

Due to their intense color many ppABs are used as dyes in industry. Their large dipole moment, high polarizability and fast thermal isomerization make ppABs ideal for the application in nonlinear optical[81,82] and photorefractive materials,[82,83] optical poling, holographic memory storage devices,[84-86] surface relief gratings and reversible optical wave guides.[87]

2.1.4 Synthesis

There are different synthetic pathways to create azobenzenes.[88] The more easily accessible azobenzenes are symmetrical, which can either be synthesized using reductive (Scheme 6a) or oxidative (Scheme 6b) coupling. The reductive pathway is in general less tolerant of different functional groups, since harsh conditions are needed to reduce the nitro-functionality. Reducing agents that are usually used include $LiAlH_4$,[89] $NaBH_4$,[90] KOH[91] and Zn/NaOH.[92] Synthesizing symmetrical azobenzenes via an oxidative (Scheme 6b) pathway is in general more functional group tolerant, since there is a wider range of available oxidizing agents that are able to oxidize the amine-functionality. Two commonly used oxidizing agents are Copper(I)-bromide[93] and (diacetoxyiodo)benzene (PIDA)[94] both of these reagents allow very mild coupling at room-temperature with a wide range of functional groups.

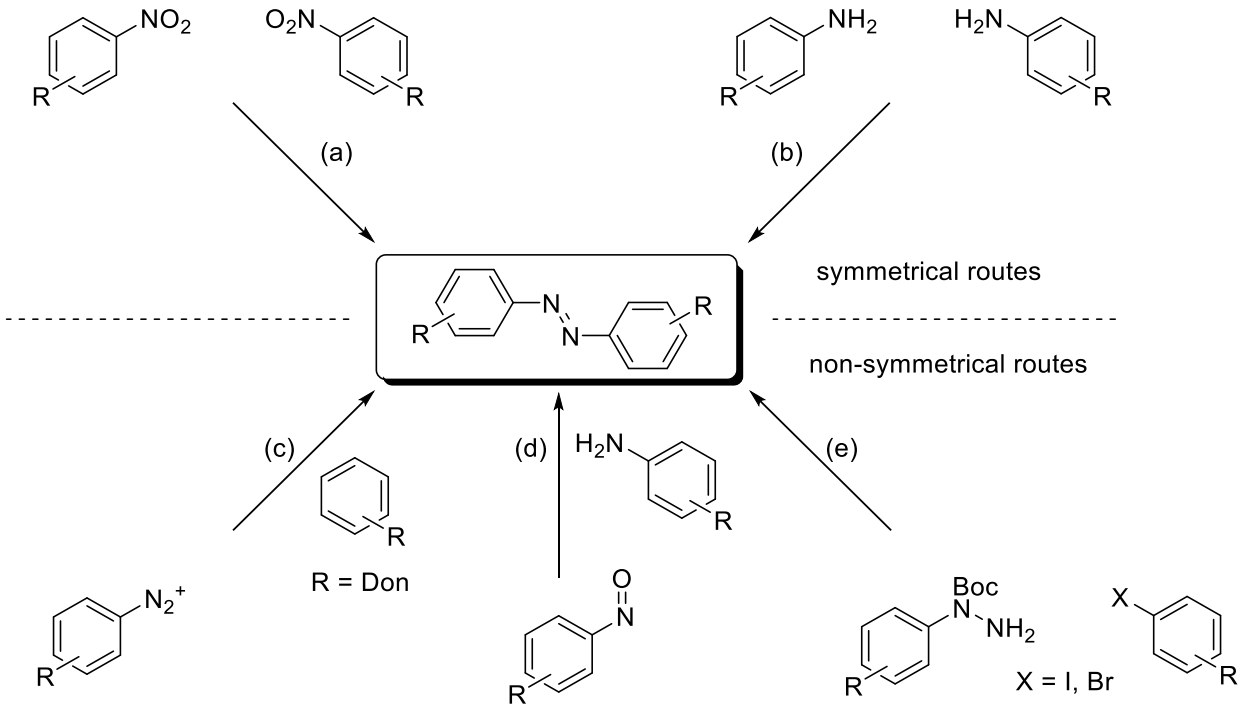

Scheme 6: Most important routes to synthesize azobenzenes. a) reductive coupling of nitrobenzenes b) oxidative coupling of aniline-derivatives c) diazonium-coupling using diazonium-salts and electron-rich benzene derivatives d) Mills-coupling of nitroso compounds with aniline derivatives e) Palladium-catalyzed coupling using halogenated benzene and a hydrazine.

To gain access to non-symmetrical azobenzenes there are three major approaches described in the literature. The oldest method is diazonium salt coupling (Scheme 6c),[95] where the first step

is the formation of a diazonium salt from the corresponding aniline derivative which then performs an electrophilic substitution. Since diazonium salts are weak electrophiles, derivatives with acceptor-substituents are sometimes used to increase their reactivity. The phenyl ring used as the nucleophile need to be very electron-rich.[96-98] Phenol- and aniline derivatives are widely used for these formations and allow a very high regioselectivity. In general, the substitution will take place in *para*-position to the electron-donating group. To bias the reaction towards an *ortho*-substitution the *para*-position needs to be blocked.

Another method to access non-symmetrical azobenzenes is the Mills-coupling (Scheme 6d).[99] Here an aniline derivative is oxidized to its corresponding nitroso-compound with a suitable oxidation agent, like ferric chloride,[100] Caro's acid,[101] potassium permanganate[102] or Oxone™.[103] The selection of the correct oxidation agent prevents over oxidation which usually leads to the formation of azoxy products. In the mechanism of the Mills-reaction the key step is a nucleophilic attack of an aniline derivative on the nitroso compound with a subsequent elimination of water. The Mills reaction allows a high control over regioselectivity and the formation of azobenzenes with hydroxyl and amine substituents in *meta*-position.
A third method has been reported rather recently. It uses a variation of the palladium-catalyzed Buchwald-Hartwig amination (Scheme 6e), where a Boc-protected hydrazine[104-106] is reacted with an aryl halide. The resulting diaryl hydrazine is oxidized using NBS/pyridine or CuI/Cs_2CO_3 to yield the desired azobenzenes. Since the yields of the coupling-reaction and the oxidation step are highly dependent on the substituents, other synthetic routes are often preferred over the palladium-catalyzed reaction.

2.2. Schiff-base based metal-complexes

Schiff bases were first described by Hugo Schiff in 1864 through the condensation of an aldehyde with an amine.[107] They are able to coordinate metals through an imine nitrogen and the hydroxyl group *ortho* to the imine. Schiff bases are considered to be "privileged ligands"[5] and are therefore still frequently used today. They stabilize a large number of metals in various oxidation states, which allows for their use in a large variety of different catalytic applications.

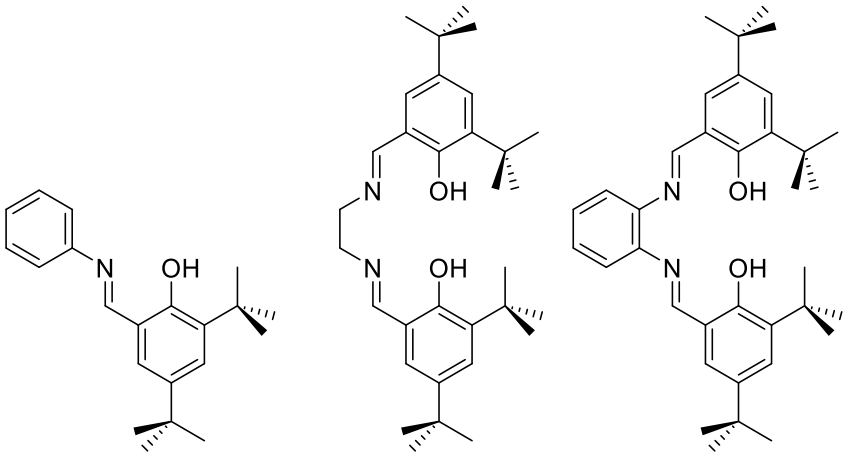

Scheme 7: Different classes of Schiff base ligands.

Schiff bases can be differentiated into two classes. The condensation of an aldehyde with an amine leads to the formation of a bidentate ligand that is usually referred to as FI- ligand (Scheme 7, left).[108,109] Using a diamine in the condensation leads to a chelating tetradentate ligand termed as salen-ligand (Scheme 7, middle).[110,111] A special case of the salen ligand are the so called salphen ligands (Scheme 7, right) where the bridging moiety is rigidified using a phenyl derivative.[112]

The ease of synthesis with many simple and well established reaction conditions make Schiff bases ideals candidate for combinatorial approaches in catalysis research.[113] The large availability of chiral amino acids and peptides allows an access to chiral ligands that can be used to make effective metal catalysts.[114]

Schiff base-complexes are often prepared *in-situ* for catalytic application using the Schiff base and a well-defined metal complex. There are essentially five different ways to prepare Schiff base complexes (Scheme 8).[111]

Using metal alkoxides (Scheme 8a) is the preferred route for early transition metals (M = Ti, Zr) since their alkoxides are commercially available and easy to handle. The reaction is an equilibrium reaction, which makes the prediction of the formed species sometimes difficult, because multinuclear complexes can also occur. Bulky substituents however can help to control the homogeneity of the complex by shifting the equilibrium towards a single species.

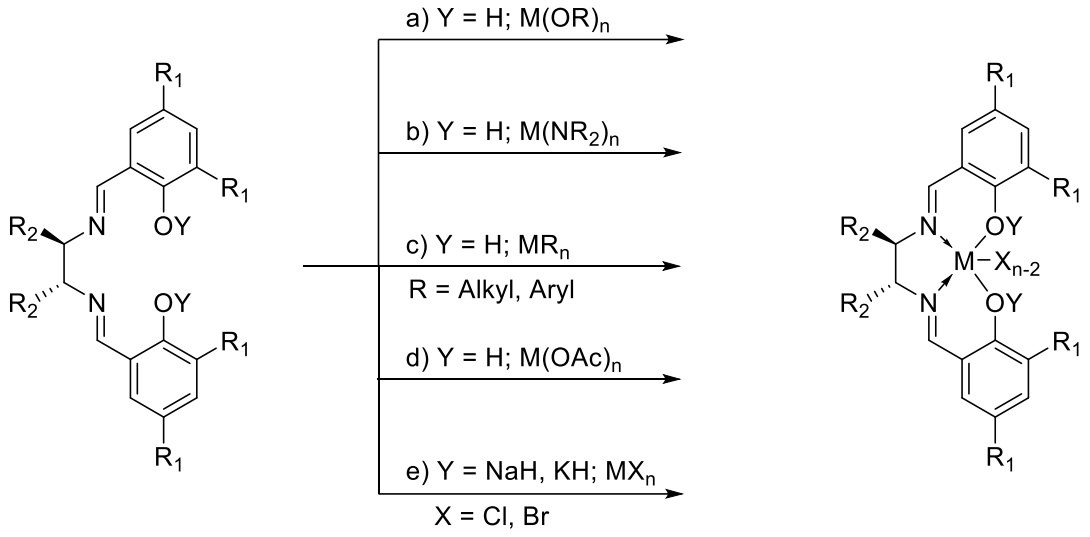

Scheme 8: Different synthetic ways to prepare Schiff base complexes. 1) using metal alkoxides 2) using metal amides 3) using metal alkyls or aryls 4) using metal acetates 5) using a base and metal halides.

Metal amides (Scheme 8b) can also be used to form Schiff base complexes with early transition metals. Here, the reaction occurs via an elimination of the acidic phenolic proton with a simultaneous formation of volatile $NHMe_2$. The reaction leads to Schiff base complexes bearing two bisimido groups that can easily be exchanged.

The preparation route using metal alkyls (Scheme 8c) is the preferred synthetic route for main group metals ($AlMe_3$, $GaMe_3$, $InMe_3$) since the alkyl derivatives are commercially available. Here the preparation is a direct exchange reaction.

Metal acetate (Scheme 8d) can also be used to prepare copper, cobalt and nickel Schiff bases by refluxing the Schiff base with the corresponding metal acetate. The methods a-d can be used for FI- complexes as well as Salen- complexes.

Procedures using metal halides (Scheme 8e) is usually just applicable for salen-complexes. Here, the first step is a deprotonation of the acidic phenol proton with a base like NaH or KH (lithium bases can attack the imide) followed by the formation of the corresponding Na_2(salen)

or K_2(salen). The driving force of the complex formation is the formation of the corresponding sodium- or potassium halide.

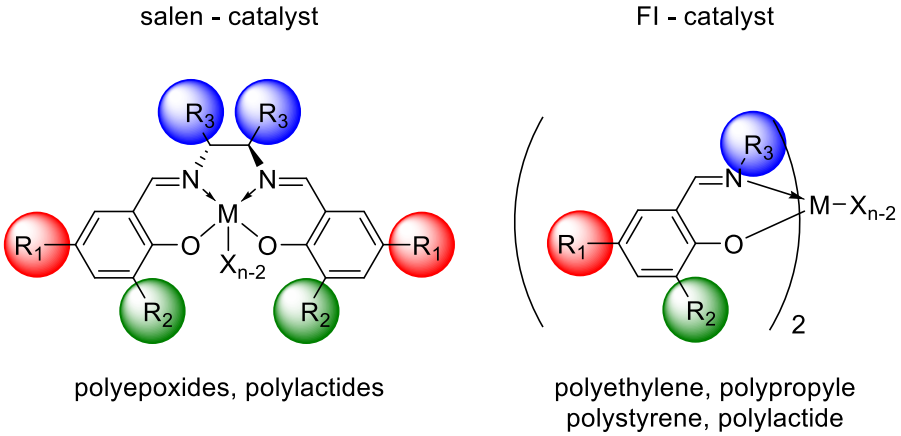

Scheme 9: Important substituents of FI- and salen catalyst, and the polymerizations they catalyze.

Salen and FI complexes are well investigated systems due to their wide range of applications in catalysis. Salen-complex have been found to catalyze different types of polymerization reactions with epoxide-[115] and lactone-monomers[116-118] among them. FI-complexes can also be used for a wide range of different polymers among them polyethylene,[108,109,119] polypropylene,[108,109,120] polystyrene[121] and polylactide[116] can be synthesized. This wide range of catalytic application has led to many investigation with different substituent so that their effects on the catalytic properties are well known. In both catalyst systems (Scheme 9) the ligands have three different substitutional sites that influence the properties of the catalyst.[116,122] The R_1 substituent (Scheme 9 red) has an electronic influence. Introducing electron withdrawing groups like chloride can increase the Lewis acidity of the metal center and therefore increase the activity of the catalyst. Usually *tert*-butyl groups are incorporated since these show the best compromise between activity and selectivity. The R_2 substituent (Scheme 9 green) is the geometrically closest substituent to the metal center and has therefore the biggest steric influence. Introducing sterically demanding moieties increases the selectivity up to a certain extend. Substituents like trityl-groups are sterically too demanding and inhibit monomer insertion. The R_3 substituent represents the Schiff base moiety which is in the case of salen ligands a bridging alkyl group. Depending on the length and the sterical demand of the group the selectivity as well as the electronic properties can be varied. Especially the length of the alkyl group can have an influence on the coordination sphere of the metal center which influences the size of the active site.

2.2.1 Salphen-complexes

Salen complexes have been extensively explored thanks to their ease of preparation and the ability to easily introduce chirality into these molecules.[123] Achiral salen ligands have received a lot less attention, especially phenyl-bridged salphen ligands have been neglected for a long time, despite the fact that they offer some advantages over their salen analogues. The conjugated π-system allows the tuning of their photophysical properties and their preparation is in general more cost efficient,[112] which renders them ideal building blocks for material science.[124] Furthermore the rigid ligand framework allows a tuning of the Lewis acidity of the metal center by introducing more substituents, which can be used to increase the reactivity of the resulting complex.

Chiral salen ligands have already proven themselves as suitable ligands in catalysis, whereas the use of salphen ligands in catalysis has scarcely been investigated to date. There are examples reported, however where salphen complexes show higher activity in catalytic application than their analogous salen complexes. Since Jacobsen[125] first reported on the use of manganese Schiff base complexes in the homogenous catalysis of epoxidation reactions, these types of systems have received a lot of attention. Indeed, there are recent developments of Mn(III)salphen complexes in the application of oxidation catalysts and antioxidants.[126]

The group of Rebek[127] has reported among others on a sophisticated salphen-based catalyst (Scheme 10). They used a biomimetic approach with a resorcinarene-supported Zn(II)salphen complex for the acetylation of choline. In this approach the bridging phenyl is integrated into the resorcinarene structure, which leads to a molecule where two reagents are brought into close proximity to each other. The Lewis acidity of the Zn(II) ion is used to bind acetic anhydride and the resorcinarene forms a host-guest complex with the choline. This proximity led to a more efficient process which could be observed by comparing the reaction rates of the pure Zn(II)salphen and cavitand, respectively with the ensemble of Zn(II)salphen and cavitand.

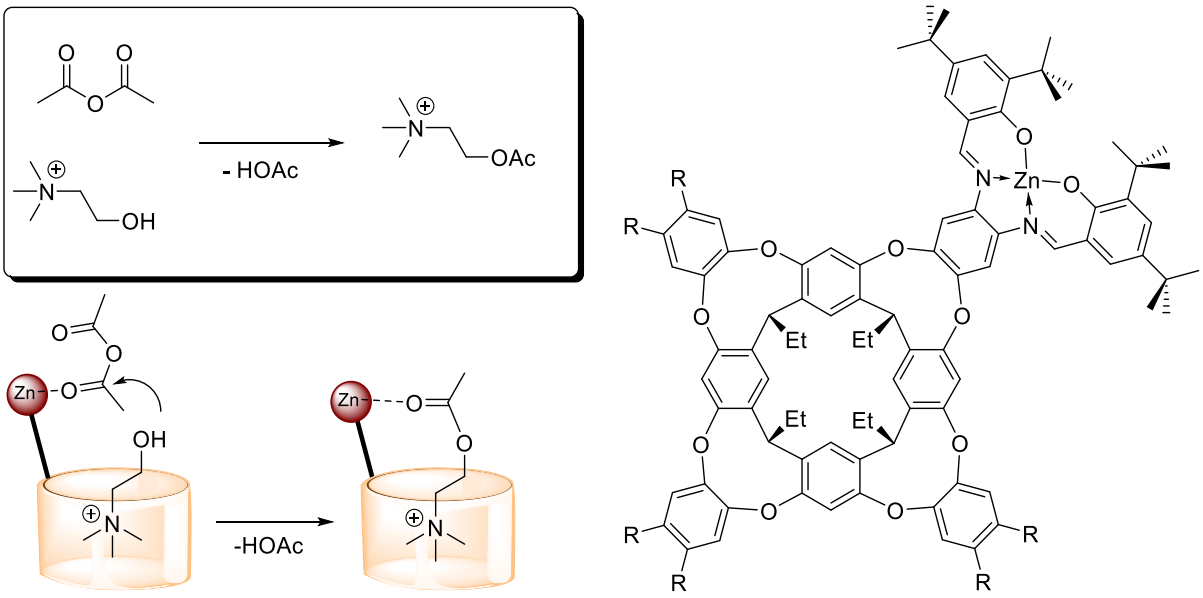

Scheme 10 Zn(II)salphen cavitand that is based on a biomimetic approach, which is active in the acetylation of choline. The proposed cooperative catalytic mechanism is shown at the bottom left.

The group of Rieger has reported on a bis-Cr(III)salphen complex that is tethered by a diarylether linker (Scheme 11).[128] These systems were successfully used in the catalysis of β-butyrolactone[129] and CO_2/propyleneoxide (PO)[130] copolymerization, and compared to their mononuclear analogues, showed a much higher activity and average molecular weights in the polymerization of lactone. Higher rates in the CO_2/PO polymerization were observed when the catalyst concentration was lowered. The better catalytic behavior was attributed to a bimetallic pathway that enabled a cooperative mechanism, where one metal center binds the polymeric chain while the other one binds and activates the monomer.[131]

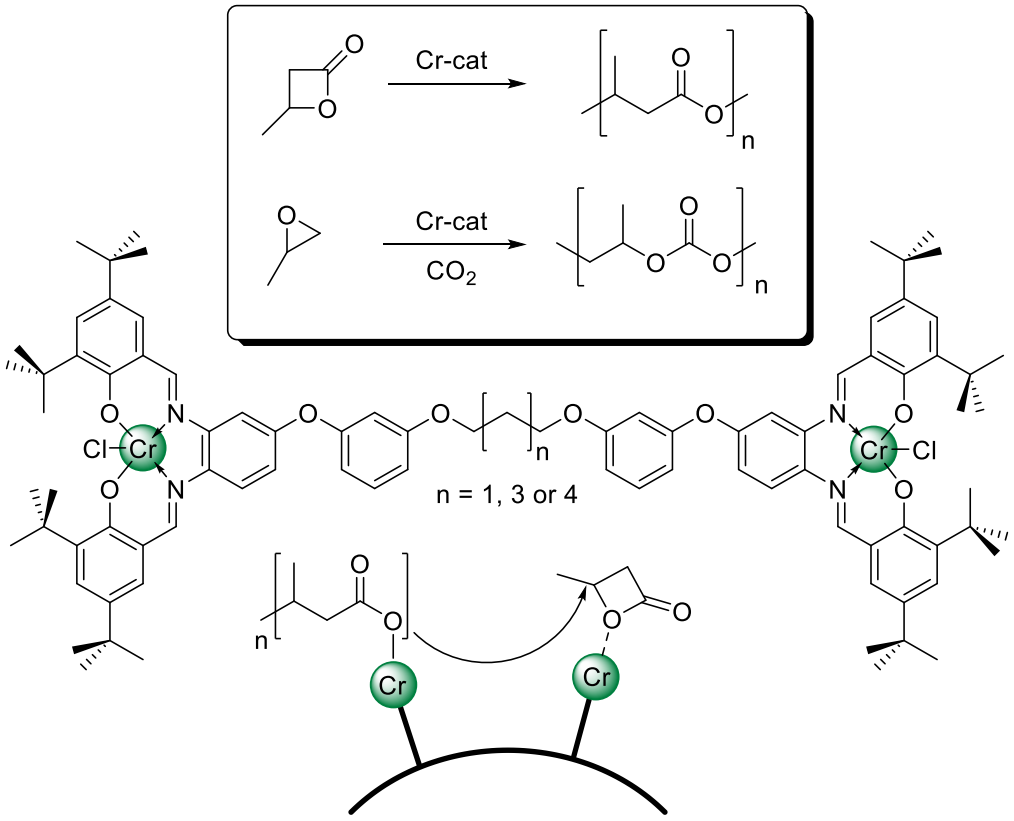

Scheme 11: bis-Cr(III)salphen reported by Rieger that efficiently catalyses the ROP of β-butyrolactone and copolymerization of CO_2/PO.

2.3 Steroselectivity in Lactide-Polymerization Reaction

The stereoselectivity of a catalyst has an influence on the tacticity (microstructure) of the polymer, which has a large influence on the physical properties of the polymer. Tacticity is defined in three classes: isotactic, syndiotactic and atactic. In isotactic polymers all the stereocenters are the same (SSSS or RRRR). Syndiotactic polymers have alternating stereocenters (SRSR) and atactic polymer have a random distribution of the stereocenters (RRSR). If a polymer has parts with different tacticities it is called a stereoblock polymer. Polymers with well-defined microstructures (isotactic and syndiotactic) have in general higher melting temperatures (T_m) than random microstructured polymers (atactic). Therefore gaining control over tacticity would allow direct control over the length of stereoblocks in polymers, which could eventually lead to well- defined tuning of macroscopic polymeric properties.

A polymer that is a good candidate for controlling tacticity is polylactide (PLA). The lactic acid monomer has an asymmetric methine carbon which leads to three possible stereoisomers of lactide (*rac*-lactide): *L*-lactide (LLA), *D*-lactide (DLA) and *meso*-lactide (*meso*-LA). Ikada and Tsuji *et al.* have reported an interesting thermal property of PLA. The T_m is raised when a stereocomplex of poly-*L*-lactide (PLLA) with poly-*D*-lactide (PDLA) is formed[132,133]. Since PLA decomposes above its T_m, this is an attractive way to improve its thermal stability. Stereocomplexes of the diblock forming PLLA-PDLA are also known.

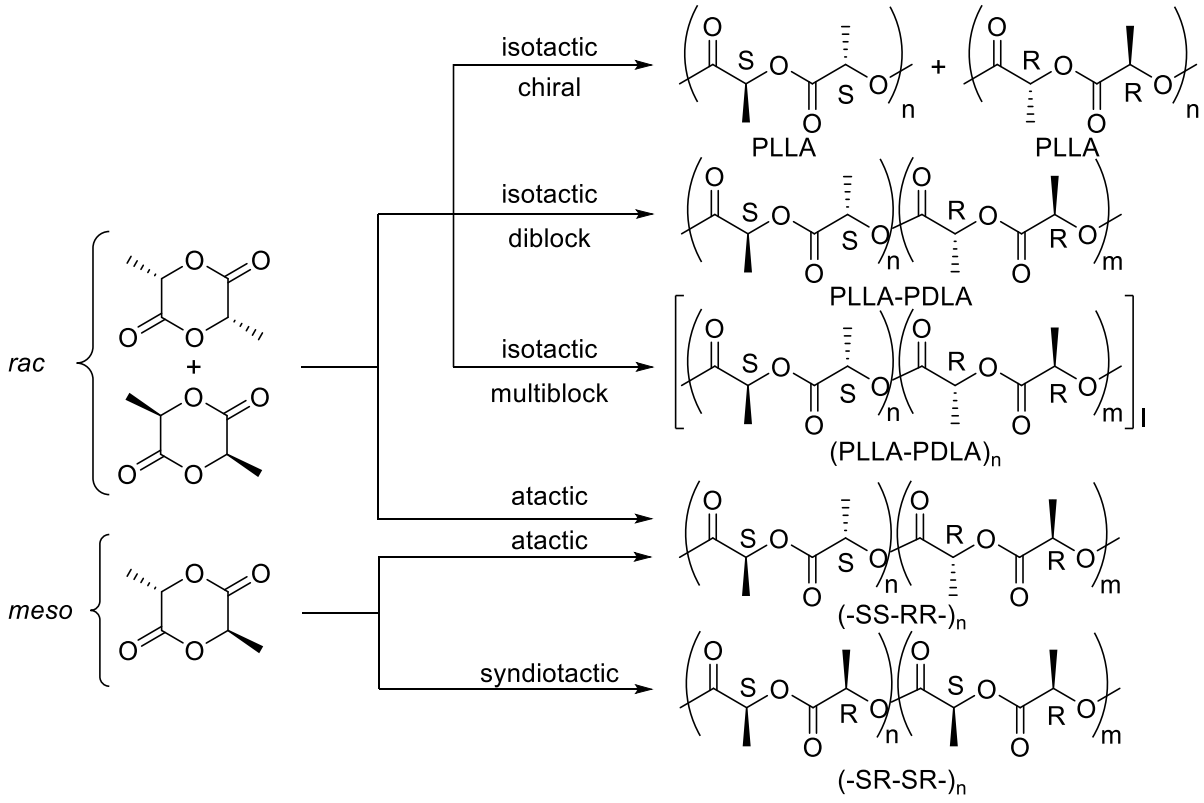

Scheme 12: Different possible microstructures that can be obtained from *rac*-lactide and *meso*-lactide.

Since the purity of the LLA is crucial for the stereochemical outcome,[134] synthetic chemists have put effort in developing stereoselective polymerizations of *rac*-lactide. Ring opening polymerization of *rac*-lactide using a conventional catalyst like $Al(OiPr)_3$ forms atactic PLA,[135] which is thermally not as stable as isotactic PLA. The ROP of *rac*-lactide can ultimately form two patterns – isotactic and atactic PLA – if the ring-opening occurs via a coordination-insertion mechanism without racemization. From *rac*-lactide three different forms of isotactic PLA can be obtained: completely homochiral, diblock stereocopolymer[136] and a multiblock stereopolymer.[137] Furthermore an atactic PLA can be formed by an alternate addition of LLA and DLA.[138] Scheme 12 shows the different possible microstructures that can be obtained by a stereoselective ROP of *rac*-lactide and *meso*-lactide.

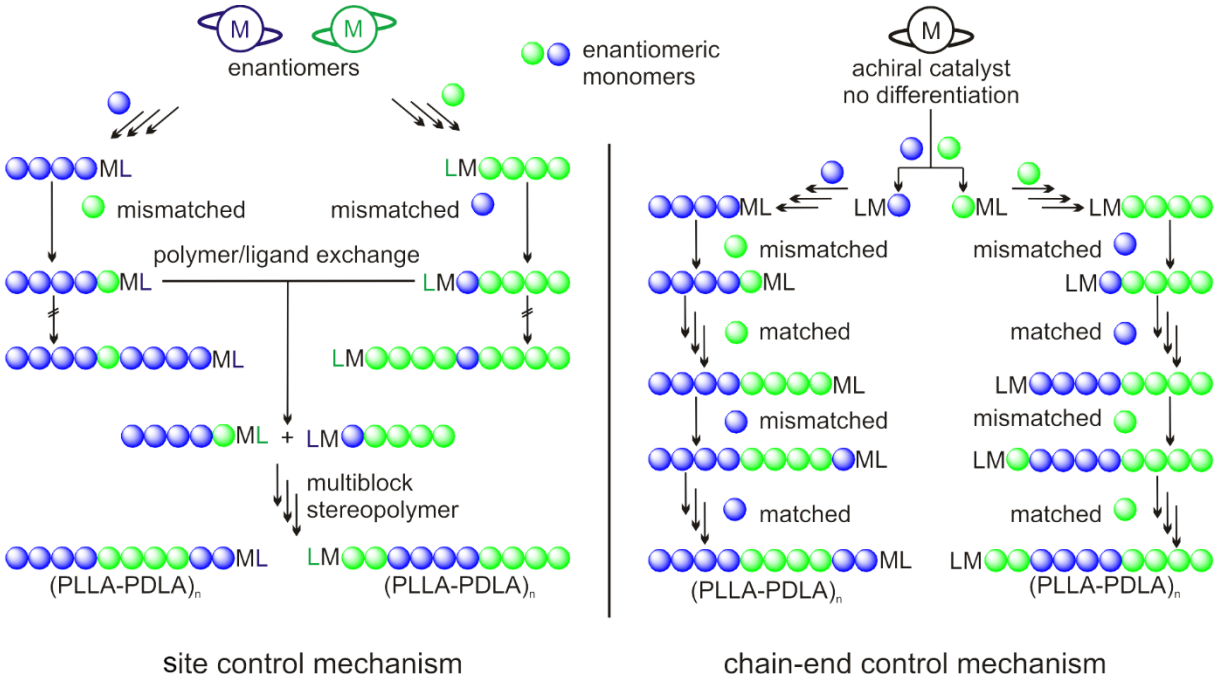

Fig. 2: Different mechanisms for the formation of stereoblock polymers.

From a mechanistic point of view (Fig. 2) stereoselectivity can be achieved via a site-control mechanism (SCM)[139] or a chain-end mechanism (CEM). With SCM the complex has a chirality that is induced by the ligands surrounding the catalytic site. This chirality differentiates between LLA and DLA which preferentially leads to the reaction of only one enantiomer. Even though one would expect an optical active polymer molecule to be formed by SCM, Coates *et al.* were able to show that the polymers can have a multiblock stereosequence, because of polymer exchanges occurring during the polymerization when a mismatched monomer is incorporated. The polymers obtained from *rac*-lactide via SCM are thermally more stable than homochiral PLLA.

In a polymerization that occurs via a CEM the metal complex as well as the ligand are achiral[138]. The initiation occurs without enantiomeric differentiation between the monomers. This leads to the situation that the chiral information is incorporated into the propagating chain-end. The monomer with the same chirality as the last inserted monomer will then preferentially be incorporated into the propagating chain-end. If a mismatched monomer is incorporated the preference for monomer insertion is reversed and the other enantiomer is preferentially incorporated into the propagating chain-end. If perfect stereoselectivity was achieved each polymer would be homochiral, although the mixture of different polymers is optically inactive. In reality no homochiral polymer is formed but multiblock stereocopolymers (PLLA-PDLA) are afforded due to several inversions of chirality during the polymerization.

When the mechanistic details of asymmetric induction are unknown, hypothetical models which give a reasonable explanation for the stereoselectivity, can be useful to design a catalyst. Unfortunately, such models for the stereoselective ROP of *rac*-lactide are rare.[140] Kondo *et al.* have postulated a working model for salen-complex catalyzed CEM (Fig. 3) based on their extensive studies of substituent effects in 3-position of the salicylidene moiety and crystal structures of different activated complexes.[116]

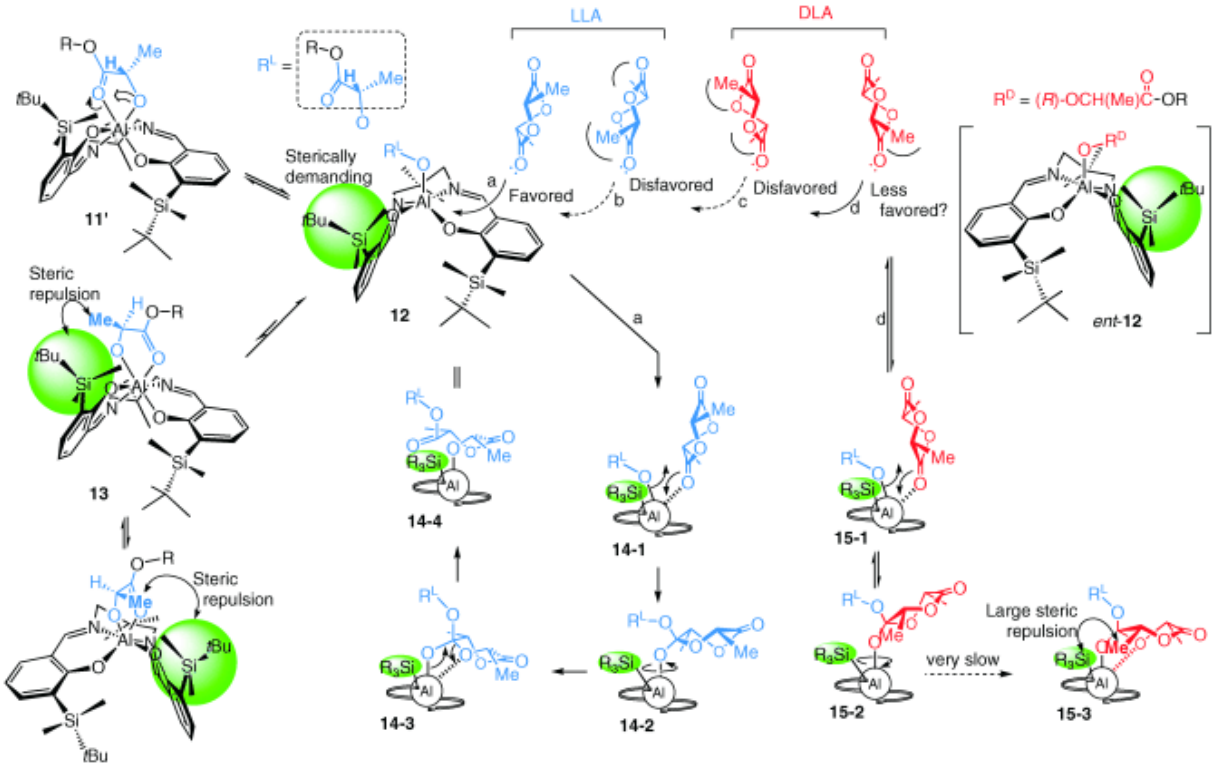

Fig. 3: Possible model for the explanation of the stereoselectivity in PLA-ROP. Reproduced by permission of John Wiley and Sons[116]

The most stable geometry of the aluminum alkoxide of (L)-lactate is expected to be complex **1**, from considerations based on the crystal structure of the non-alkylated complex. A decoordination of the carbonyl oxygen reorganizes the geometry around the aluminum center to be pentacoordinated, which results in the formation of the complex **2**. This opens one coordination site for an approaching monomer. The rotation around the Al-O bond is hindered due to the steric demand of the TBS group and the methyl group of the lactate (complex **3**). The flipped geometry as seen in complex **3**, shows no relief in steric repulsion because the methyl group is still facing the other TBS group which covers the whole face of the lactate moiety. Therefore complex **1** is supposed to be more stable than **3** and **3'**. This leads to the assumption that R in complex **1** and R_L in complex **2** occupy the space behind the TBS group and that the monomer insertion occurs on the opposite site of the aluminum center (paths a-d). From NOE

experiments it was shown that the geometry of **1** is not fixed in solution. Nevertheless the approach of *rac*-lactate is most likely as illustrated in Fig. 3 from the open site of complex **2**. The LLA molecule that has its methyl groups pointing away from the TBS groups most likely approaches the aluminum center from the opposite site of the R_L group to minimize steric repulsion between the TBS and the methyl group and the R_LO group to form complex **4-1**. The alkoxide R_LO attacks then the carbonyl group to afford complex **4-2** and after rotation around the Al-O bond the four membered ring in **4-3** is formed[141] which leads to the ring opening reaction of LLA to give complex **4-4**. The geometry of the inserted monomer is arranged in the most favorable conformation, which has the polymer terminus of the alkoxide of the alkyl (L)-lactate in complex **1**. The incorporation of LLA occurs continuously. Inclusion via path **a** can be disturbed by bulkier substituents (e.g Ph_3Si).[116] For the DLA monomer two possible incorporation pathways are imaginable, path **c** is disfavored for the same steric reasons as path **b**. Path **d** on the other hand, has methyl groups that are kept away from the TBS group, and could take place although there is still some steric repulsion between the methyl and the TBS group (complex **5-1**) The alkoxide R_LO can then attack the carbonyl carbon to afford complex **5-2**. The following ring opening polymerization requires the formation of a four membered ring **5-3**, but this can only occur after a rotation around the Al-O bond, which is restricted due to steric repulsion that occurs between the TBS and the methyl group during that process. This leads to a more favorable back reaction to **5-1** and a following decoordination of DLA. Nevertheless, once a DLA monomer overcomes the barrier and forms **5-3** it will incorporate into the polymer chain and the stereochemistry will be reversed. DLA monomers are then incorporated continuously and the LLA incorporation is the least favorable.

2.4. Photoswitchable Catalysis[b]

Here, the increasing number of photoswitchable catalystsystems is covered, that display external control over thermal (ground-state) chemical reactions. After describing key design criteria for merging photochromic and reactive units, different approaches for photoswitchable catalytic systems are discussed.[5]

2.4.1 General Design Considerations

In order to design photoswitchable systems that are able to control a ground-state, (i.e. thermal) chemical reaction, a suitable photochromic moiety[6] has to be incorporated into the system. The chromophore must be chosen in a manner that the structural differences between their two switching states are translated into different chemical reactivity. Therefore, one has to optimize intrinsic switching properties of the chromophore as well as the way it interacts with the active center(s).

The performance of a chromophore is best described by the efficiency and robustness of the light-induced forward and backward switching. The degree of possible photoconversion, i.e. the composition of the photostationary states (PSSs), is governed by the ratio of the absorption of both switching forms at the irradiation wavelength used multiplied by the ratio of the quantum yields of the forward and backward photochemical reactions. Ideally, only one form of the switch can be selectively addressed and undergoes the desired photochemical reaction with a high quantum yield. In addition to efficiency, the repeated addressability of the switch requires clean and highly reversible photochemistry. Depending on the chromophore used, either both switching forms are thermally stable and can only be interconverted by light (P-type chromophore, such as diarylethenes, Scheme 13, right) or one of the forms is meta-stable and reverts back thermally to the more stable form (T-type chromophore, such as azobenzenes, Scheme 13, left). While the first requires the use of two different irradiation wavelengths, to switch the system between its ON and OFF states, the latter is only ON or OFF when under constant irradiation.

In catalysis the ON state is associated with a higher reactivity as compared to the OFF state and reactivity difference between both states are used to remote-control a desired chemical process.

[b] Parts of the introduction have been published in R. Göstl, A. Senf, S. Hecht, *Chem. Soc. Rev.* **2014**, *43*, 1982–1996.

The chromophore that are used for these processes usually undergo significant geometrical and/or electronic changes (Scheme 13) that lead to reactivity difference between the switched states. Large geometrical changes are typically achieved via *trans* → *cis* isomerization reactions of azobenzenes, leading to a largely reduced distances between the phenyl termini in the bent, non-planar *cis*-configuration when compared to the extended, planar *trans*-configuration. Electronic changes can be induces by electrocyclic ring-closing/ring-opening reactions of 1,3,5-hexatriene systems. Irradiation of diarylethenes, spiropyranes/spirooxazines or fulgides result in substantially different electronic properties of the ring-closed isomer as compared to the ring-open form. It is important to maintain the switching behavior throughout the reaction and therefore the excitation of the photochromic moiety should be selective and local, without interfering quenching processes by energy or electron transfer.[7]

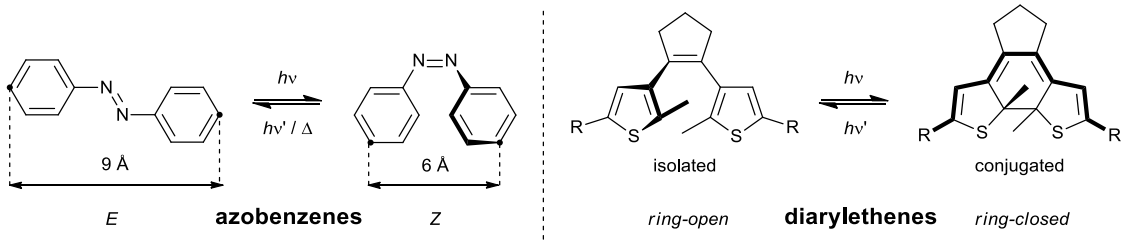

Scheme 13: Molecular structure changes upon either *trans* → *cis*-isomerization of azobenzene or 6π-electrocyclization of diarylethene photoswitches.

The chromophore can be incorporated either directly by a covalent connection to one of the components participating in the reaction, or indirectly by a non-covalent interaction with the same. Here the focus is on covalent connections since they offer the advantage that they operate independent of concentration as opposed to supramolecular approaches. In general, the coupling of a photochromic system to control another thermal reaction can be realized through various concepts depending on the geometrical or electronic alteration of the switch and the point of interactions. Such interactions at the active site can occur either at the level of the substrate, product or template, leading to stoichiometric processes with maximum overall quantum yields of unity ($\Phi \leq 1$), or at the level of the catalyst or effector, giving rise to an amplification of the light stimulus where one photon can trigger several chemical transformations.

Using catalytic processes has a large influence on the photoefficiency with which the reaction can take place. In order to achieve full conversion each photoresponsive molecule needs to be switched, which leads to problems when trying to address the photoresponsive groups *in-situ*. Most reactions take place at a reasonable rate only at concentrations in excess of the ones

typically employed in photochemistry by several orders of magnitude. This problem can be overcome to a certain extent by using a photoresponsive catalyst, which lowers the overall concentration of the absorbing photochrome in the reaction mixture. Furthermore with a photoresponsive catalyst it is possible to amplify the light stimulus in the system, since the photoreaction that is needed to isomerize the catalyst molecule triggers multiple chemical conversions (turnover).

Reaction control in catalysis can be divided into two different approaches, one is to control the activity of the catalyst and the other is to control the selectivity, as discussed below.

2.4.2 Activity Control

Almost all photoswitchable catalyst systems reported to date focus on modulating catalytic activity. For this a catalytically active molecule is functionalized with a photoswitchable entity. Ideally, the difference in catalytic activity between the two forms of the chromophore differs significantly enough, leading to an ON/OFF switching of the catalyst (Fig. 4). There are several strategies that can be employed to achieve control over the activity of a catalyst. Herein, the focus will be on the control of cooperative effects, steric shielding of the active site, and modulating the electronic properties of a catalyst, which are the more promising approaches. Additional approaches such as using photochromic effector molecules and activating or inhibiting the catalyst system are described in the literature.[11,142]

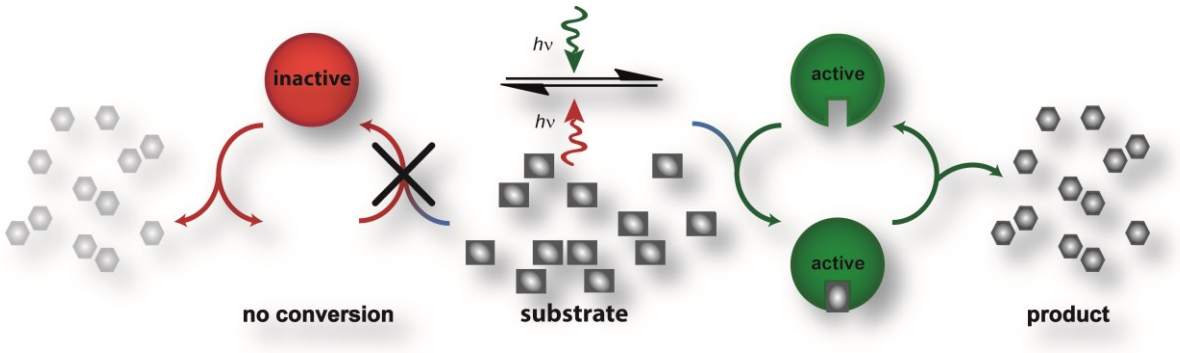

Fig. 4: Concept of photoswitching the activity of a catalyst: Photoswitching converts a catalyst from an inactive to an active form, which turns substrate into product, while the inactive form shows no conversion (turnover). Thereby, one switching event can lead to the formation of many product molecules (amplification).

Cooperative effects play an important role in biological and synthetic catalytic systems and have therefore also been exploited to photomodulate reactivity. The basic principle relies on a large geometrical change during the isomerization process that allows the variation of the distance between two catalytic active sites. Cacciapaglia *et al.* reported the first successful use of a photoswitchable cooperative effect in catalysis.[46] The *bis*-barium complex of an azobis(benzo-18-crown-6) ether **6** was used to catalyze a basic ethanolysis of tertiary anilides (Scheme 14). By reversible *trans* → *cis*-isomerization of the azobenzene spacer the catalytic activity could be controlled. The thermodynamically more stable *trans*-**6** has only a low catalytic activity. Photoswitching the azobenzene moiety into the *cis*-form changes the geometry of the *bis*-barium complex into a more favorable concave conformation in which the two barium centers are in close proximity to each other. In the catalytical active complex one barium center serves as binding site for a carboxylate anchoring group on the anilide substrate while the other barium center binds a nucleophilic ethoxide ion. The close proximity of these two pre-organized starting materials gives rise to the increased catalytic activity of the *cis*-isomer.

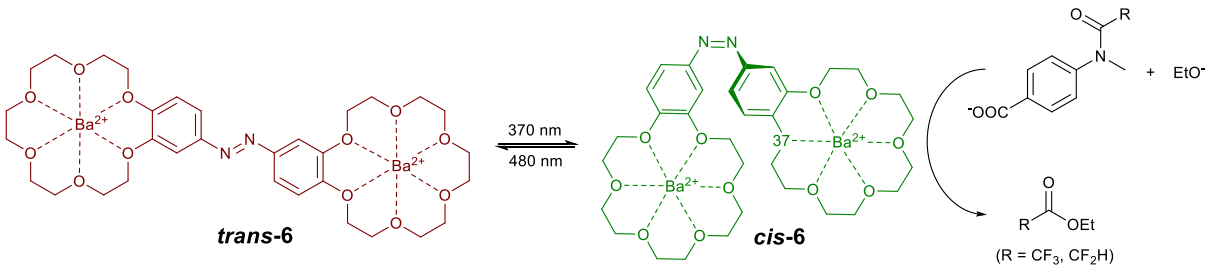

Scheme 14: In the photoswitchable cooperative catalyst 6, *trans* → *cis* photoisomerization brings both barium centers and hence the two coordinated starting materials into close proximity to catalyze the ethanolysis of tertiary anilides.[46]

Cooperative effects have also been used in a similar way to photoreversibly control the Morita-Baylis-Hillman reaction.[45] A bifunctional cooperative acid catalyst was functionalized by Imahori and coworkers with an azobenzene moiety to activate or deactivate the cooperative effect, which led to a reversible control of the reaction rate.

Steric effects can influence the activity as well as selectivity of a catalyst for a given reaction. To gain control over the activity of a catalyst using this concept, a photoswitch is needed that induces a large geometrical change to shield or deshield the substrate binding site of the catalyst. An approach where this concept was successfully used has been reported previously by our

group.[44,143] The lone pair of the *N*-alkylated piperidine base **7** can reversibly be shielded by *trans* → *cis* -isomerization of a rigidly connected azobenzene "wiper" (Scheme 15). It was shown through titration experiments that the piperidine base has a lower basicity in the resting state *trans*-**7**. Switching the azobenzene moiety into the *cis*-conformation exposes the piperidine electron lone-pair, which led to an increase in basicity. The different basicities were used to photocontrol the conversion of a base-catalyzed nitroaldol (Henry) reaction. Later a related catalyst was immobilized on various solid surfaces, such as silica gel or silicon wafers, to prevent the loss of spatial resolution due to diffusion of the catalyst in solution.[47]

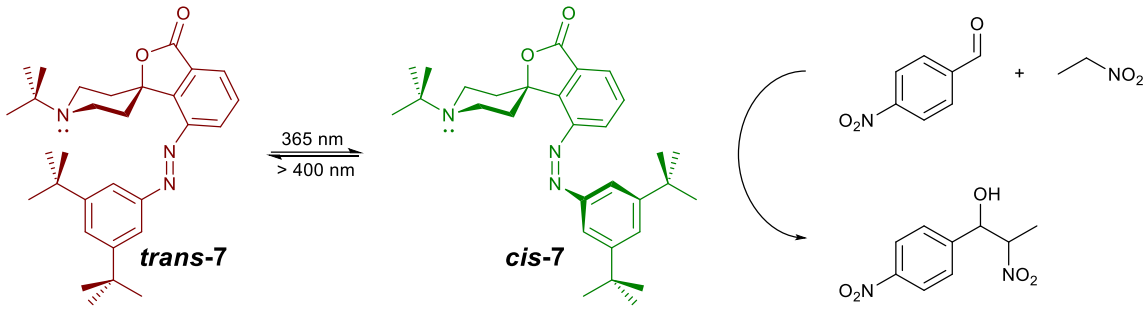

Scheme 15: *trans* → *cis*-photoisomerization of an azobenzene moiety controls the accessibility of a piperidine base, which can be used to catalyze a nitroaldol (Henry) reaction.[44,143]

Electronic effects can significantly influence the active site and hence electronic fine-tuning constitutes one of the main strategies in catalyst design. Therefore, it is no surprise that efforts were put into photomodulating the electronic properties of a catalyst. The basic concept is founded on breaking or forming a conjugated system between the active site and an electronically activating group. Recently, Bielawski and Neilson used this concept to control the activity of a catalyst.[144] An *N*-heterocyclic carbene (NHC) functionality was incorporated into the backbone of a dithienylethene (DTE) **8** (Scheme 16). The length of the conjugated π-system modulates the electronic properties of the NHC-functionality. In the presence of visible light and a base the NHC **8o** catalyzes transesterification and amidation reactions. Upon irradiation with UV-light to the ring-closed derivative **8c** the rate of a transesterification and an amidation reaction was significantly decreased. This process was reversibly switched several times between a slow and a fast reaction rate. On the basis of NMR-experiments with an isotopic label at the C2 "carbene" carbon, the authors could rationalize the observed activity differences by showing that the ring-open form **8o** exists as an imidazolium species while the ring-closed species **8c** forms the less active alcohol adduct.

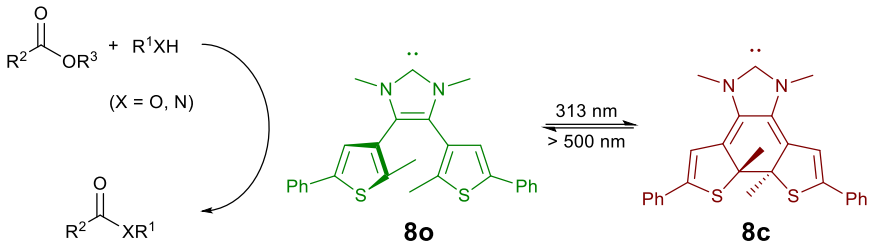

Scheme 16: Ring-open *N*-heterocyclic carbene (NHC) 8o catalyzes transesterification, amidation as well as ring-opening polymerization reactions, upon irradiation to its corresponding ring-closed isomer 8c exhibits significantly reduced catalytic activity is seen.[144,145]

This photomodulation of the nucleophilicity of an NHC center was further used to switch the activity of a Rh(I)-complex **9** (Scheme 17).[146] It was shown that the Rh-metal center functionalized with the photochromic NHC ligand **9o** catalyzes the hydroboration of various alkenes, such as styrene, with modest activity differences between the two different switched forms. In this case the rate-determining reductive elimination step was slowed by the lower donor capability of the NHC-ligand in its ring-closed form.

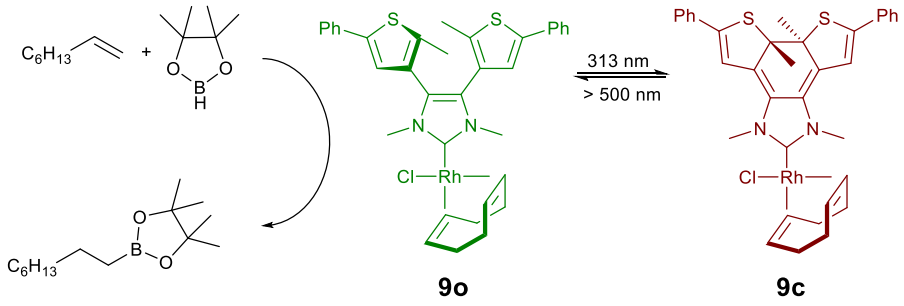

Scheme 17: Photoswitching of a dithienylethene-based *N*-heterocyclic carbene (NHC) ligand modulates the activity of the derived Rh(I)-complex in the hydroboration of styrene.[146]

Recently, Bielawski and coworkers were also able to show the first photoswitchable attenuation for the ring-opening polymerization (ROP) of δ-valerolactone as well as ε-caprolactone using their dithienylethene-based NHC **8** (see Scheme 11).[145]

2.4.3 Selectivity Control

The previous examples impressively show how much progress has been made in the field of photoinduced activity control of catalysts. Although efforts on activity control have thus far been the main focus of research in this field, approaches to photoswitch the selectivity of catalysts are equally important. For this a catalytically active entity is combined with a photoswitch that leads to a difference of chemo-, regio-, and stereo-selectivity between the two forms (Fig. 3). Until now efforts to reversibly switch the catalyst's chirality and thereby modulating its stereoselectivity have been limited.

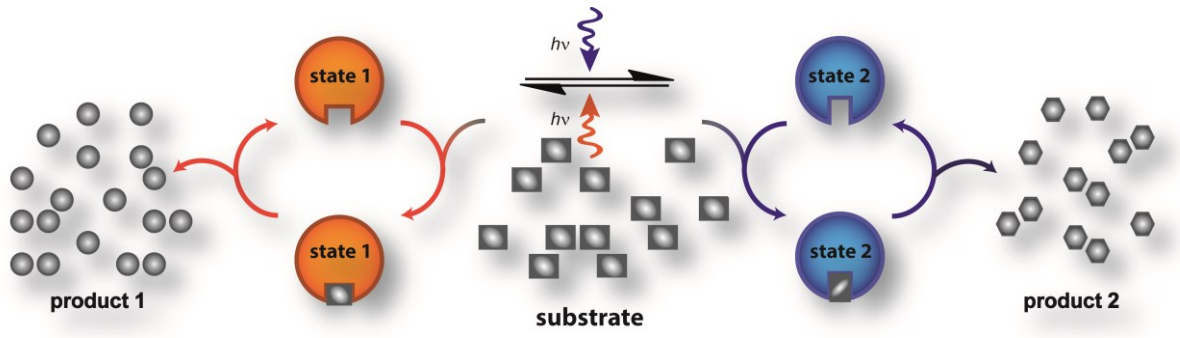

Fig. 5: Concept of photoswitching the selectivity of a catalyst: Photoswitching interconverts a catalyst between two forms exhibiting different selectivity in a given transformation. Again, one switching event can lead to the formation of many product molecules (amplification).

The first successful approach to photochemically switch the stereoselectivity of a catalyst was reported by Branda and coworkers.[147] Their dithienylethene-based chiral bis(oxazoline) ligand **10** is only able to chelate to the catalytical active copper center in its more flexible ring-open form (Scheme 18). This complexation generates a chiral environment around the copper center and thereby allows a cyclopropanation reaction to take place stereoselectively. Hence, in the open form **10o** an *ee* of 30-50% was observed whereas the closed form **10c**, where the rigidity of the ligand prevents chelation, only showed a very low *ee* of 5%. Irradiating the sample with visible light led to recovery of the original chiral information and gave an *ee* of 11-37%.

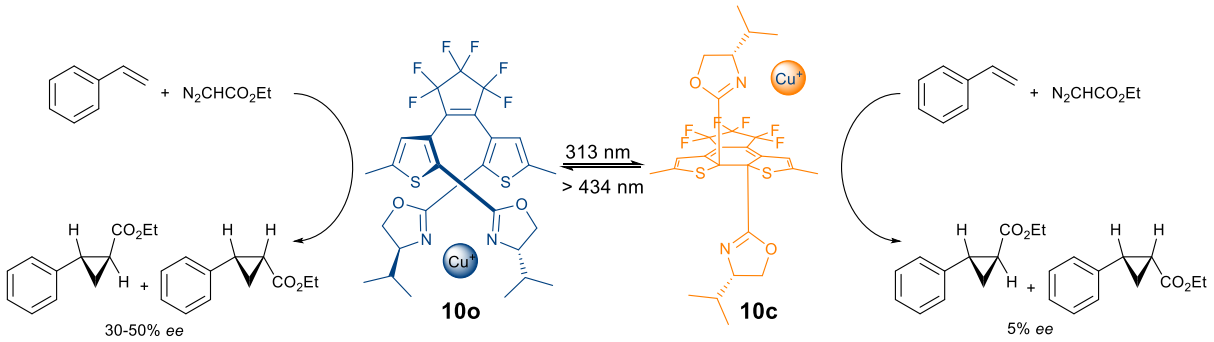

Scheme 18: Photoswitching of a dithienylethene-based bisoxazoline ligand leads to modulation of its chelation ability and hence chirality of the corresponding copper complexes, which display different degrees of stereoselectivity for the cyclopropanation of styrene.[147]

Feringa and Wang combined both of these concepts to photoswitch the activity and selectivity of a catalyst (Scheme 19).[148] Their rotatory molecular motor, that has four switching states, was transformed into a photoswitchable bifunctional organocatalyst by attaching a Brønsted base and a thiourea hydrogen-bonding donor group, which are known to cooperate in the catalysis of Michael additions, among other reactions. The thermodynamically stable (*P*,*P*)-*trans*-**11** isomer shows a negligible catalytic activity with no stereoselectivity (*e.r.*, S:R= 49:51) in the Michael addition. However, upon irradiation helix inversion takes places and the (*M*,*M*)-*cis*-**11** isomer is formed, which shows a higher activity in the Michael addition and forms the product in considerable enantiomeric excess (*e.r.*, S:R = 75:25). Heating the (*M*,*M*)-*cis*-**11** isomer to 70 °C triggers a thermal isomerization step that forms the (*P*,*P*)-*cis*-**11** isomer, which also catalyzes the Michael addition however yielding the opposite stereoisomer (*e.r.*, S:R = 23:77). Subsequent photochemical and thermal isomerization give rise to the original catalytically reactive (*P*,*P*)-*trans*-**11** isomer via (*M*,*M*)-*trans*-**11**.

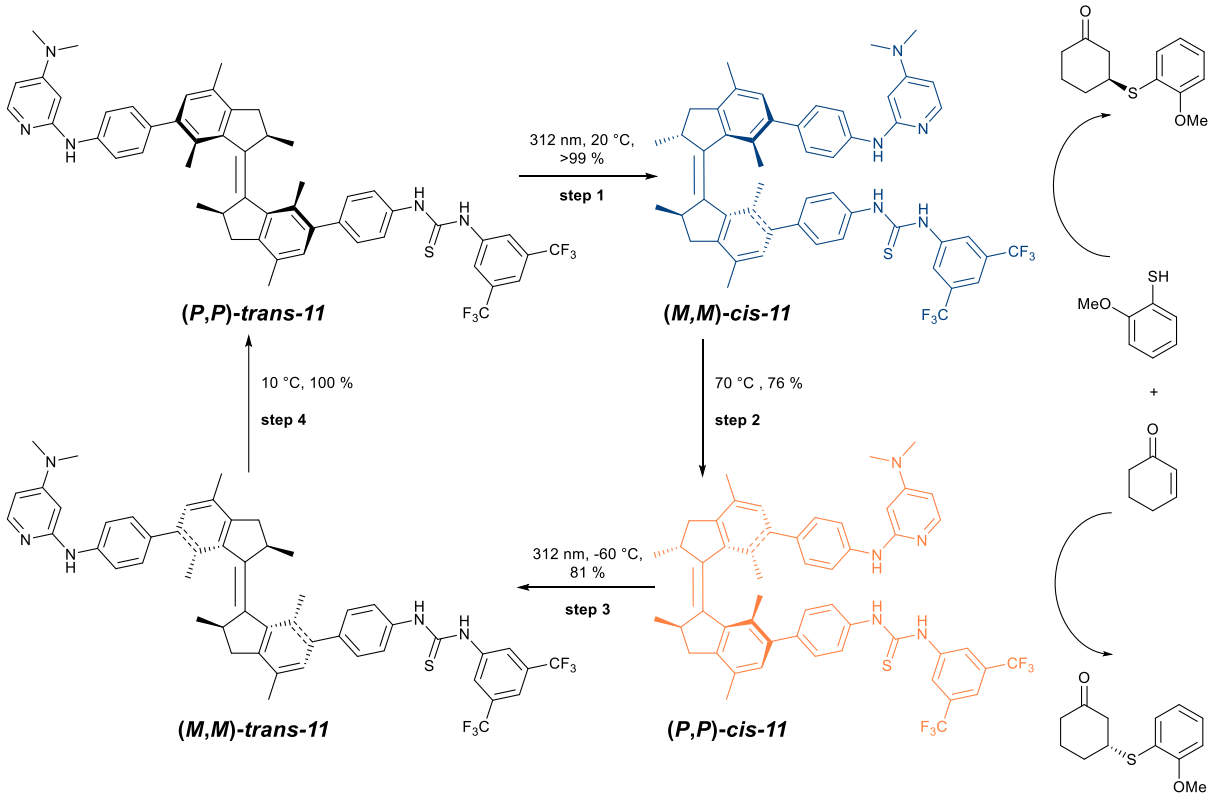

Scheme 19: Modulation of the relative orientation of a pyridine basic and a thiourea hydrogen-bonding site embedded in a molecular motor leads to a photoswitchable bifunctional organocatalyst, which allows for control over the activity and stereoselectivity of a Michael reaction.[31]

Recently the group of Feringa reported a photoresponsive phosphine ligand that can be used for Pd-catalyzed reactions.[149] They used a combination of the light driven molecular motor bridging two phophine moieties (Scheme 20), which allowed for the switching between several stereoisomers with distinct ligand properties. The chiral helicity that is switched within the molecule during the photochemical processes can be used to control the enantiomeric outcome of Pd-catalyzed desymmetrization reactions. This shows that chirality can be controlled in Pd-catalyzed reaction. However the drawback of this system is that the complex cannot be switched *in situ*. Because only the ligands are photoresponsive, it has to be switched to the desired state before the complex can be formed.

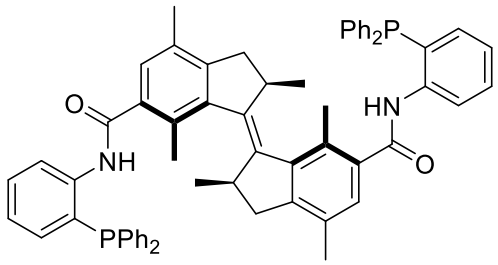

Scheme 20: Chiral photoresponsive phosphine ligand reported by Feringa.

3. Results and Discussion

3.1. Photoswitchable FI and salen complexes

3.1.1 Challenges in combining photoswitches with organometallic complexes

Organometallic chemistry has had an unprecedented impact on modern synthetic chemistry starting with the discovery of the Grignard reaction[150] and other organometallic species such as lithium[151] and cuprate[152] reagents which offered new synthetic tools to the organic chemist. Further development in organometallic catalysis with the discovery of asymmetric hydrogenation,[153-155] alkene metathesis[156-158] and cross-coupling reactions[159-161] added even more possibilities to create new molecules. With so many possible applications it is not surprising that efforts were made to control organometallic reactivity either by intrinsic switching[162] or by external stimuli.[20] To date, there is but one example of a photoswitch-functionalized ground-state organometallic catalyst.[144] The reason for this is that there are many challenges that need to be faced to introduce a photoswitchable functionality into an organometallic molecule. The first challenge lies in the fact that metal-complexes are chromophores which can be excited by light, a phenomenon that has been applied in photoredox catalysis.[163] Therefore, to overcome the excitation of the metal center a molecular design has to be found that guarantees a separate excitation of the photoswitch without interference by the metal center.

Equally important is possible electron transfer from the photoswitch to the metal-center.[164] It has been shown that the organometallic-complex and its oxidation state greatly influence the switching capability of a neighboring photoswitch.[165] Therefore the selection of the catalytically active metal has to be compatible with the chosen switch, and vice versa.

Since these challenges need to be met in all switching states, a reliable prediction on the control of the reaction is difficult to make, and a lot of the research is still based on trial and error.

3.1.2 Azobenzene functionalized FI and Salen complexes

Gaining control over the selectivity of a reaction is an interesting challenge especially in the field of polymerization reactions, since it would allow new possibilities to create polymeric microstructures that are not accessible by available methods. For this purpose a switchable system based on salen-complexes was envisioned. Founded on the mechanistic considerations highlighted in chapter 2.3 a flexible catalyst design was proposed that allowed a versatile introduction of a photoswitchable group. Choosing salen catalyst as a model system would further allow to modify the system easily by changing the metal center or even by using a different Schiffs base moiety to form a FI catalyst. FI catalysts are important catalysts for poly(propylene) polymerizations that have gained considerable attention in industrial research for their easily adaptable synthetic route.[108,121]

For this purpose a photoswitchable azobenzene group was introduced into a catalytic system to sterically shield or deshield the catalytic active site (Fig. 6).

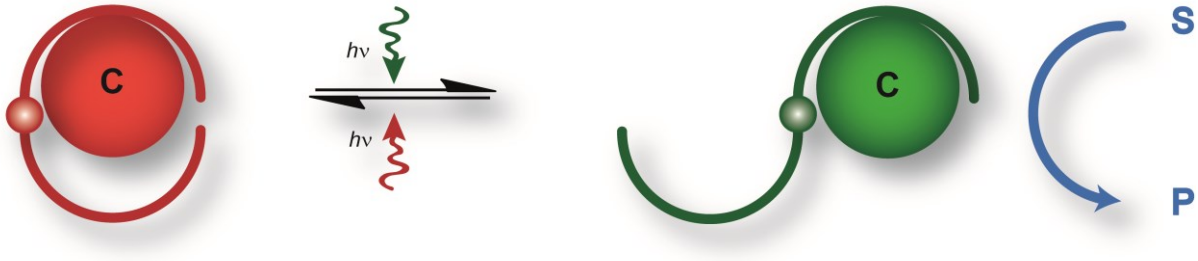

Fig. 6: Schematic representation of a steric shielding/deshielding of a catalytic active site.

Since there is only little known about the photochemistry of salen-complexes, different catalytically active metals were screened for their stability when irradiated with light, before any photoswitching studies were done. The screening also included metals that were not active in the polymerization of lactide but for other types of polymerization reactions. For this purpose an unfunctionalized salen ligand was synthesized and then complexed with different metal reagents ($AlMe_3$, $TiCl_4$, $Co(OAc)_2{\cdot}4H_2O$, $CrCl_3$, $Zn(OAc)_2{\cdot}2H_2O$, $Ni(OAc)_2{\cdot}4H_2O$, $Pd(OAc)_2$) to give the complexes shown in Scheme 21.

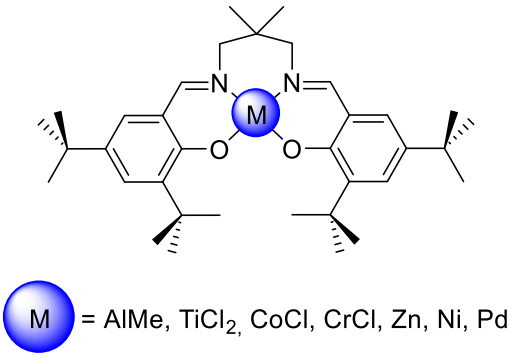

Scheme 21: Different salen-complexes that were tested for their stability during irradiation with 365 nm light.

Those complexes were then screened for their stability during irradiation with light of a wavelength of 365 nm (Fig. 7), a commonly used wavelength for azobenzenes. The Al-, Ti-, Co and Cr-salen complexes were stable while the Zn-, Ni- and Pd-salen complexes were observed to react during irradiation. There were small differences in the stability, as the Al- and Ti-salen showed no visible degradation in the absorption spectrum, whereas small changes in the absorption spectrum of Co- and Cr-salen were visible, but well within an acceptable range, so that the complex could be irradiated during the timeframe of a typical polymerization. Based on these results all of the following studies made use Al-, Ti-, Co and Cr- metal centers, due to their favourable photostability properties.

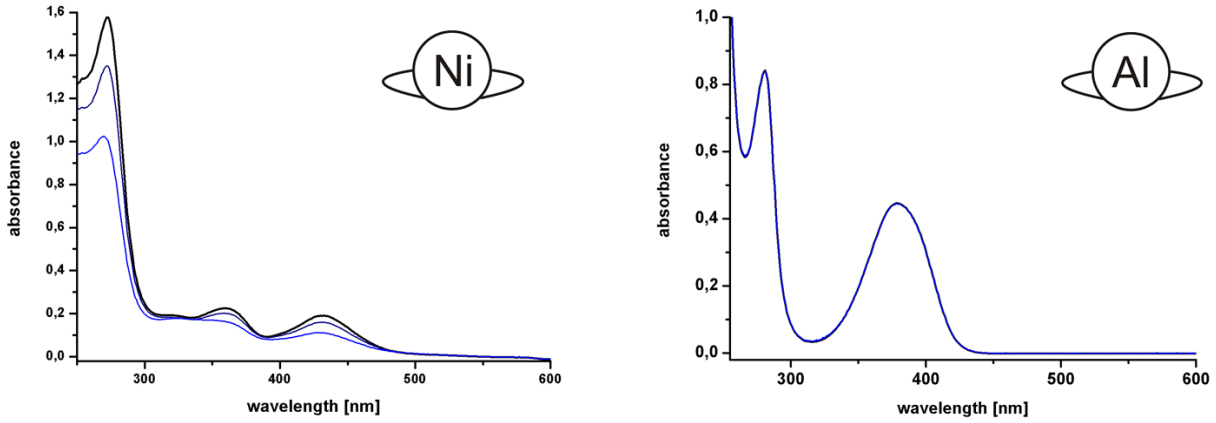

Fig. 7: Examples of the irradiation experiment (λ = 365 nm) with different salen-complexes. Left) Ni-salen had the lowest stability and showed a fast degradation after 10 min of irradiation. Right) Al-salen had the best stability and showed no degradation after 2 h of irradiation.

To gain control of stereoselectivity the steric influence of the R_2 group of the salen (Scheme 9 on page 14) ligand can be exploited. For this purpose a sterically demanding azobenzene was introduced in the *ortho*-position of the hydroxyl-group of a Schiff-base, which would allow to reversibly change the steric demand around the catalytically active center.

To study this effect in detail different *ortho*-azobenzene substituted salicylaldehydes were synthesized.

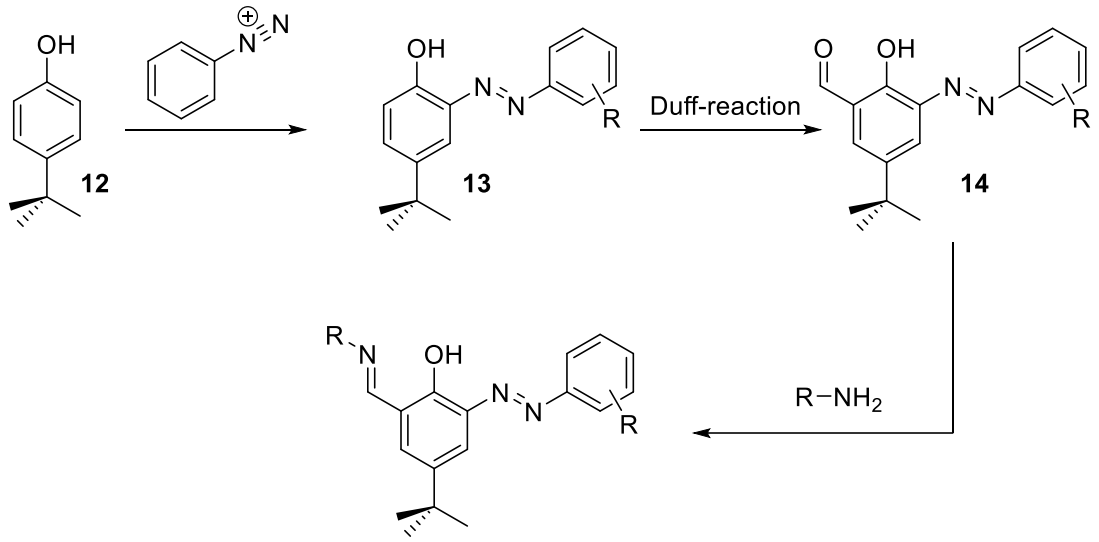

Scheme 22: Synthetic pathway to *ortho*-substituted azobenzene Schiff-base moieties.

A direct azobenzene-coupling with salicylaldehyde did not yield the desired product, so a synthetic route via the *ortho*-hydroxyazobenzene was chosen. The first step of the synthetic route was the diazonium-coupling of an aniline derivative with the phenol derivative **12** to yield the *ortho*-hydroxyazobenzene **13**. In the next step several different formylation reactions were tested but did not yield the desired product. Only Duff-conditions afforded the desired azobenzene-functionalized salicylaldehyde **14**. This salicylaldehyde was then further reacted with different amine- and aniline-derivatives to give a small library of azobenzene-functionalized Schiff-bases **15**-**20**.

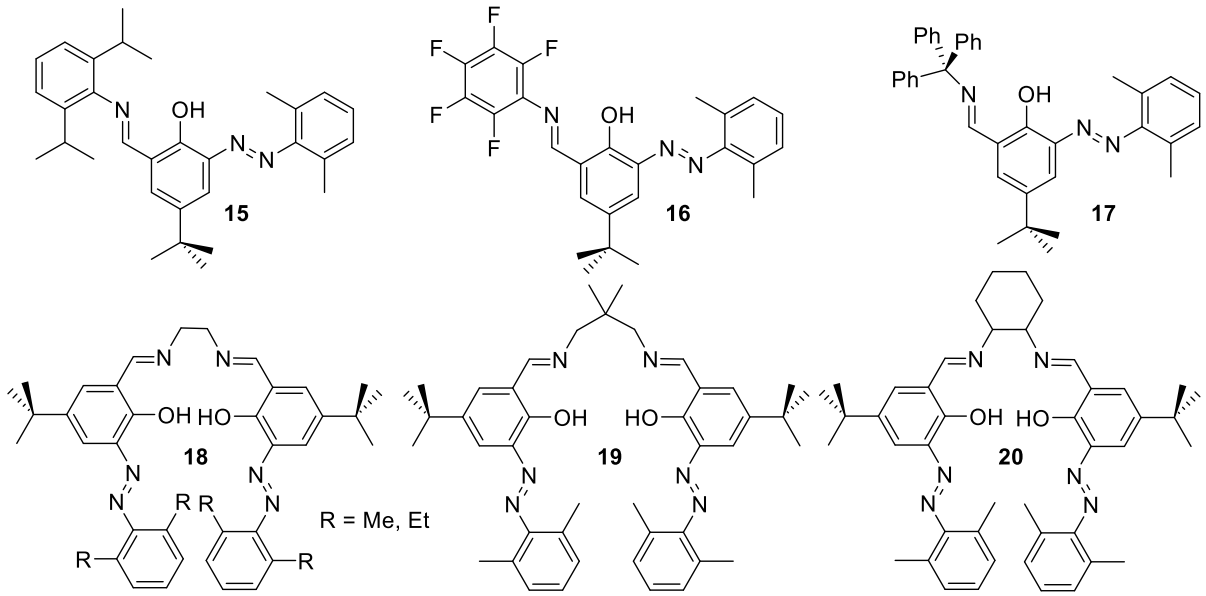

Scheme 23: Library of synthesized *ortho*-substituted azobenzene Schiff-bases 15-20.

The first complex to be synthesized was the titanium complex **21**. It was obtained by adding Titanium(IV) isopropoxide to a solution of ligand **19** in toluene at low temperature.

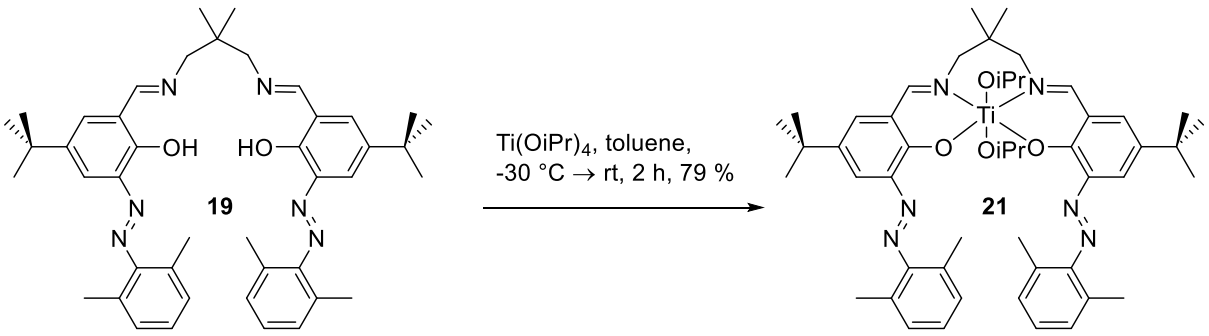

Scheme 24: Synthesis of azobenzene-functionalized titanium(IV) salen complex 21.

The ^{1}H-NMR-spectrum of complex **21** is seen in Fig. 8. The spectrum shows two sets of signals that are due to the coordination sphere, as the complex is formed with the two isopropyl-groups positioned *cis* to each other. This conformation leads to the possibility of two diastereomeric pairs, which are observed via NMR.

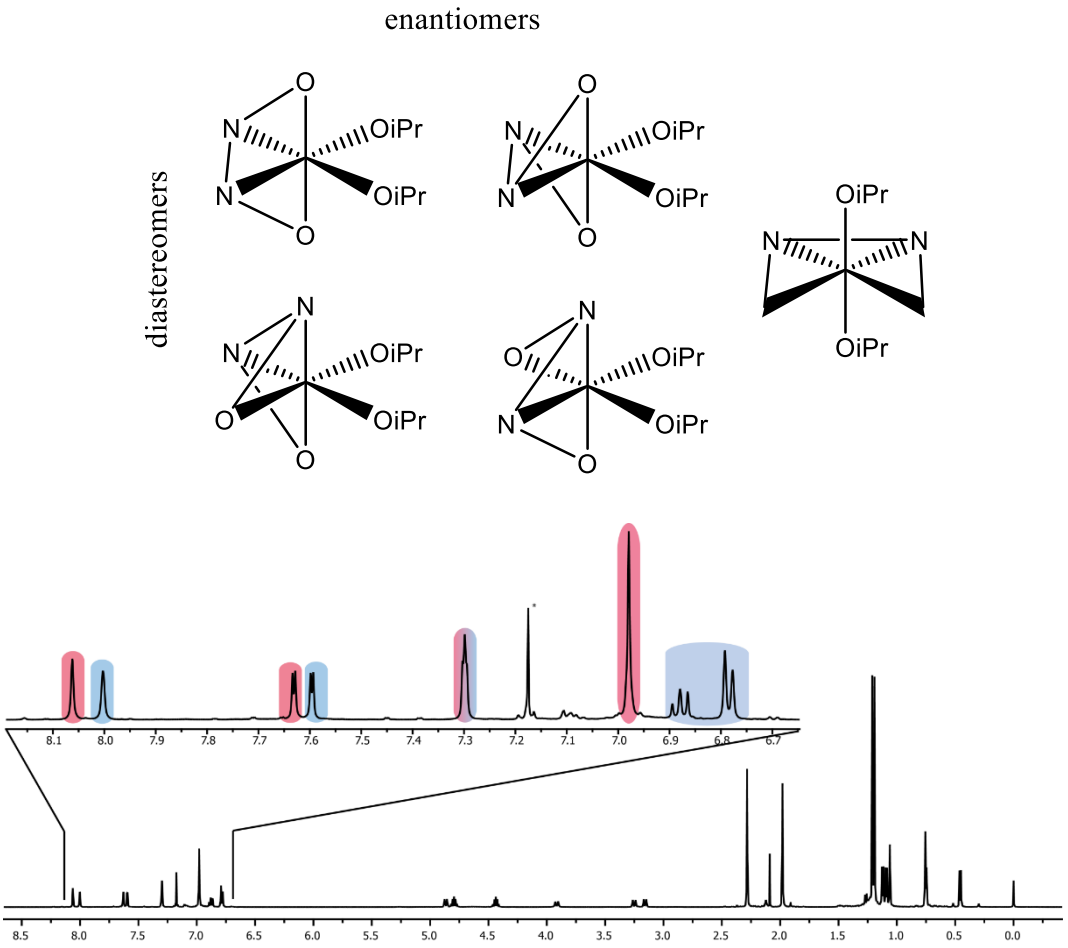

Fig. 8: Top) pairs of diastereomers that can be formed Bottom) ^{1}H-NMR spectrum of complex 21 in CD_2Cl_2. Highlighted are the signals that could be assigned to a diastereomer.

The photochemistry of complex **21** is not straightforward. When a 10^{-5} M solution of the complex in toluene is irradiated with light at a wavelength of 313 nm, at first an irreversible process takes place. A second process then sets in (Fig. 9 (left) blue) and this photochemical process is reversible. The solution can either be irradiated with light at a wavelength of 365 nm or a thermal process can take place that leads to *cis* → *trans*-isomerization of the azobenzene (after the irreversible process). This azobenzene switching process was repeated several times without noticeable fatigue.

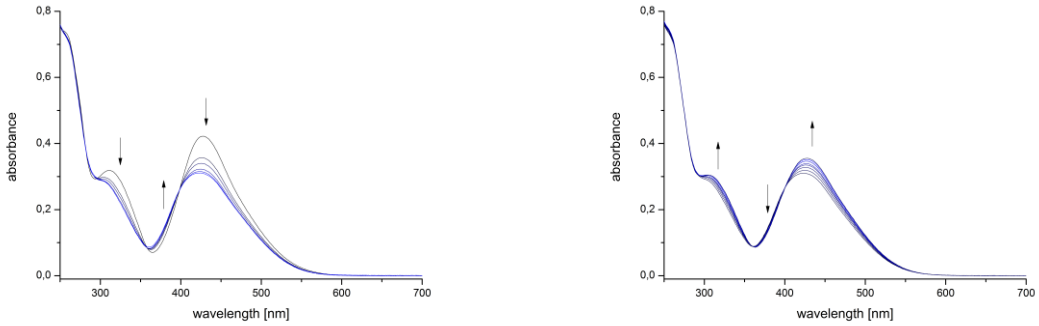

Fig. 9: Photochemical analysis of titanium-complex 21 in toluene (c ≈10^{-5} M). Left) Irradiation with light (λ = 313 nm) blue lines reversible unimolecular photochemical process. (timeframe 5 min) Right) Thermal *cis* → *trans*-isomerization at 25°C (timeframe: 5 h).

A characterization of the photochemical process with intermediate and final product could not be obtained, due to the air-sensitive nature of the complex. Since the complex had to be handled in the glovebox an extinction coefficient could also not be obtained. To gain insights into the first photochemical process, the spectrum was compared with the spectrum of the ligand (Fig. 10). The ligand spectrum shows a total of four bands while the complex and the intermediate only have three bands. This rules out the possibility that the metal center dissociates from the the chelating ligand. Laser flash photolysis studies made with salen complexes that included aluminum(III),[166,167] nickel (II),[168] manganese (III)[169,170] and chromium (III)[170] centers suggest that the non-chelating ligands are dissociating when the LMCT band is excited. This most likely also happens with the azobenzene-functionalized titanium(IV) salen complex and photodissociation of ispropoxide is likely taking place. Since the binding energy of the isopropoxide ligand to the metal-center is similar as compared to the polymer chain binding site, it is very likely that the polymer chain will also be released during irradiation. This would make controlling the polymerization impossible. Due to this intrinsic problem of the molecular design this approach was not studied further.

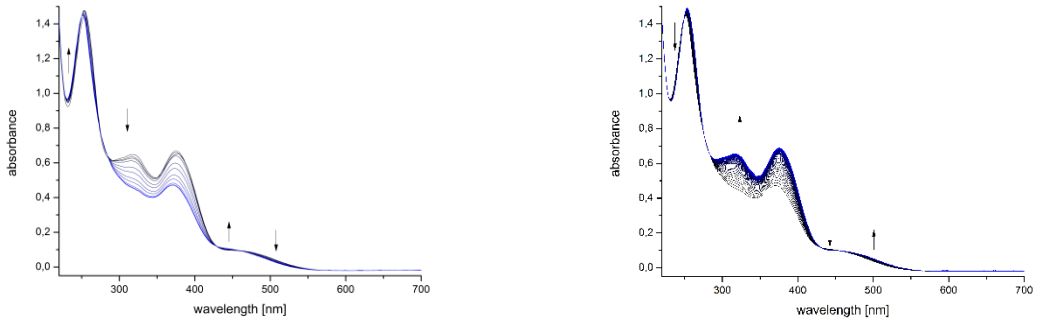

Fig. 10: Photochemical analysis of ligand 19 in ACN. Left) Irradiation with light (λ = 313 nm). Right) Thermal *cis* → *trans*-isomerization at 25°C (timeframe 8 h)

3.1.3 Photoswitchable binuclear Co-Salen complex

In 2005[171] Coates and co-workers reported on a cobalt salphen catalyst **22** that is highly active and selective in the ROP of racemic propylene oxide, as the formed polymer was highly isotactic. This very unusual finding for an achiral catalyst led to further study on the stereoselectivity of the complex. X-ray analysis of single crystals **23**, which is also isospecific, revealed the presence of chiral clefts that are postulated to be the reason for the stereoselectivity in a solid-state mechanism.[172]

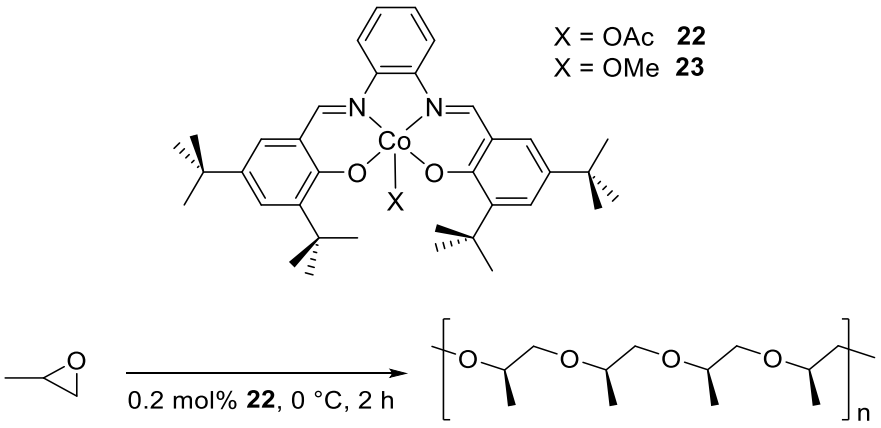

Scheme 25: Cobalt(III)-salphen complex that is stereoselective in PPO reported by the workgroup of Coates and the polymerization condition used.

In the following years the system was optimized and it was found that biaryl-linked binuclear cobalt salen catalysts mimic the chiral cleft that yields isospecific polymerizations of propylene oxide.[131] These systems were then experimentally and theoretically investigated[173] to gain insights into the influence of the Co-Co distance and the dihedral angle. For the system to efficiently catalyze the polymerization the two metal-centers have to be 4 -7 Å apart from each other. The dihedral angle on the other hand does not play a crucial role, as theoretical studies showed that it could be between 60° and 80°.

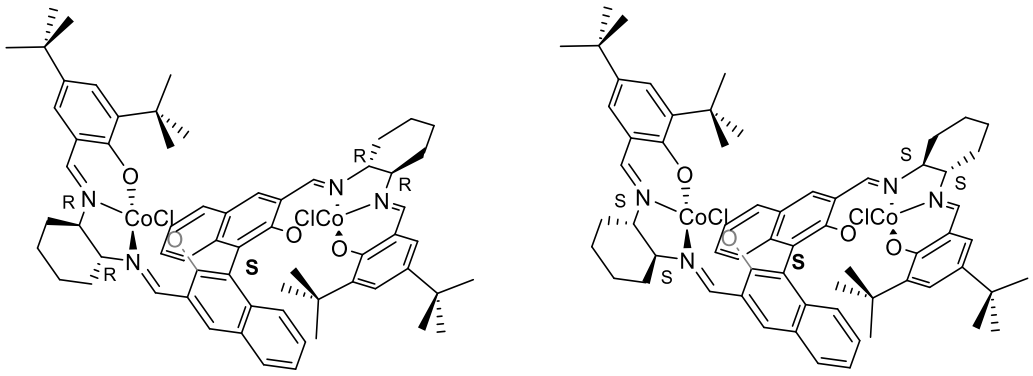

Scheme 26: Improved Co(III)-complex reported by Coates. A biaryl linker was introduced between two salen moieties to induce chirality into the molecule.

Based on these findings a photoswitchable catalyst was envisioned where the cooperative effect of the two metal centers can either be switched "ON" or "OFF". This can be realized by incorporating a photoswitch that undergoes a large geometrical change in its isomerization reaction, conceptually shown in Fig. 11. In the inactive state the two metal centers are too far away from each other so that they cannot interact in a cooperative fashion. Applying a light stimulus will trigger an isomerization reaction that leads to a large geometrical change, which will bring the two metal centers in close proximity to each other, so that they can interact with each other and catalyze a polymerization reaction. To turn the catalyst "OFF" again a light stimulus of a different wavelength is applied which switches the catalyst back into its initial inactive form. Ideally, this process is reversible and on a timescale that is faster than the polymerization.

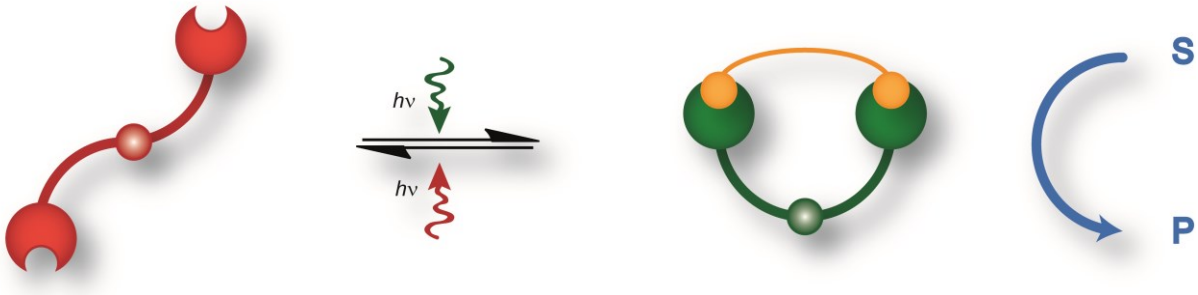

Fig. 11: Schematic representation of the concept of photoswitchable cooperative effects in transition metal catalysis. The inactive form (red) can be transferred with light into an active form (green), where both metal centers can interact with each other and therefore catalyze a reaction. The switching process is ideally reversible.

The simplest molecule that combines two metal-moieties with a photoswitch is shown in Scheme 27 where two salen-moieties are incorporated onto an azobenzene. MM2-calculation

for the *trans* as well as the *cis* state revealed that this is an ideal candidate for photoswitchable cooperative control. The distance between the two metal centers in the *trans*-**24** is approximately 12 Å, which is well above the distance where the two metal-centers can interact in a cooperative manner. In the *cis*-isomer, the two metal centers are only 7 Å apart from each other which is within the distance where cooperative effects can take place. Furthermore, the dihedral angle will also help a cooperative interaction, as *trans*-**24** is planar and has therefore an orientation that is not favorable for an interaction.

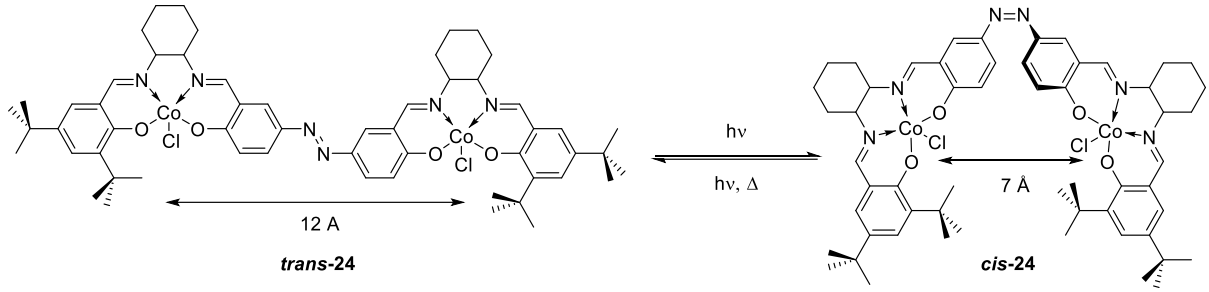

Scheme 27: Conformational change of the azo-functionalized dinuclear cobalt salphen complex 24 with its switching states and the calculated distances between the metal centers in both forms.[c]

The important precursor for the dinuclear complex **24** is the azobenzene-functionalized disalicylaldehyde **30** shown in Scheme 28. The synthesis is not straightforward, since normal formylating protocols of the easily accessible dihydroxyazobenzene were not providing adequate yields. Other approaches to directly couple the salicylaldehyde **25** either oxidatively or reductively to the corresponding azobenzene failed due to the lack of compatibility of the salicyl-functionality with the reaction conditions. The same is true for Pd-catalyzed coupling reaction to form the desired azobenzene. Therefore, the salicyl-functionality was protected. In the first step the aldehyde was protected as an acetal **26** and in a subsequent step the alcohol-functionality was masked using a TBS-ether **27**. The fully protected nitro compound was then reduced using H_2 and Pd-C to the corresponding aniline-derivative **28**. An oxidative coupling using copper(I) bromide led to the formation of the fully protected azobenzene **29**. The protecting groups were removed in one step using iodine in acetone, which yielded the desired disalicylaldehyde-azobenzene **30** in good yields.

[c] All synthesis were performed using *rac-trans*-cyclohexyldiamine

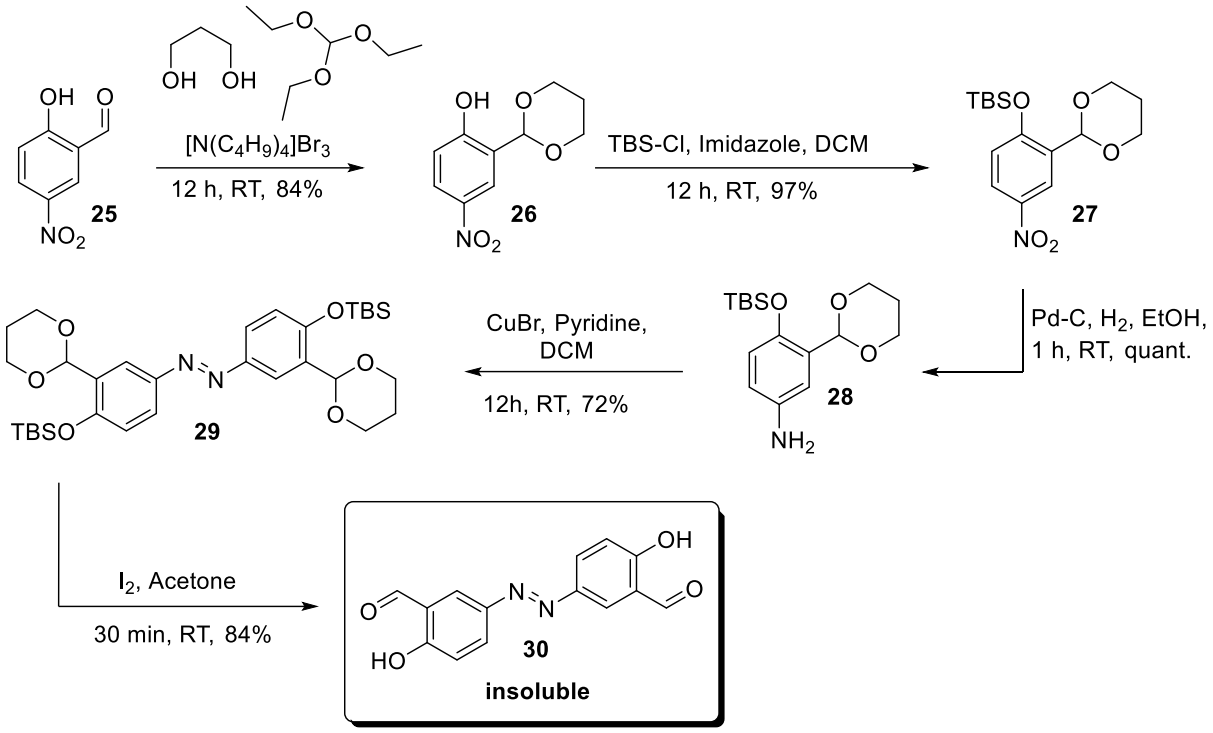

Scheme 28: Synthetic route to disalicyl azobenzene 30 that is an important intermediate in the synthetic route towards complex 24.

The solubility of **30**, however was too low to be used directly in an imine-reaction. Different approaches were explored to overcome this problem, such as keeping the TBS-protecting group intact and allowing for an *in-situ* deprotection, so that one imine is formed while the molecule is not fully deprotected. Several protocols were tested for the approach, but they all led to a complete deprotection.

For the last approaches different reaction condition were tested using the nitro-salicylaldehyde **27**. For the introduction of an asymmetrical salen-moiety the ammonium-protected half-salen can be used.[174] Usually, the ammonium is deprotonated using a light base like triethylamine to restore the nucleophilicity of the amine. Here, different additives were tested under which the deprotection as well as the imine formation can occur. One test reaction used no additives since the ammonium-ion with its light acidity could deprotect the salicylaldehyde. Other additives were acetic acid or triethylamine. All of these reactions showed no conversion at room temperature after five days. Increasing the temperature to 80 °C however showed a deprotection under the acid catalyzed conditions and a product formation using triethylamine after two days.

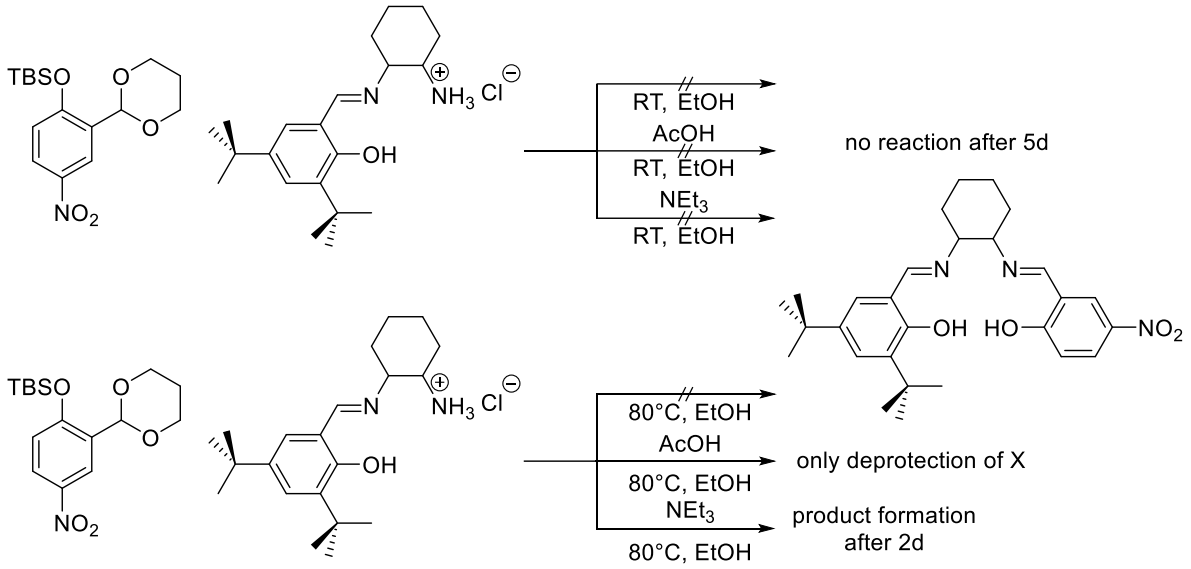

Scheme 29: Different synthetic strategies towards unsymmetrical salphen ligands.

Using the same conditions in the reaction with the protected azobenzene **29** did not yield the desired product. A yellow precipitate formed, that was confirmed to be the deprotected azobenzene, leading to the conclusion that the salicyl-moieties are fully deprotected before the imine-formation can take place.

To overcome the issue of the low solubility a new molecular design was envisioned. The low solubility of **30** results very likely from the flat geometry which allows for efficient stacking of the molecules. To prevent this stacking another phenyl-ring was introduced into the design and MM2-calculations were performed to ensure an optimal geometry of the complex. Different substitution patterns were calculated and the best fit showed complex **31** where the salicyl-moiety was in a *meta*-position to the azobenzene (Scheme 30). This substitution pattern predicts a Co-Co-distance of 12 Å in the *trans*-isomer and only 6 Å in the ideal *cis*-isomer, so the distances remain well within the optimal range.

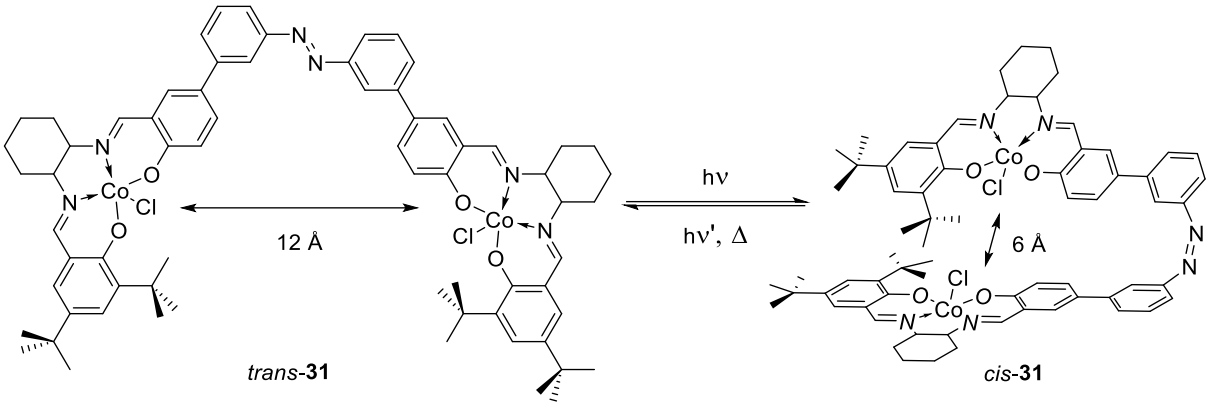

Scheme 30: Second generation of the azofunctionalized dinuclear cobalt salphen complex 31 in its two isomeric forms.

For the ligand synthesis the salicyl-azobenzene core **34** needs to be synthesized. For this the pinacolboron-functionalized salicylaldehyde was synthesized from the corresponding bromine derivative via Suzuki conditions. The dibromoazobenzene **33** was coupled oxidatively using PIDA, and then subsequently used in a Suzuki-coupling with **32** to form the disalicylazobenzene **34**. For the unsymmetrical salen-moiety the ammonium protected half-salen **35** was reacted with **34** to form the azobenzene-functionalized ligand **36**. The yield for this step is low due to a challenging purification. Recrystallization attempts did not yield the pure product. NMR studies showed that the impurities contained an aldehyde functionality. To successfully remove the impurity a preparative GPC had to be used, leading to a large loss in yield.

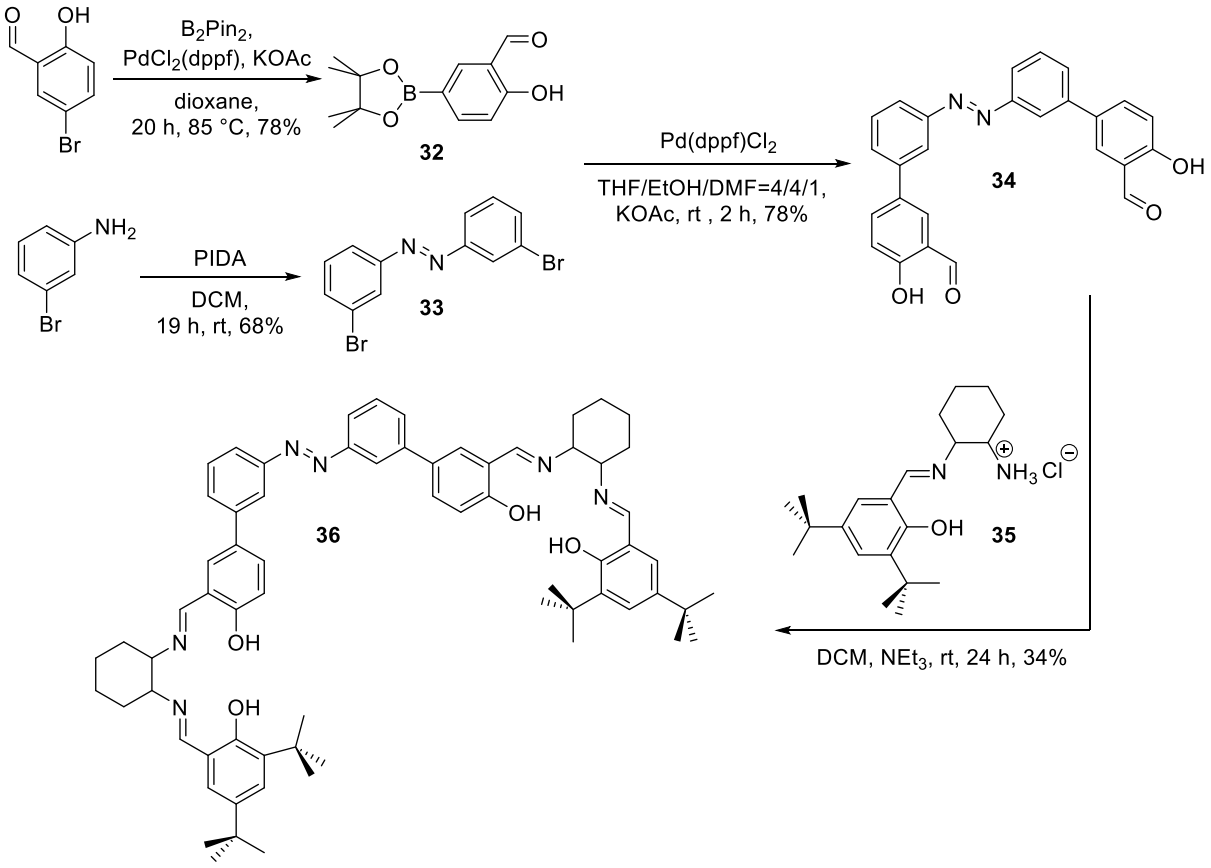

Scheme 31: Synthetic route to the azofunctionalized salphen ligand 36.

The ligand **36** was characterized using NMR-spectroscopy and mass spectrometry. The ^{1}H-NMR spectrum (Fig. 12) shows the characteristic broad peaks for the two hydroxyl-protons around 13.5 ppm.

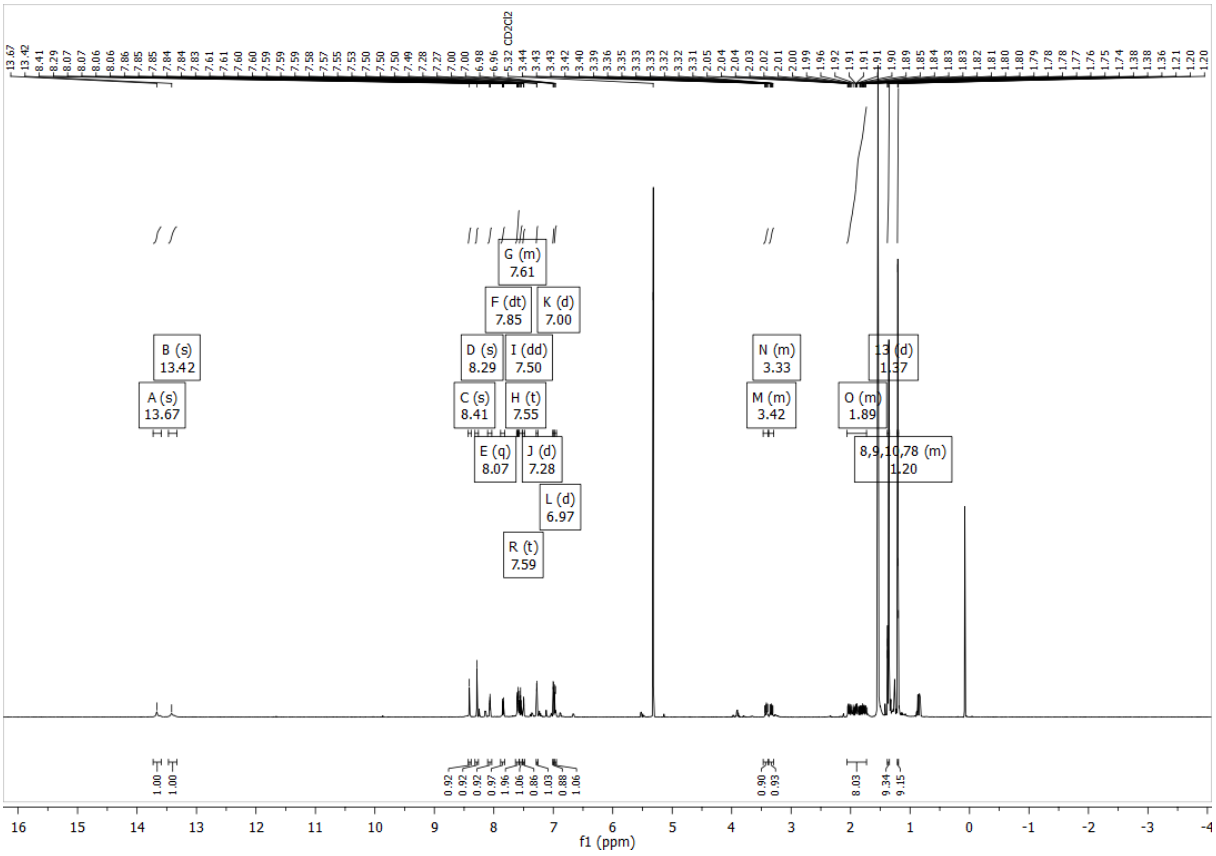

Fig. 12: ^{1}H-NMR (500MHz) spectrum of ligand 36 in CD_2Cl_2.

The complex was then formed using cobalt(II) acetate to form the catalytically inactive Co(II)-complex. This is then subsequently oxidized using tosylate in air to form the tosylated Co(III)-complex. An anion exchange using sodium chloride gave the desired complex **31**.

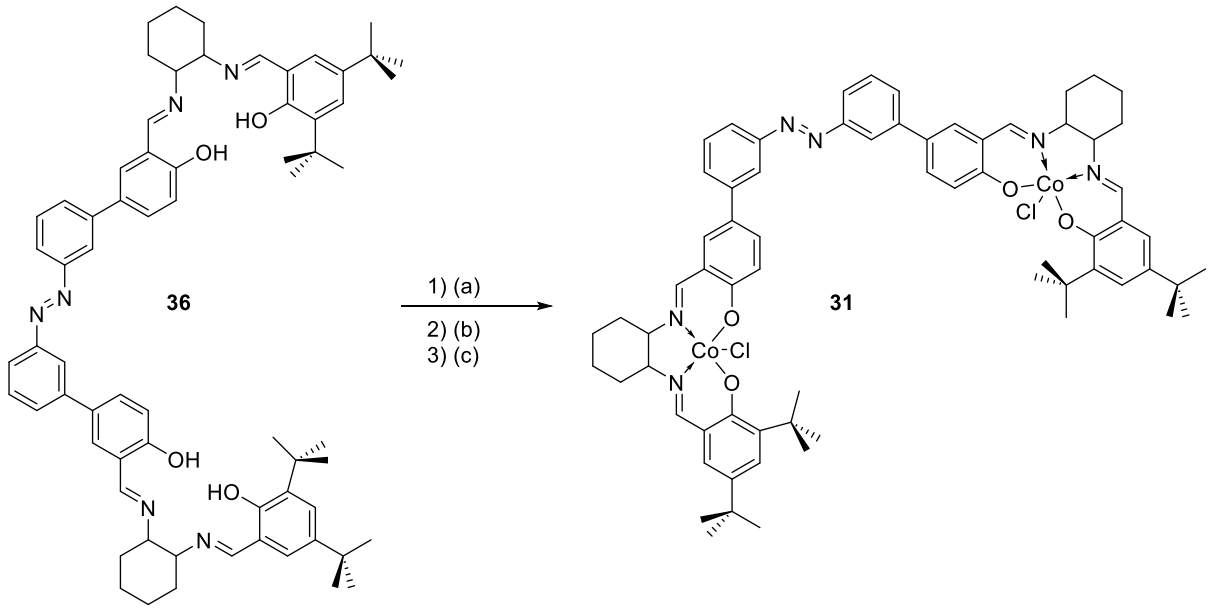

Scheme 32: Synthesis of complex 31. a) $Co(OAc)_2$, 1 h, 70 °C then 1 h, 80 °C, EtOH/CH_2Cl_2, 55% b) TsOH, 72 h, rt, CH_2Cl_2 c) NaCl(aq), CH_2Cl_2, 51% (two steps).

The photochemical investigation of the ligand **36** showed expected azobenzene behavior. Irradiation of a 10^{-5} M solution in acetonitrile using 313 nm light shows a clean photochemical process yielding a photostationary state (PSS) with a *cis*-content of 76% determined using the Fischer method.[175] The *cis* → *trans* isomerization can either be initiated thermally or using light of a wavelength of 435 nm which yields a PSS of 90% *trans*-content. Irradiation of complex **31** showed changes in the absorption spectrum, but they were small[d] and not photochemically reversible. The complex had a thermal back-reaction (~ 3h until completion) but it was too slow to be used as an effective triggered in the polymerization of propylene oxide that is usually run at 0 °C for these type of complexes. The low PSS for the isomerization is attributed to electron-transfer reaction which takes place from the azobenzene moiety to the metal center. The non-existing photochemical back-reaction is probably caused by an overlap of the n → π* band of the *cis*-azobenzene with the LMCT-band of the metal center, which made an effective switching process impossible.

[d] A PSS using the Fischer method could not be obtained. Measurements at three wavelengths led to different results. Since the absorption change occurs mostly on the shoulder of a band, it is assumed that the absorption of the underlying band interferes with the measurement.

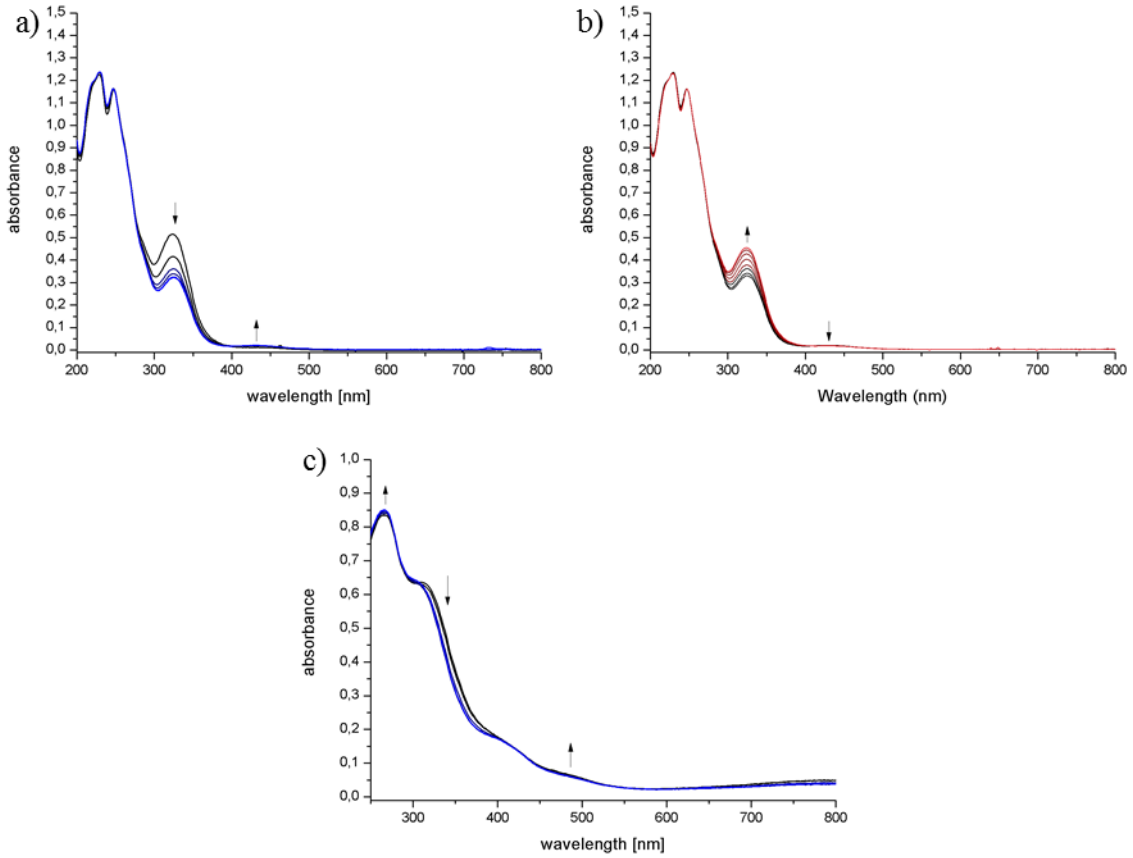

Fig. 13: Photochemical analysis of ligand 36 in ACN (M = 2.08 x 10^{-5}) and of complex 31 in DCM (M ~ 10^{-5}). a) *trans* → *cis*- isomerization of 36 with λ = 313 nm b) *cis* → *trans*- isomerization of 36 with λ = 435 nm c) irradiation of 31 with λ = 313 nm for 20 min.

3.1.4 Photoswitchable binuclear Cr-Salphen complexes

To overcome the poor switching performance in complex **31** different approaches were explored. First a methyl-group was introduced in the *para*-position to the azobenzene moiety to introduce a twist between the two phenyl rings (Scheme 33), which should reduce interactions between the metal-center and the azobenzene. To this end azobenzene **37** was synthesized and then used in an analogous Suzuki cross-coupling to afford disalicylaldehyde **38**. This was then used in an imine-condensation with **35** to form the desired ligand **39**. The crude ^{1}H-NMR showed the formation of the ligand with two different imine-signals. But the ligand could not be isolated in a pure form. Neither recrystallization, column chromatography nor GPC purification led to a ligand that was sufficiently clean to perform the complexation reaction. Complex formations with the crude ligand led to reaction mixtures that did not allow for an isolation of the complex.

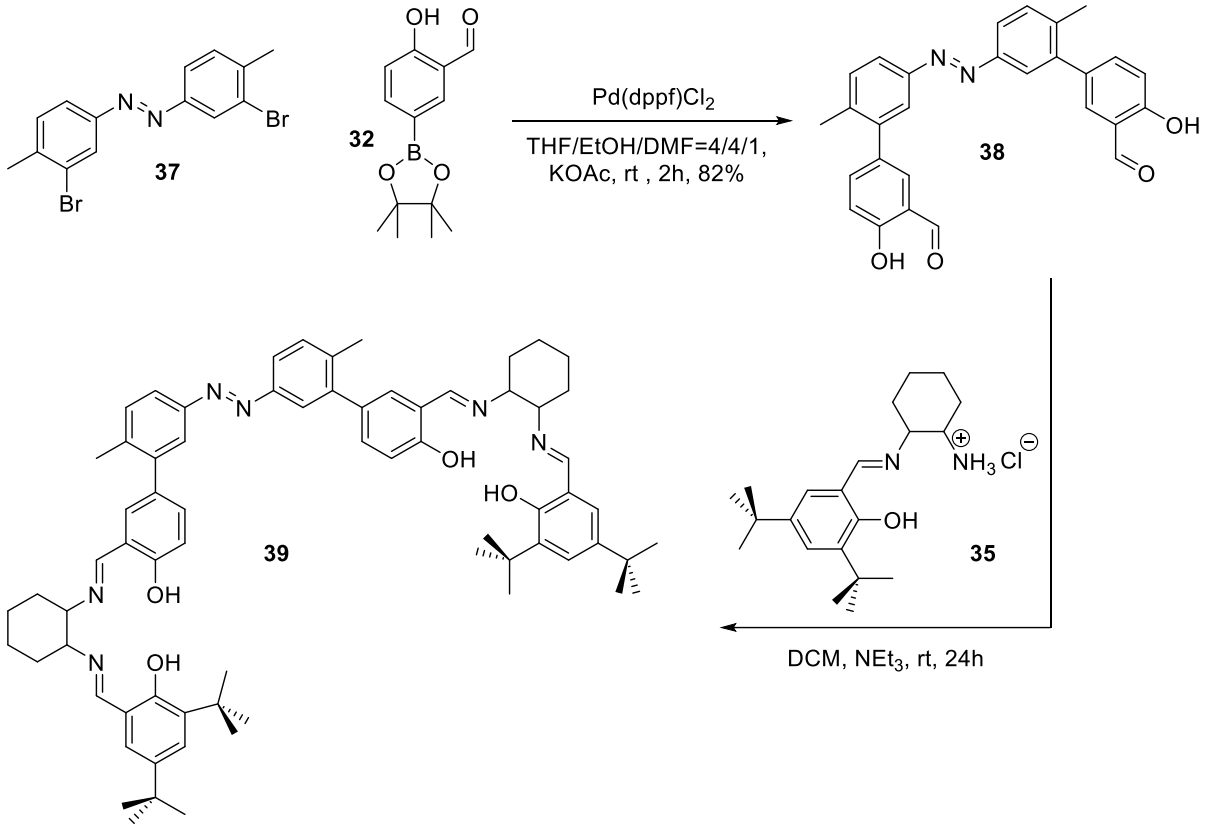

Scheme 33: Synthetic route towards ligand 39.

To overcome the purification problem a different molecular design was chosen, that was already described by the group of Jacobsen.[176] The complex **40** in Scheme 34 should also prevent interaction between the azobenzene and the metal-center, due to the flexible linker chosen.

Arylesters are known to undergo photo-Fries-rearrangement[177] but the excitation wavelength for these to occur are generally higher in energy than those needed for the azobenzene isomerization. For this molecule the central dicarboxylic azobenzene **42** in Scheme 34 had to be synthesized. However, the molecule **42** was insoluble such that it could not perform the following esterification reaction with **41**.

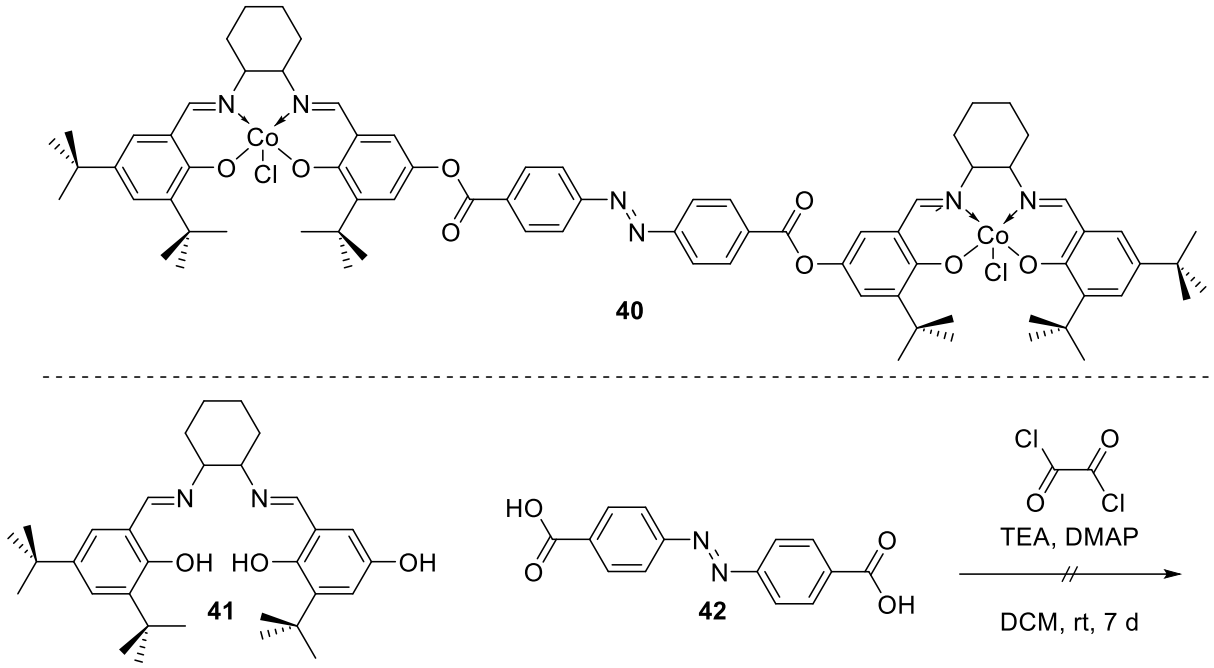

Scheme 34: Photoswitchable dinuclear Co-complex 40 with an ester bridge.

The next approach was to tune the absorption properties of the azobenzene. It was recently shown that introducing fluoro-substituents in the *ortho*-position of the azobenzene leads to a separation of the n $\rightarrow$ π^* band which allow for a separate addressability of both isomers in the visible region. This would allow an excitation of the azobenzene with light of lower energy, which should decrease possible interactions between the metal-center and the azobenzene. Ligand **43** shown in Scheme 35 should allow for excitation of the azobenzene moiety with visible light.

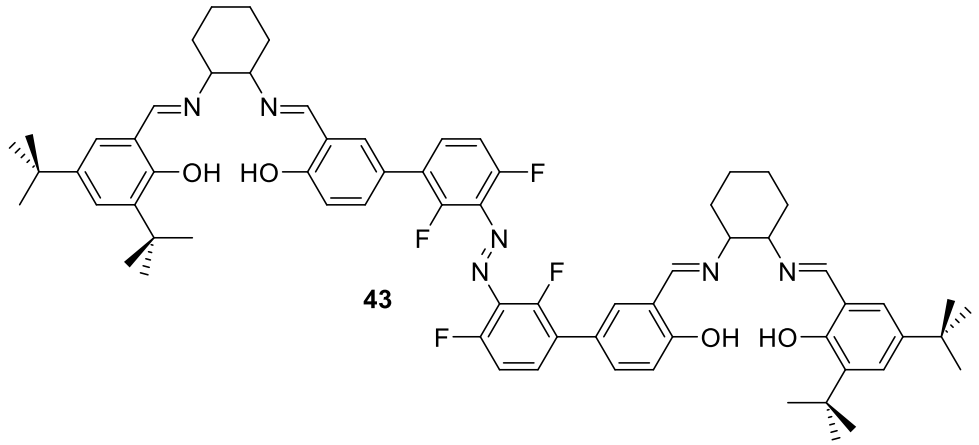

Scheme 35: Tetrafluorazobenzene ligand X.

For the azobenzene synthesis difluoroaniline derivative **44** (Scheme 36) was prepared. Tetrafluoroazobenzene **45** was synthesized using Mills-coupling conditions, but it was not stable enough to be used in further reaction. It could be isolated and analyzed as a red solid, but turned brown after a few hours. To overcome these stability issues the boron and bromo-substituent were exchanged. Suzuki-Miyaura-borylation of the difluoroaniline **44** gave the desired borylated difluoroaniline derivative **46**, however even with an extensive screening of coupling conditions the yield of 5% could not be increased. A last approach was taken where only two fluoro-subsituents were introduced on one phenyl ring of the azobenzene and the difluoroazobenzene **47** could be isolated in reasonable yield. However the subsequent Suzuki-coupling did not yield the desired disalicyl aldehyde, as NMR and UPLC analysis showed that only one coupling occurred on the non-fluorinated phenylring to afford molecule **48**.

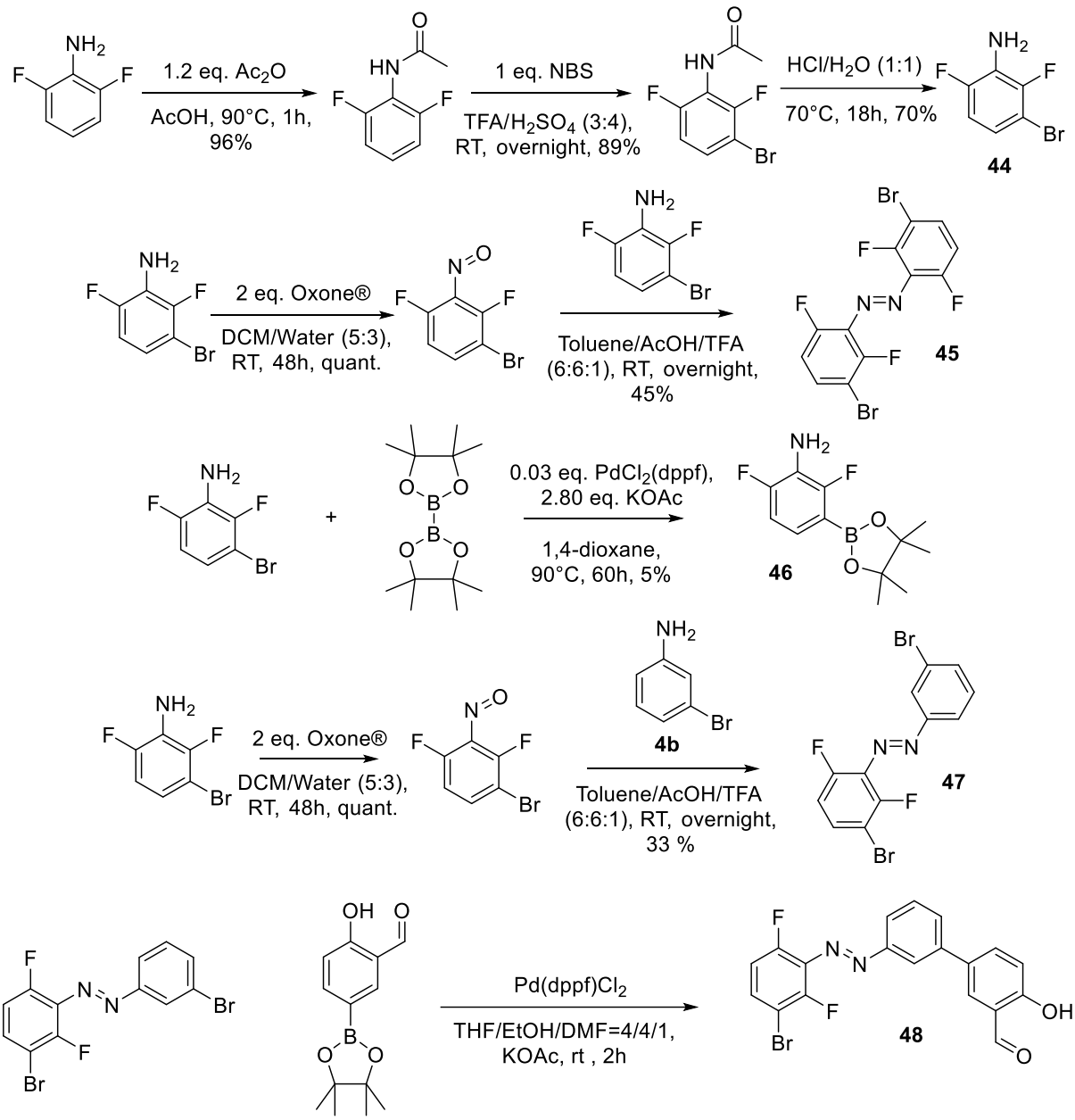

Scheme 36: Synthetic steps toward ligand 43.

Since tuning the properties of the azobenzene moiety was not succesful, the absorption properties of the metal-center were modified. Salphen-ligands allow easy tuning of the absorption properties due to their rigid diamine bridging moiety. Chromium-salphen complexes can be efficient catalysts for the ROP of β-butyrolactone (β-BL). The workgroup of Rieger has studied a large amount of different salphen complexes and their catalytic activity in the ROP of β-BL.[128,129,178] They were able to show that complex **49** in Scheme 37 has a relatively low activity in the ROP of β-BL with a conversion of only 30% after 24 h. The dinuclear complex **50** in Scheme 37 showed a conversion of 86% after already 15 h. Further concentration

dependance investigations of the polymerization reaction showed that the dinuclear complex undergoes a cooperative mechanism during the polymerization reaction.[128]

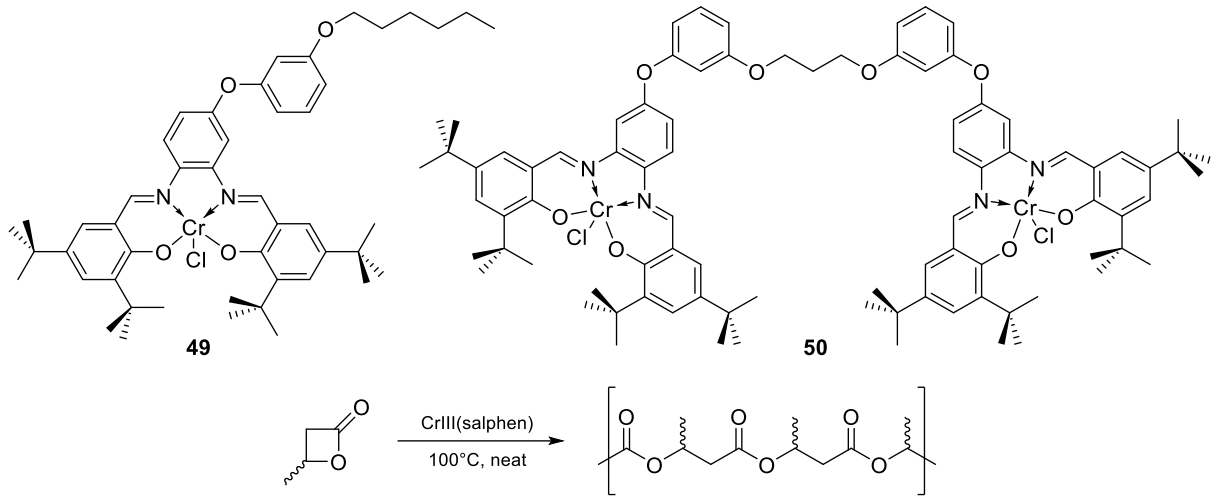

Scheme 37: Top) Two Cr(III)-salphen complexes investigated by the workgroup of Rieger. Complex 49 on the left shows only a relatively low activity in the ROP of β-BL (bottom) with a conversion of 30% after 24 h. Complex 50 on the right side showed a conversion of 86% after already 15 h.

Based on these results two azobenzene-functionalized binuclear Cr-salphen complexes were synthesized that can be used in the ROP of β-BL. The catalyst was envisioned to exist in two different states, where one state is active in the ROP of β-BL and can be converted by light of a discrete wavelength into the inactive state. In this case, the active state consists of a binuclear complex where the two Cr-centers are in close proximity to each other so that they can interact in a cooperative catalytic cycle. In the inactive state both Cr-centers are too far away from each other to interact in a cooperative fashion.

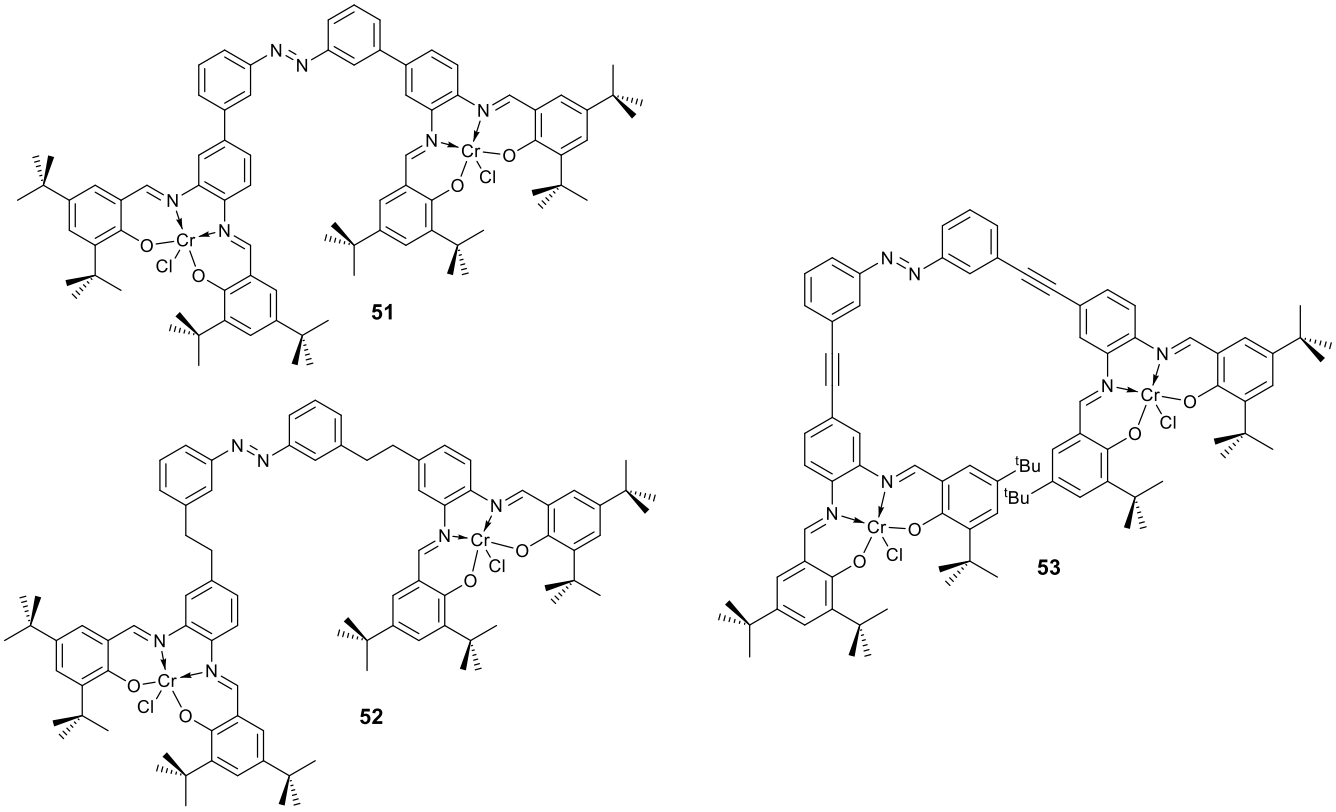

Scheme 38: Overview of the investigated complexes.

For this purpose three salphen moieties were functionalized with different azobenzene derivatives, since azobenzenes undergo a large geometrical change during the light induced *trans* → *cis*-isomerization (Scheme 38).[53] In one case the metal-moieties are directly linked to the azobenzene **51**, one with an ethylene spacer **52** to break the conjugation and one with an acetylene spacer **53** to increase the distance between both moieties.

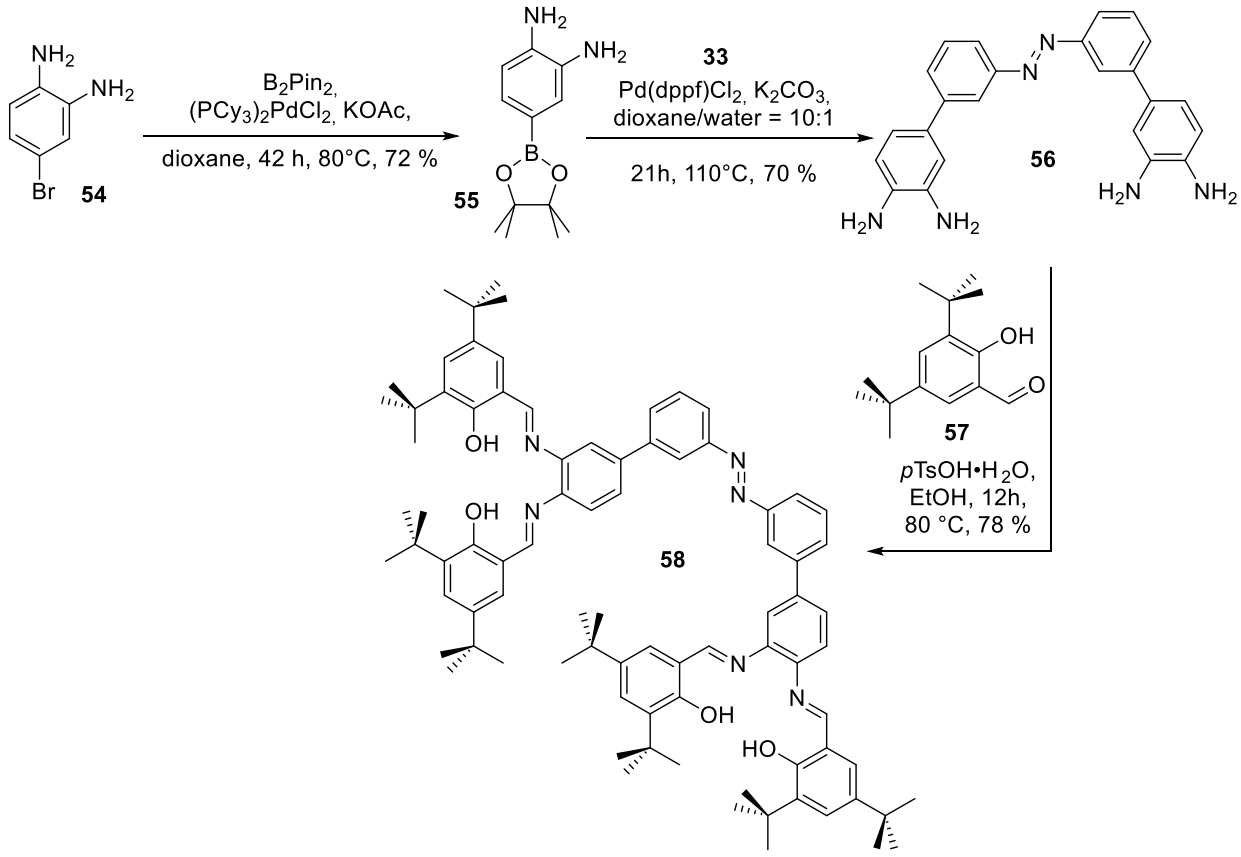

Scheme 39: Synthetic route to ligand 58.

The synthesis of ligand **58** starts from the bromo-functionalized diamine **54**. In the first step the pinacolborane derivative is formed using Suzuki-coupling conditions. The pinalcolboron-derivate is then reacted in a Suzuki-coupling with the dibromo-azobenzene **33** to form the azobenzene-functionalized diamine **56**. The salphen-moiety is formed in an imine-formation reaction using di-*tert*-butylsalicylaldehyde **57**. The ligand **58** was characterized using NMR spectroscopy, mass spectrometry and FTIR spectroscopy. The ^{1}H-NMR-spectrum (Fig. 14) shows the characteristic hydroxyl-signals around 13.5 ppm.

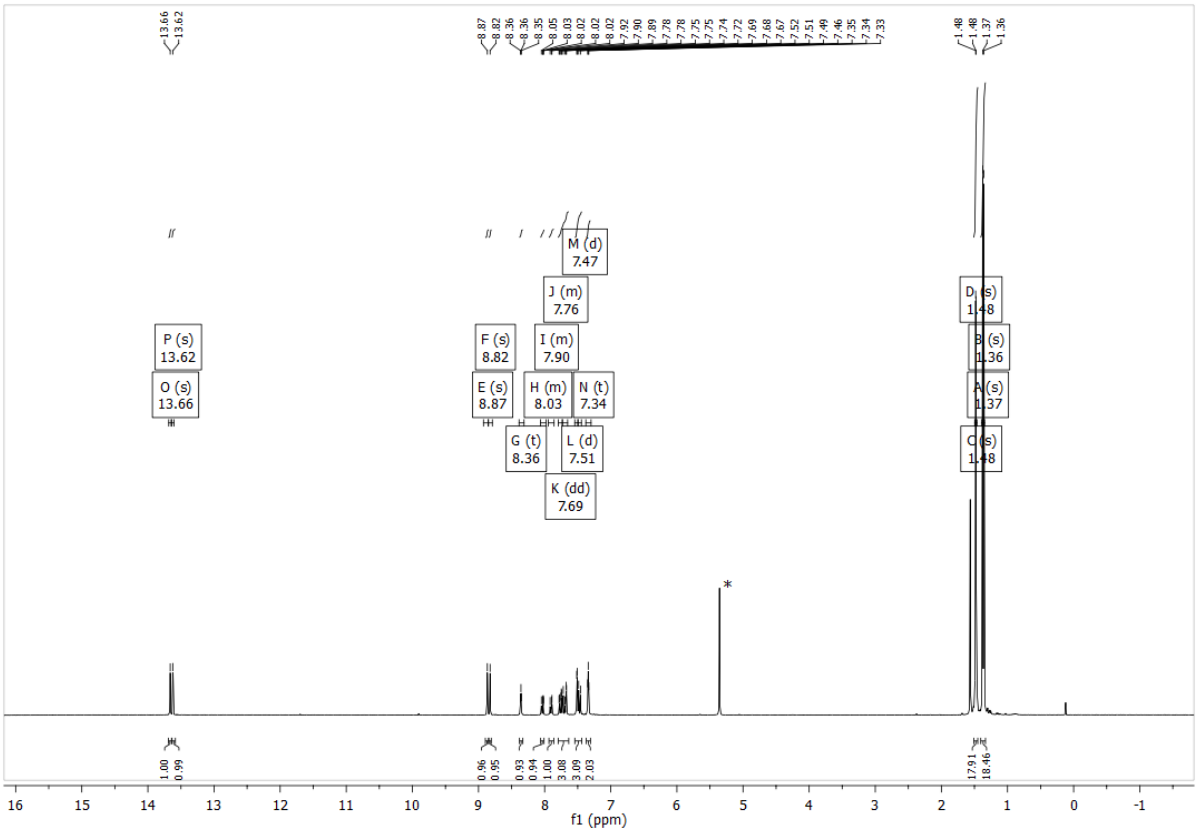

Fig. 14: ^{1}H-NMR (500 MHz) of ligand 58 in CD_2Cl_2.

The complex **51** is formed using $CrCl_2$. The first step is an insertion of the Cr (II) metal into the salphen moiety, which is then oxidized to the catalytically active Cr (III)-species in air using lutidine.

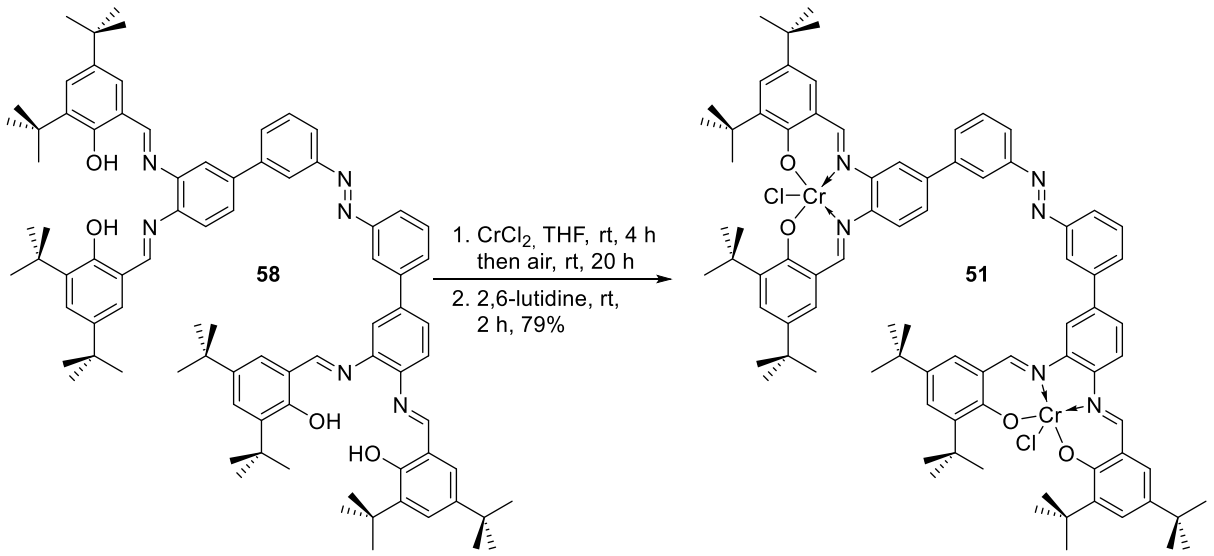

Scheme 40: Synthesis of complex 51.

The synthetic route for complex **52** starts out from diaminobenzene **54**. To avoid selectivity issues in the azobenzene-coupling to come, the amino functionalities were masked using Boc-

protecting groups. The Boc-protected diamine **59** was then used in a Sonogashira-cross-coupling to form alkyne derivative **60**. The alkyne was then reduced to form the flexible linker between the azobenzene and salphen-moiety. This alkyl bridged amine **61** was afterwards used in an oxidative azobenzene-coupling using copper(I)bromide. In the next step the Boc-groups were removed and the free amine-functionalities in **62** were used in an imine formation to yield ligand **63**.

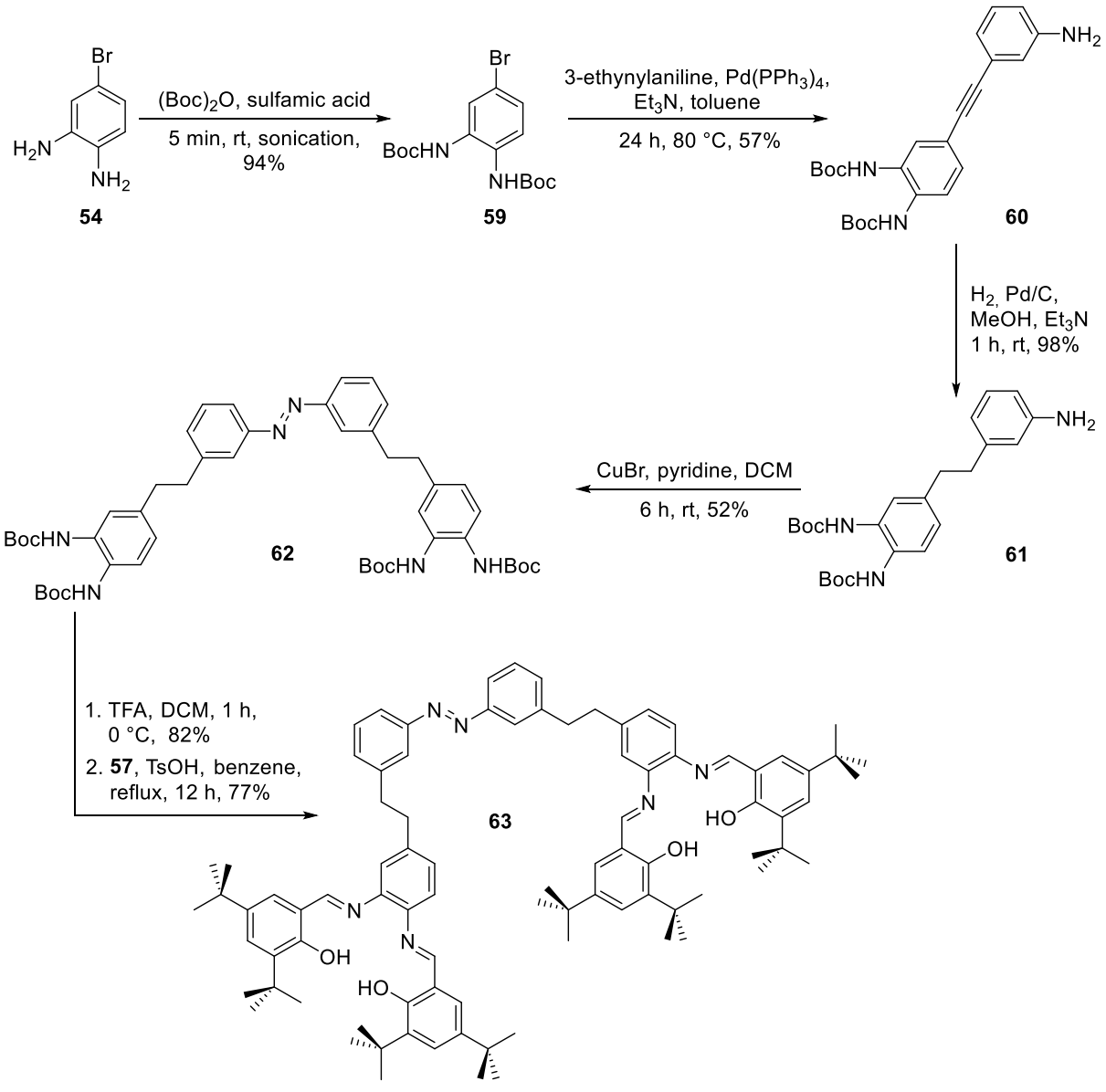

Scheme 41: Synthetic route towards ligand 63.

The ligand **63** was characterized using NMR spectroscopy, mass spectrometry and FTIR spectroscopy. The ^{1}H-NMR-spectrum of the ligands shows the characteristic broad signals for the hydroxyl-protons around 13.6 ppm. The complex **52** is formed using the same conditions as for complex **51**.

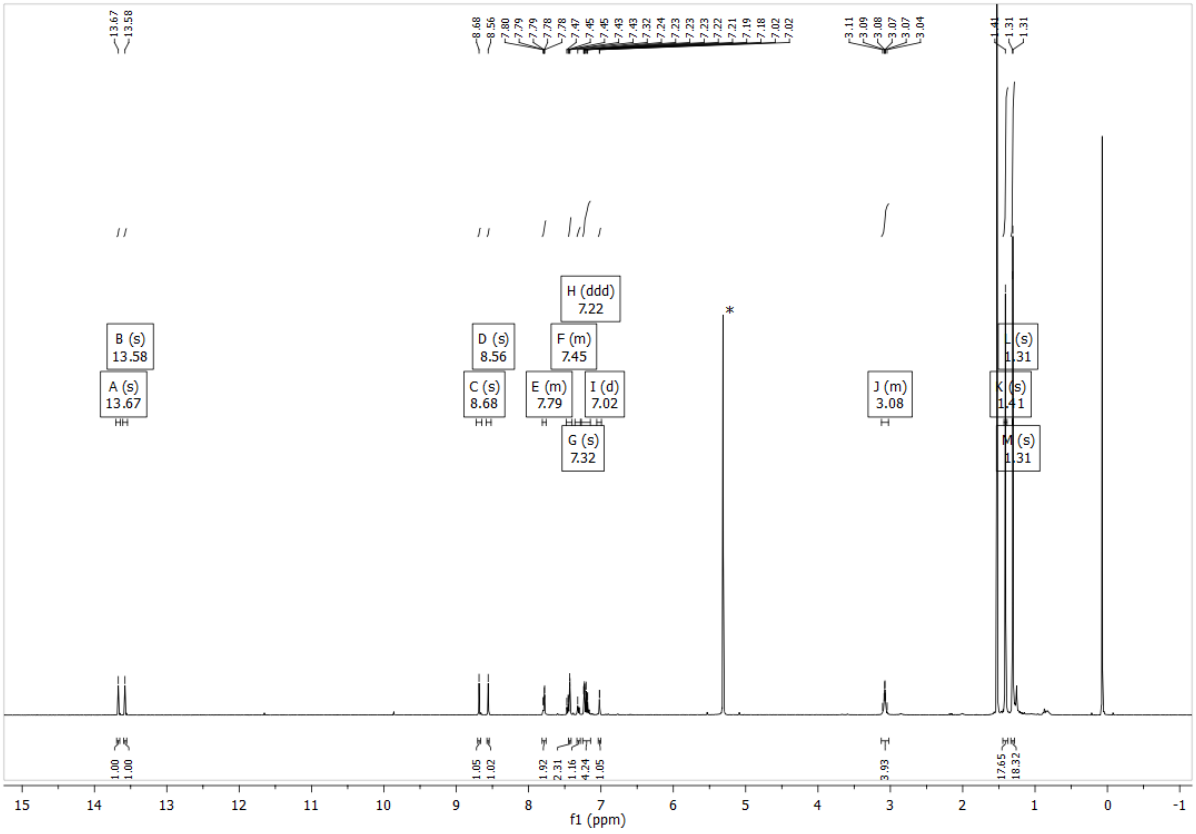

Fig. 15: ^{1}H-NMR (500 MHz) of ligand 63 in $CDCl_3$.

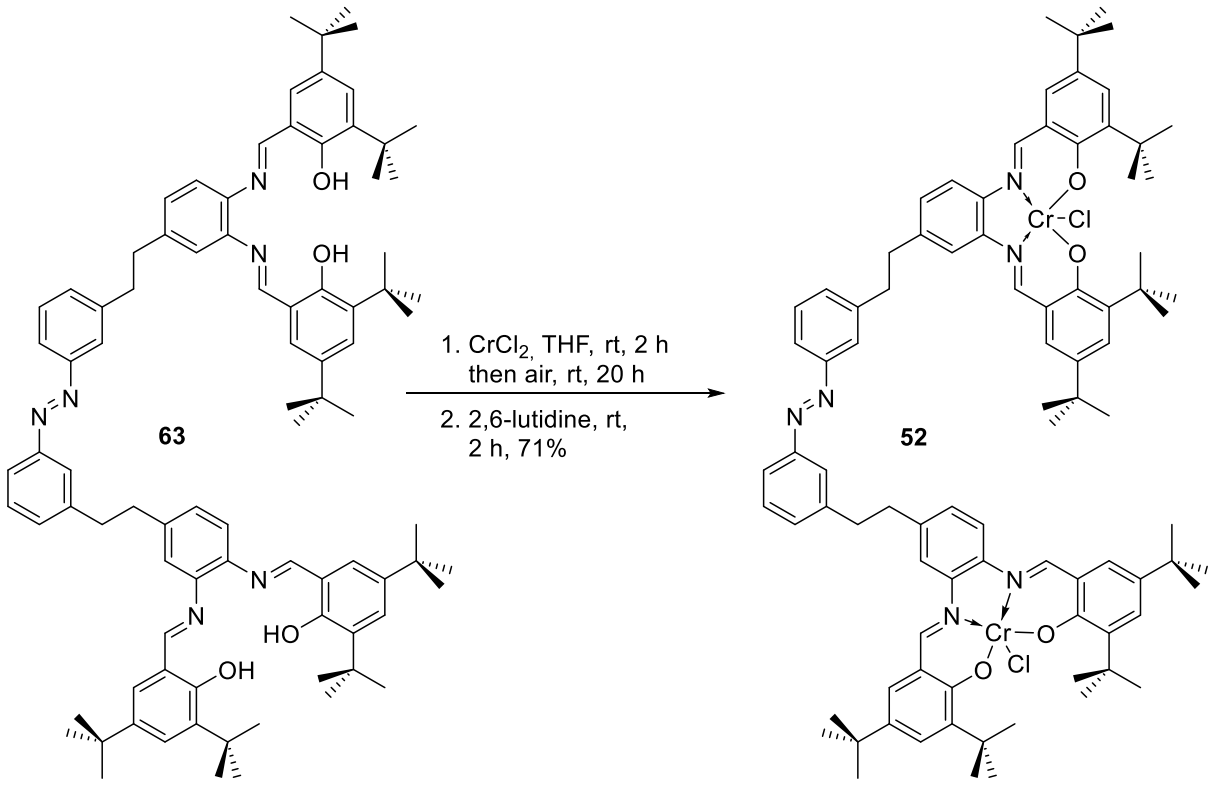

Fig. 16: Synthesis of complex 52.

Furthermore ligand **66** was synthesized with a rigid acetylene spacer. The synthesis starts from the acetylene derivative **60**, an oxidative azobenzenes coupling using PIDA afforded Boc-protected azobenzene **64**. Deprotection and imine-formation yielded the desired ligand **66** in low yield. Photochemical investigation of the ligand revealed only poor isomerization behavior (PSS <5% *cis*-content). Since the isomerization behavior was generally observed to worsen following insertion of the metal center, the ligand was not synthesized again to investigate the photochemistry of the corresponding complex.

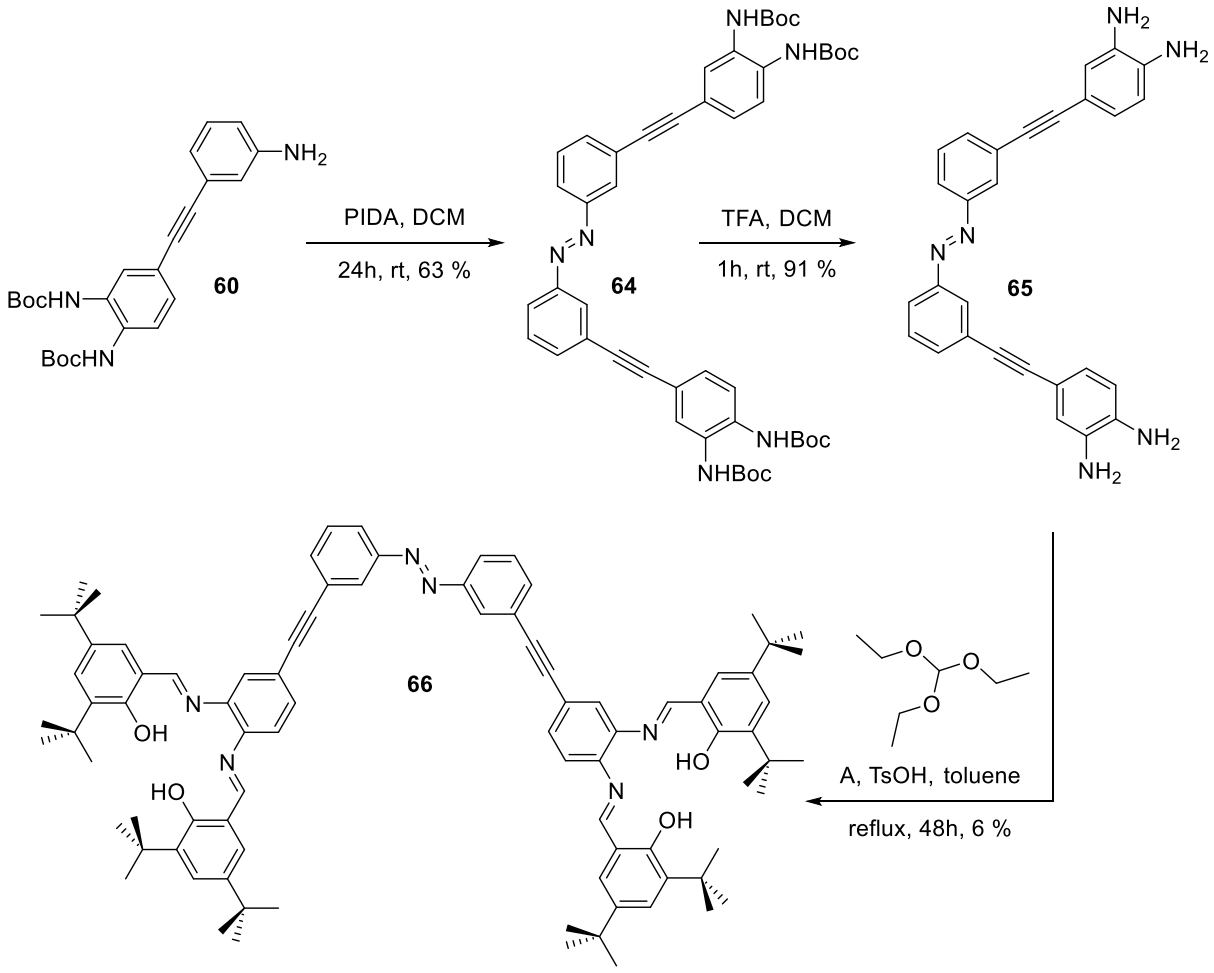

Scheme 42: Synthesis of azobenzene-functionalized salphen ligand with an acetylene bridge.

The photochemical investigation (Fig. 17) of complexes **51** and **52** shows that the **51** complex when irradiated with light of a wavelength of 365 nm can only reach a PSS of 37% *cis*-**51** content (Fig. 17a/c), determined using the Fischer's method.[175] This PSS, however, is insufficient for a noticeable change in reactivity between the two stages. The **52** complex on

the other hand, where the azobenzene moiety and the metal centers are well separated from each other, can reach a PSS of 65% *cis*-**52** (Fig. 17d/f) content in dichloromethane at 25 °C when irradiated with UV light (λ = 365 nm). For both complexes the photochemical back-reaction (Fig. 17 b/e) using a wavelength of 436 nm did not work, as **51** showed no change in absorption and **52** shows no clean photochemical reaction. However, the thermal back-reaction is possible in the case of complex **52**, and has a thermal half-life of 2.3 h at 25 °C. In the following, the polymerization behavior of complex **52** is described.

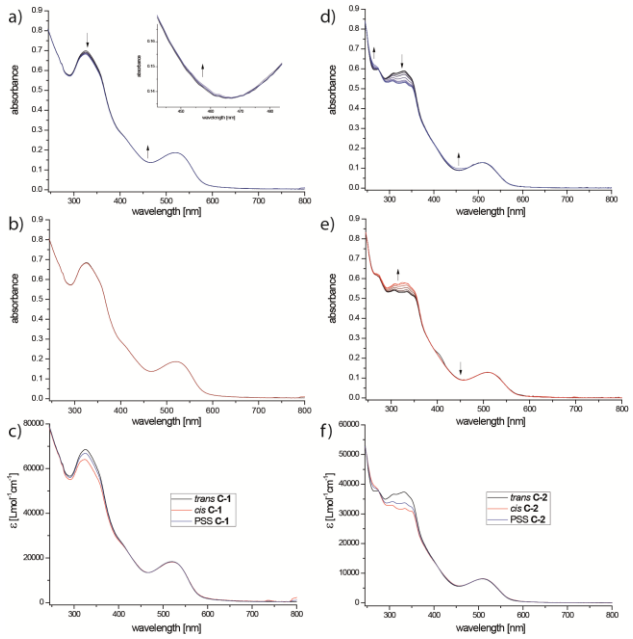

Fig. 17: a) Irradiation of *trans*-51 in CH_2Cl_2 using a wavelength of 365 nm until the PSS is reached. Inset: change of absorbance between 440 – 485 nm b) Irradiation of the PSS from (a) using 436 nm c) ε of *trans*-51 and *cis*-51 as well as an approximation of the PSS as a comparison. d) Irradiation of *trans*-52 in CH_2Cl_2 using a wavelength of 365 nm until the PSS is reached. e) Irradiation of the PSS from (d) using 436 nm f) ε of *trans*-52 and *cis*-52 as well as an approximation of the PSS as a comparison.

For the ROP of β-BL (Scheme 37 Bottom) a neat mixture of the catalyst solvated in the monomer was used. In all comparable studies a freshly prepared solution of catalyst and monomer in a 1000:1 ([monomer]:[Cr]) ratio was prepared to study their behavior under irradiation and in the dark.[e]

[e] For reproducibility the catalyst-monomer mixture was divided into two different flasks to ensure the same catalyst-monomer ratio for both experiments.

The complex *trans*-**52** shows a monomer conversion of 68% after 20 h in the dark determined by ^{1}H-NMR spectroscopy, whereas a solution irradiated with 335 nm[f] shows a conversion of only 27% (Fig. 18a). Calculating the rate constants using the approximation that the initial density is equal to the monomer density the rate constants k_{trans}= -11.1 · 10^{-5} M·s^{-1} for *trans*-**52** and k_{PSS} = -4.7 · 10^{-5} M·s^{-1} for **52** at the PSS while irradiating with 335 nm at 100 °C are obtained, which corresponds to a $k_{ON/OFF}$ = 2.4 (Fig. 18b). The polymers formed in both cases are comparable. The molecular weight distributions are 7.7 · 10^{4} g/mol for *trans*-**52** and 6.8 · 10^{4} g/mol for the **52** at the PSS with PDIs of 1.14 and 1.18. The switching of the catalyst has no influence on the tacticity of the polymer. Furthermore, the *in situ* switching behavior of the complex **52** was investigated and it showed that there is no fatigue in the switching of the catalyst during the ROP of β-BL (Fig. 18c). On the timescale of the polymerization it was possible to perform one complete switching cycle while monitoring the difference in activity. The activity change for the *in situ* switching is $k_{ON/OFF}$ = 2.1.

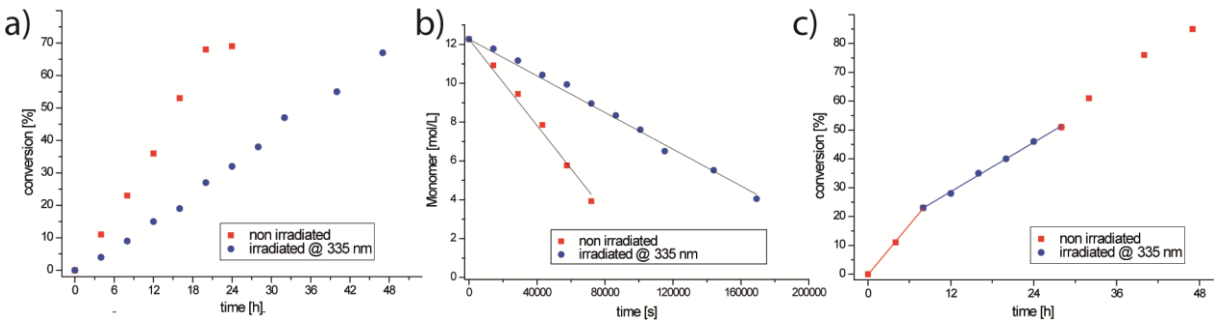

Fig. 18: a) Polymerization reaction that was studied using complex 52. All Polymerizations were preformed neat at 100 °C using a [monomer]:[Cr] ratio of 1000:1. b) A batch of catalyst and monomer was divided into two flasks. One reaction was kept in the dark (red squares) and the other was irradiated using 335 nm (blue circles). The conversion was determined using ^{1}H-NMR spectroscopy. c) Kinetic rates were plotted for the polymerization in the dark (red squares), irradiated with 335 nm (blue circles) d) For the *in situ* switching experiment the polymerization was stirred in the dark for 8 h (red line), the sample was then irradiated for 20 h. using 335 nm (blue line) and finally it was stirred in the dark until the reaction was complete (red squares).

Table 1: Results of Polymerization of b-BL (100 °C, 1:1000 Cr/b-BL ratio).

catalyst	conversion[a]	M_W [10^4 g/mol]	PDI	P_m[b]
50[128]	86[c]	10.8	1.9	n.d.
***trans*-52**	53[d]	7.7	1.14	0.51
52 (PSS)	19[d]	6.8	1.18	0.52

[f] Prior to the irradiation of the polymerization experiments it was ensured that the switching behavior at 335 nm is the same as at 365 nm.

[a] Determined by integration of signals in ^{1}H-NMR spectrum. [b] Determined by integration of carbonyl signals in ^{13}C-NMR spectrum.[179,180] [c] polymerization time 15 h. [d] polymerization time 16 h. n.d. not determined.

Herein, the first example of a photoswitchable metal complex is presented that can be used *in situ* to control the activity in polymerization reactions using light. Different azobenzene-functionalized Cr-salphen complexes were photochemically studied and the results show drastic differences in switching behavior, where a electronic separation between the azobenzene and the metal chromophore is in favor of the switching behavior. Furthermore the *ex situ* vs. *in situ* switching behavior of activity in the ROP of β-BL of complex **52** showed no significant change in the $k_{ON/OFF}$ ratio.

3.2 Photoswitchable reactivity control in Dynamic Covalent Chemistry[g]

Dynamic covalent chemistry (DCC) has gained a lot of interest in recent years because of its potential application in adaptive materials. These are materials that can respond to environmental changes and self-repair. Usually adaptive materials are based on reversible bonds,[181,182] that rely on supramolecular, non-covalent interactions[183-185] or DCC.[186-189] Light is among the available triggers the most attractive because it is non-invasive and allows for high temporal and spatial control of the effect. There are two ways how light can be used to influence the making and breaking of reversible bonds in polymeric materials. To date only one of these approaches has been reported, with the groups of Weder and Rowan[190] inducing the breaking of a reversible metal-ligand coordination bond upon local heating induced by light, and thereby providing the ability to heal a polymer during illumination. Another way would be to use light to control the kinetics of an intrinsic exchange based on reversible covalent linkages. A photoswitchable dynamic covalent crosslinker could be used to modulate the ability of a polymer network to self-heal after illumination with UV and visible light.

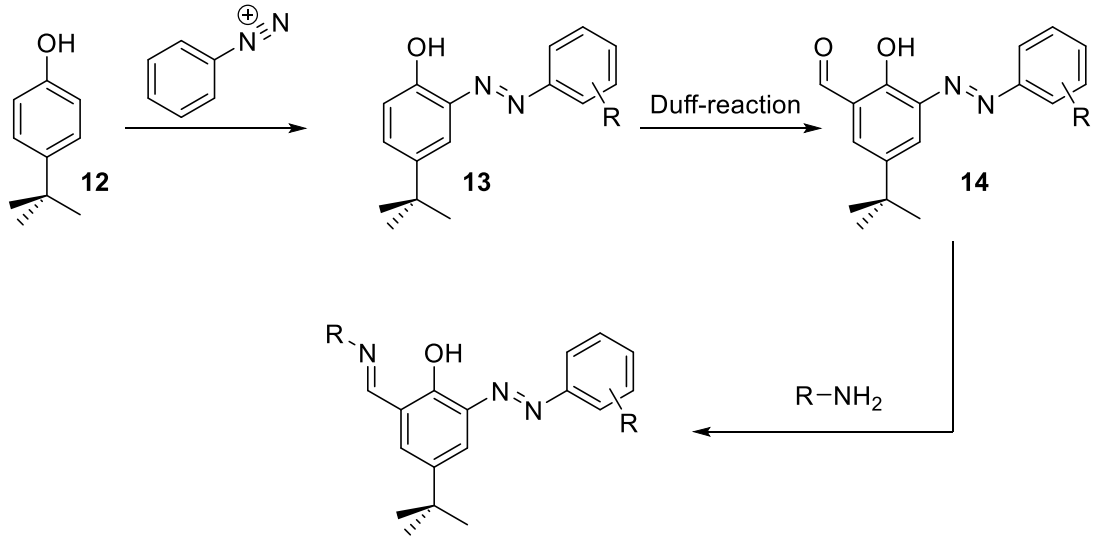

Scheme 43: Synthetic pathway to *ortho*-substituted azobenzene Schiff-base moieties.

The photochemical analysis of the FI- and salen-ligands (Scheme 23 on page 37), showed some interesting results. The photochemical behavior is not like expected for an *ortho*-hydroxyazobenzene which usually exhibits a low PSS and short thermal half-life.[68] A clear

[g] Parts of this chapter have been submitted in M. Kathan, P. Kovaříček, C. Jurissek, A. Senf, A. Thünemann, S. Hecht "Self-healing dynamic polymers controlled by light"

isomerization of these species can be observed and the thermal half-life can be in the range of hours.

DFT-calculations on a B3LYP 6-31G+ level (Fig. 19, Fig. 20) showed that the Schiff-base motif should indeed prevent the fast thermal isomerization. The electron-density in the HOMO-orbitals of the *trans* and *cis* isomers are different. For the *trans*-azobenzene the electron-density lies on the azobenzene moiety, which is also where the hydrogen-bond should be located. In the *cis*-isomer, however, the electron-density is located around the imine-bond, which means that the proton is located on that side of the molecule and should not protonate the azobenzene bond.

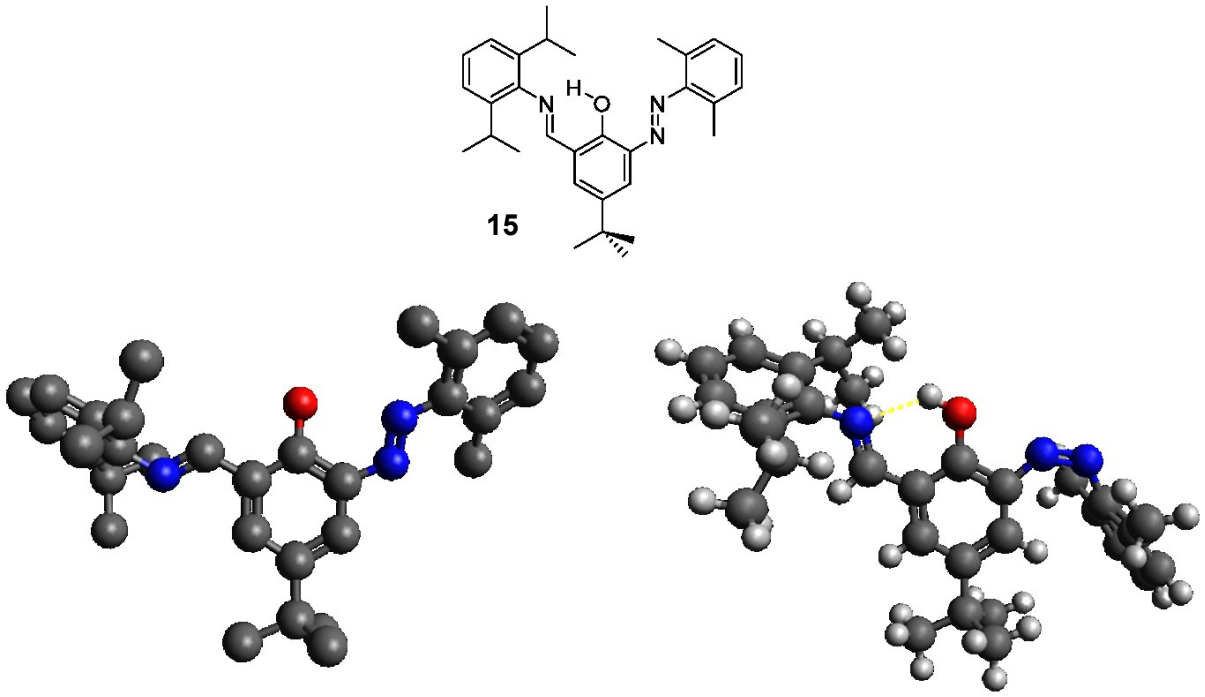

Fig. 19: Investigated azobenzene-functionalized Schiff-base 15 and their geometry optimized structural models in the *trans*- and *cis*-isomer.

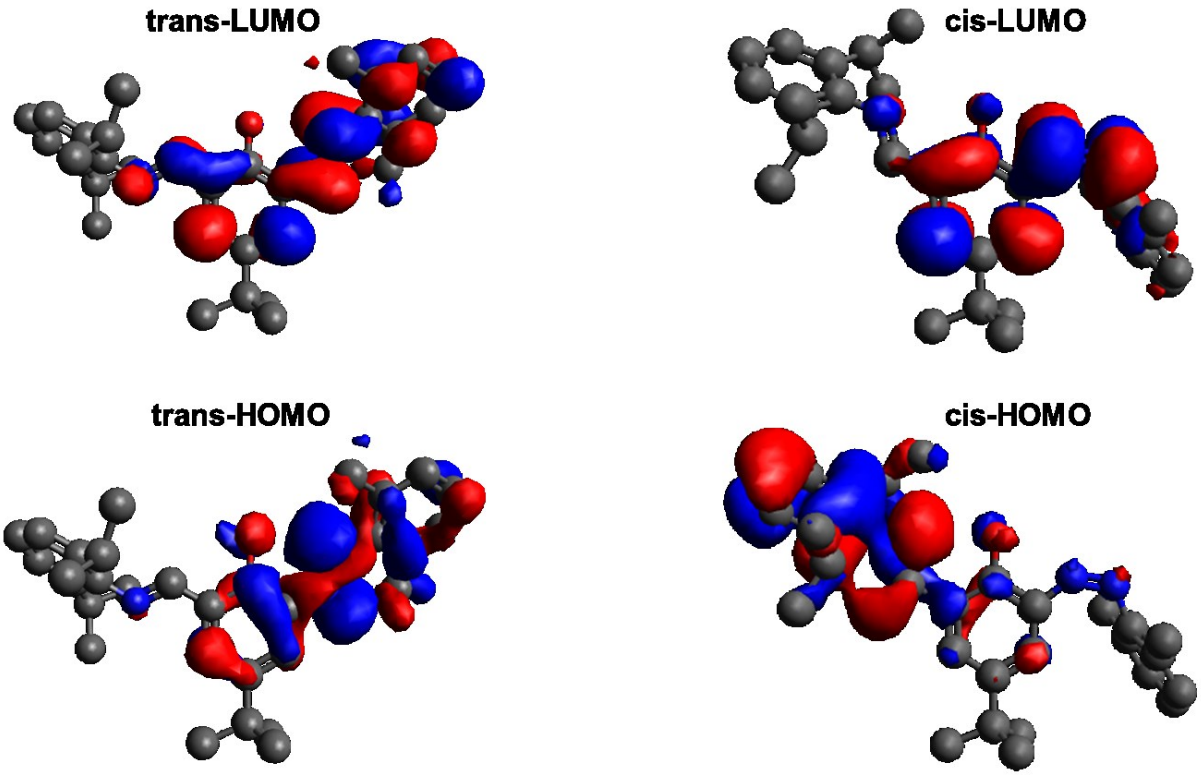

Fig. 20: DFT calculation of the HOMO/LUMO distributions in the *trans*- as well as *cis*-state of the investigated azobenzenes-functionalized Schiff-base 15.

Due to the fast thermal-back reaction of *ortho*-hydroxyazobenzenes their scope of application is limited. The acidic hydroxyl-proton can intramolecularly protonate the N=N-bond which leads to a single bond. A solution to overcome this limitation seems to be the introduction of a hydrogen-bond acceptor that prevents the protonation in the *cis*-state. The Schiff-base motif seems to be an ideal structural motif for that since the hydroxyl-proton is hydrogen-bonded to the imine.

The photochemistry was studied for these compounds and will be discussed for azobenzene **15** (Scheme 44).

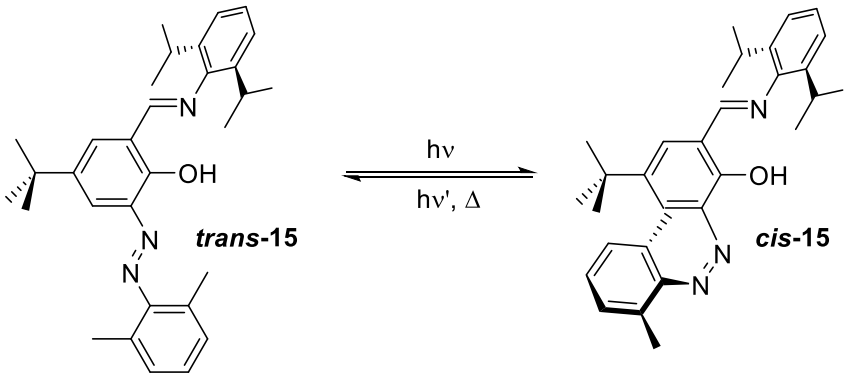

Scheme 44: Photochemical isomerization of the azo-bond in Schiff-base 15.

The photochemical investigation of azobenzene **15** (Fig. 21) supports the theoretical studies. Irradiating a 10^{-5} M solution of **15** in acetonitrile using 365 nm light shows a clean photochemical reaction behavior, but has a poor conversion with an estimated *cis*-content of 20% in the PSS. The *cis*-isomer for all these compounds is relatively stable compared to ortho-hydroxyazobenzenes,[68] azobenzene **15** needs to be irradiated with 235 nm light to isomerize it back to the *trans*-isomer within a reasonable time interval (70 min). Without irradiation it takes 4.5 h to reach the initial state. The kinetic profiles for the back-isomerization show no first-order kinetics, which is due to a pH dependence of the back isomerization.[53,68] Even though no quantitative data on the thermal half-life can be obtained for the azobenzenes **15**-**20** (Scheme 23 on page 37) the thermal stability increases roughly by an order of magnitude (ranging from several minutes to several hours) with the introduction of the aldehyde functionality.

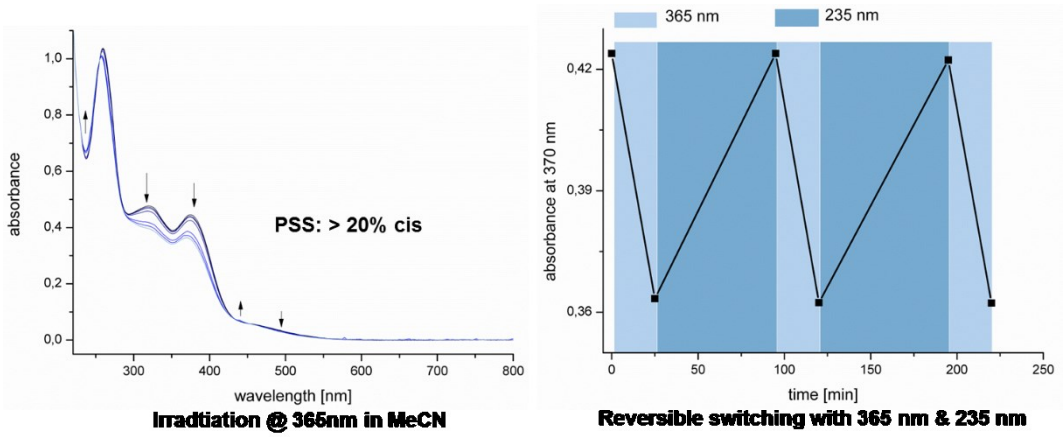

Fig. 21: Photochemical analysis of azobenzene-functionalized Schiff-base 15.

The initial research focused on the design of a photoswitch, which allows for reactivity modulation of an appended aldehyde group (Fig. 22 left).

For this purpose azobenzene **67** (Fig. 22 right) was synthesized. Upon irradiation with UV light, the azobenzene is readily converted into the *cis*-isomer, which displays an enhanced carbonyl group reactivity[191,192] and can be returned to the less reactive form by using visible light and/or heat. Photoisomerization of the *trans*-configured azobenzene **67** unmasks an activating *ortho*-hydroxyl group[193] in *cis*-**67**.

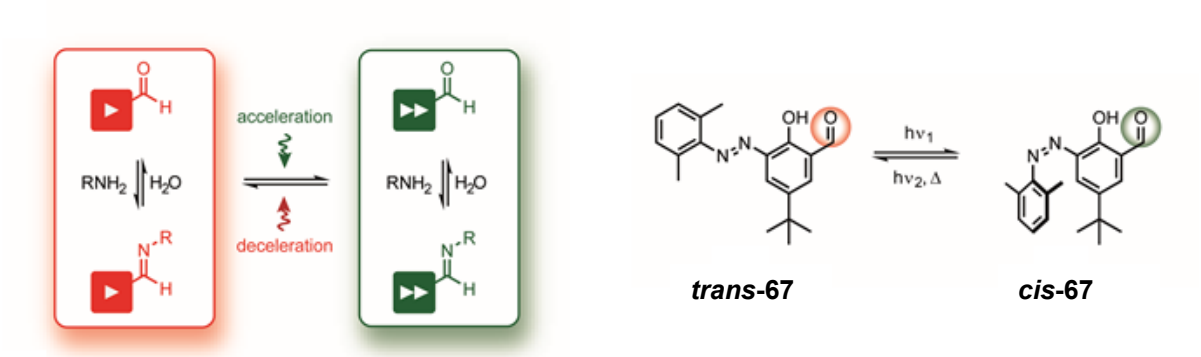

Fig. 22: Left) Conceptual control over kinetics in DCC. Light is used to induce a photochemistry that increases the imine exchange rate. Light of a different wavelength can be used to decelerate the imine exchange again. Right) Azobenzene molecule 67 that was used to control the imine exchange reaction.

The reactivity difference of the aldehyde electrophiles was investigated in a condensation reaction with an amine-based nucleophile. **67** was treated with pyridine-4-carboxhydrazide, and the formation of the corresponding acylhydrazones was followed by UV-vis absorption spectroscopy.[h]

The kinetics followed by UV-vis spectroscopy were investigated first without any catalyst, however, no reaction (change in the spectrum) could be detected within one hour. When an excess of trifluoroacetic acid (TFA) was added, the reaction started to proceed when it was heated above 60 °C. Finally, a piperidine/TFA mixture was used, fulfilling the role of a buffer and a catalyst of the condensation, as previously reported.[194] Due to the thermal back-reaction, the azobenzene **67** derivatives require constant illumination to maintain a constant ratio of isomers during the course of the reaction. Therefore, the reaction was performed in a stirred fluorescence cuvette under constant illumination by monochromatic light and followed by UV-vis spectroscopy employing an orthogonal probe beam. Due to the concentration limitations of UV-vis measurement, the amine reactant had to be replaced by a hydrazide derivative leading to the formation of acylhydrazones which exhibit higher stability towards hydrolysis. Furthermore, to achieve sufficient conversion over a reasonable time scale, the reaction was performed in the aforementioned piperidine-trifluoroacetic acid (TFA) buffer.

When azobenzenes **67** were mixed with pyridine-4-carboxyhydrazide in buffered CH_3CN (~10^{-5} M, 1:1 ratio, 6 mM piperidine + 3 mM TFA buffer, at 25 °C), slow formation of the corresponding acylhydrazone was observed by band evolution in the UV-vis spectrum. Conversion at equilibrium was determined by UPLC-MS analysis. The condensation

[h] Kinetic experiments were performed by P. Kovaříček.

experiments were conducted either with exclusion of light or they were pre-illuminated with light of a wavelength of 313 nm until the PSS was reached and illumination was continued after the hydrazide reactant was added. A significant increase in the reaction rate was observed when the azobenzene was illuminated, the reaction rate increased from $1.2 \cdot 10^{-2}$ M^{-1} s^{-1} in the *trans*-**67** to $2.6 \cdot 10^{-2}$ M^{-1} s^{-1} in the illuminated mixture.

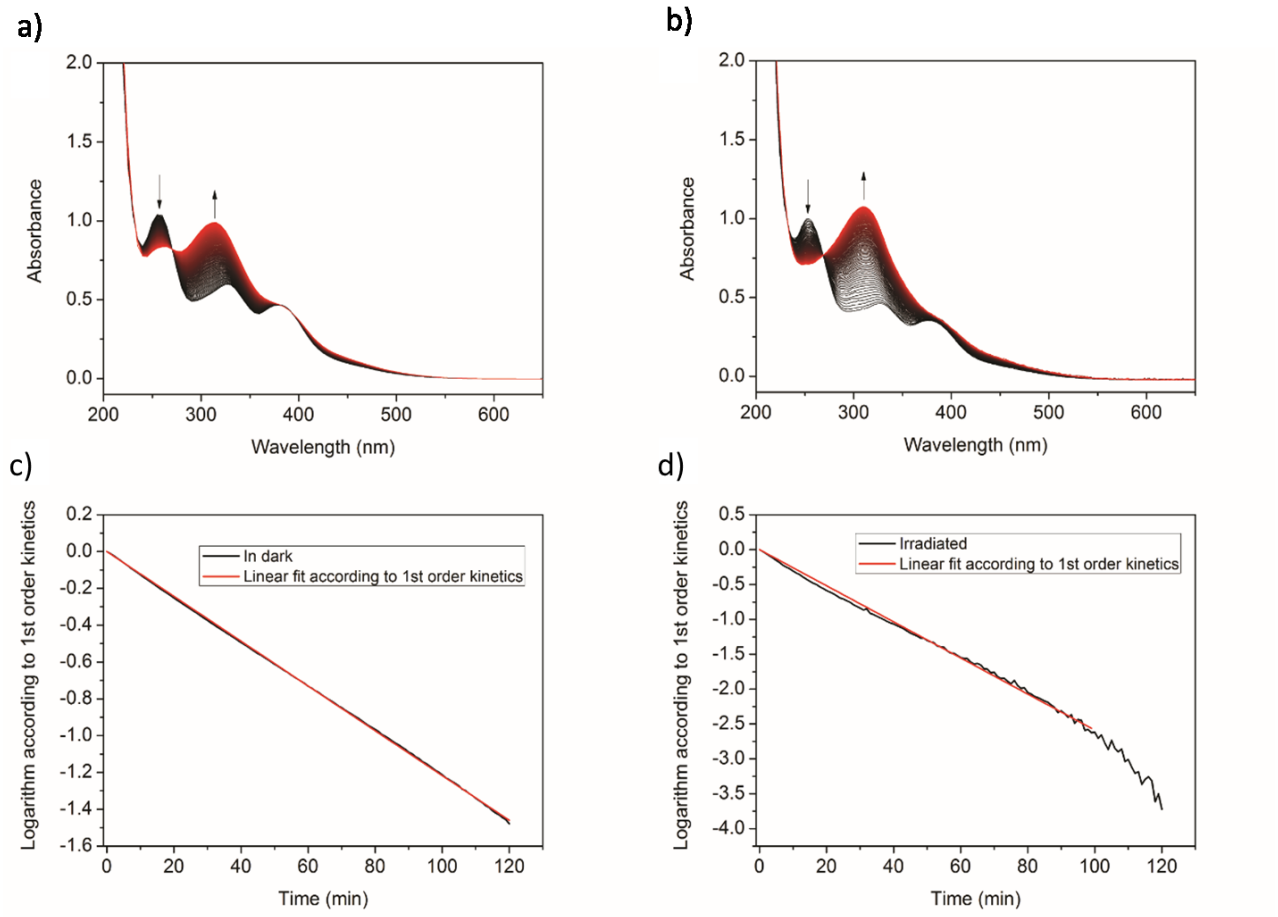

Fig. 23: Kinetics of hydrazine formation from azobenzene 67. a) Stacked UV-Vis spectra recorded over the course of the condensation of 67 with pyridine-4-carboxhydrazide (both reactants $3.8 \cdot 10^{-5}$ M) in dark in acetonitrile in the presence of a piperidine-TFA buffer ($6 \cdot 10^{-3}$ M piperidine, $3 \cdot 10^{-3}$ M TFA) at 25 °C. b) Stacked UV-Vis spectra recorded over the course of the condensation of AB with pyridine-4-carboxyhydrazide (both reactants $3.8 \cdot 10^{-5}$ M) under constant irradiation at 313 nm in acetonitrile in presence of a piperidine-TFA buffer ($6 \cdot 10^{-3}$ M piperidine, $3 \cdot 10^{-3}$ M TFA) at 25 °C. c) Fitting of the first-order kinetics of the reaction of 67 with hydrazide in the dark. The concentration data were processed by the formula: $\ln [c] - \ln [c_0] = -kt$. d) Fitting of the first-order kinetics of the reaction of AB with hydrazide under irradiation. The concentration data were processed by the formula: $\ln [c] - \ln [c_0] = -kt$.

In conclusion, it can be said that under continuous illumination, leading to the formation of the photoisomer *cis*-**67**, the condensation rates were significantly higher compared to the

corresponding dark samples composed solely of *trans*-**67**. The rate of the condensation is increased by a factor of 2.2 in the PSS (Fig. 23), containing ca. 22% of the *cis*-isomer, which exhibits a thermal half-life in the range of several minutes at room temperature under these conditions. However, the azobenzene illustrates the drawback of a more reactive switch with a short thermal half-life, which prevents a large and permanent acceleration of condensation kinetics.

Furthermore it was envisioned that a molecule with two salicyl moieties could be used to control self-healing capabilities of polymers using the kinetic differences in DCC. For that reason the molecule **30**[i] (Scheme 45) was investigated in more detail. However the azobenzene shows even at lowered temperatures of 10 °C no noticable change in absorption. Here, the tautomerization described in Scheme 4 occurs too fast to observe a significant change in absorption.

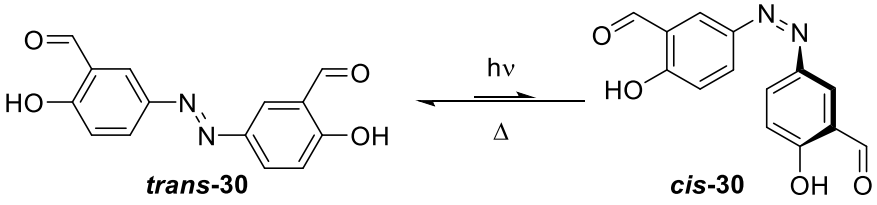

Scheme 45: Photoisomerization of azobenzenes X.

Nevertheless the imine formation for the molecule was investigated and it shows that the azobenzenes **30** undergoes an imine formation with isonicotinylhydrazine. Experiments to investigate the light-controlled combinatorial chemistry for azobenzenes **30** showed no difference in reactivity between an irradiated solution and a non-irradiated. The PSS that is reached is most likely not large enough to see a change in reactivity.

[i] Synthesis of **30** is described on page 35

4 Conclusion and Outlook

The goal of this thesis was to design and synthesize photoswitchable catalysts for polymerization reactions. For this purpose existing organometallic catalysts were functionalized with azobenzene moieties to introduce a photoresponsive group into the catalytically active molecule.

In chapter 3.1.2 salen and FI ligands were functionalized with azobenzenes in the *ortho*-position of the ligating Schiff-base moiety. The complexes, however, did not show reversible photochemistry which was attributed to intramolecular processes that led to the release of a non-chelating ligand, which made them unsuitable for polymerization control.

In chapter 3.1.2 an approach was described where two salen-moieties were tethered together by an azobenzene. Here the large geometrical change of the azobenzenes was used to induce cooperative effects between two metal centers in the ring-opening polymerization of propylene-oxide. After computational calculation to get an optimized structure for that effect, the target molecule was successfully synthesized. The complex however showed no reversible photochemistry. It had a unimolecular process to the *cis*-azobenzene but showed no reversible switching back to the *trans*-azobenzene. The thermal back-isomerization was too slow to be used as an effective trigger in the polymerization of propylene oxide that is usually run at 0 °C for these type of complexes. The non-existing photochemical back-reaction was attributed to the large overlap of the n $\rightarrow$ π^* band of the *cis*-azobenzene with the LMCT-band of the metal center, which made an effective switching process impossible.

In chapter 3.1.3 the same cooperative approach as in chapter 3.1.2 was used for the ring-opening polymerization of β-butyrolactone. To overcome the problematic overlap of the LMCT with the n $\rightarrow$ π^*-band of the *cis*-azobenzenes a salphen moiety was used as the catalytic active center, which offered due to the delocalized π-system, better control over the absorption properties of the metal center. Three different target molecules were synthesized that differ in the linker between the azobenzenes and the salphen moiety. In one case the azobenzene was directly attached to the salphen-moiety and the other two molecule had bridges (acetylene, ethylene) between them. The acetylene brigded ligand showed already very poor isomerization behavior. The directly linked complex showed very poor photochemical properties which led to a PSS of only 37% *cis*-azobenzene content. The ethylene bridged molecule on the other hand showed decent photochemical properties and a PSS with 65% *cis*-azobenzene content. In both cases the

molecules did not perform photochemical back-reactions, which is also due to a large overlap of the n → π* and LMCT bands of the metal center. For the ethylene linked molecule however the thermal back-reaction is fast enough under the conditions that are usually used for β-Butyrolactone polymerizations. The catalyst showed an increased activity by a factor of 2.4 in the *trans*-isomer compared to the *cis*-isomer and it also allows for an *in-situ* switching of the complex.

In chapter 3.2 ortho-azobenzene functionalized Schiff-bases were used to control the reactivity in DCC. It was shown that there is an increase in the imine formation when comparing the *trans*-azobenzene and the reaction under constant irradiation by a factor of 2.2.

The azobenzene functionalized organometallic molecules reported in this thesis have in common that the photochemistry of azobenzenes is significantly affected by the metal-centers. One way how this could be overcome is to use negative photochromic compounds that absorb further red of the spectrum than the metal centers used for the polymerization reactions. Indigo-type molecules would be one candidate that could be used to replace the azobenzenes moiety since they have an absorbance spectrum with a π → π* band above 600 nm.[195,196]

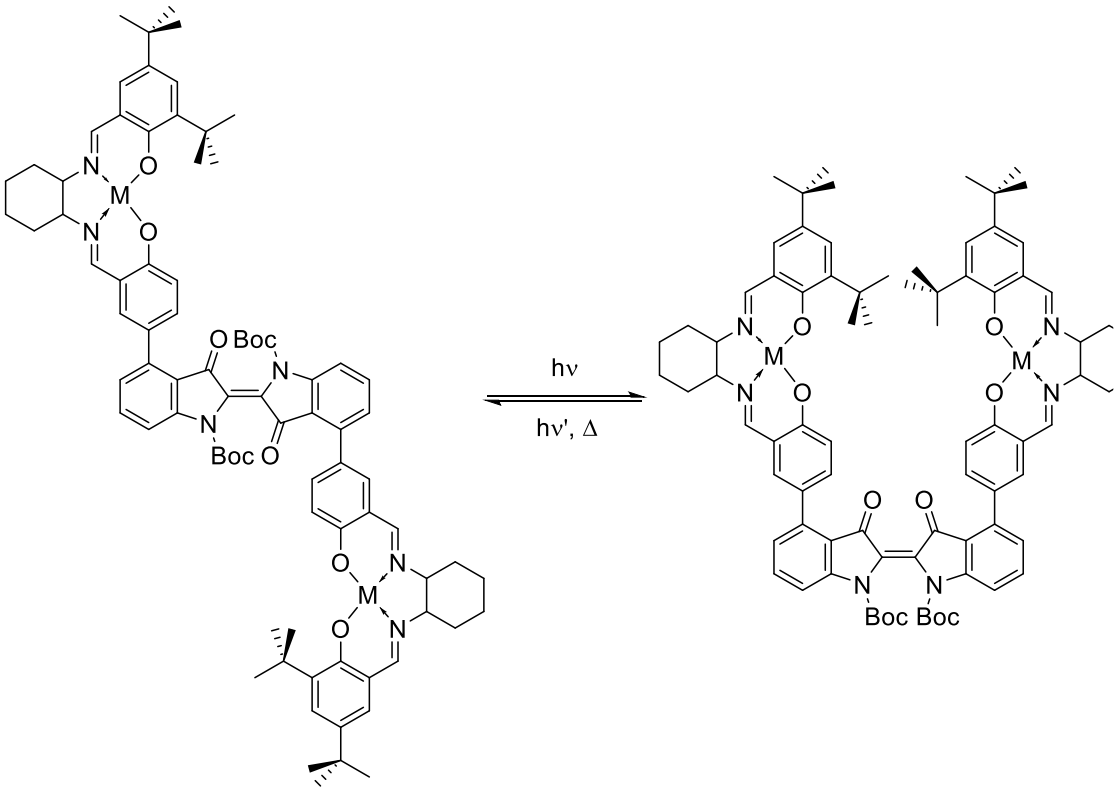

Scheme 46: Possible way how to incorporate an indigo-switch into a catalytic system that allows for the control of cooperative effects during polymerization reactions.

A possible way to use cooperative effects of certain catalysts is shown in Scheme 46. The system can be irradiated using wavelengths above 600 nm which should not affect the LMCT band of the metal center. The indigo chromophore shows just like azobenzenes large geometrical changes, but since both states in the indigo have delocalized π-systems in the two states they are better defined compared to the azobenzenes.

In chapter 3.1.2 the possibility of tacticity control in polymerization reaction with a chain-end mechanism was also discussed. A promising approach to control stereochemistry in chemical reaction was already presented by the group of Feringa.[148,149] The overcrowded alkene switch developed in his group could be used to control tacticity in polymerization reactions.

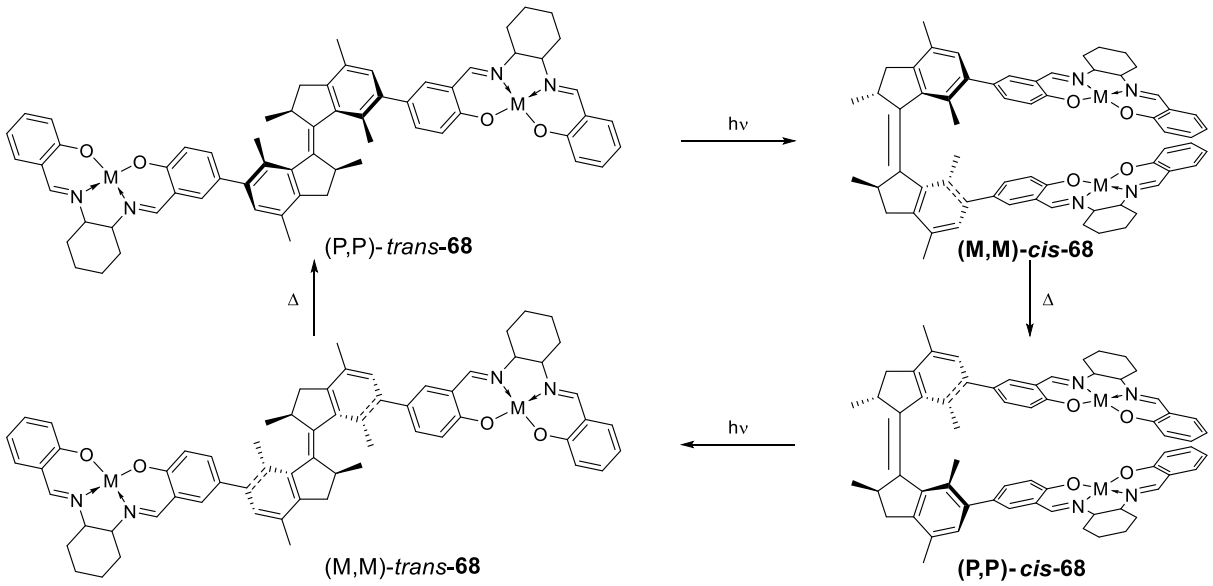

Scheme 47: Possible use of an overcrowded alkene switch to gain control over stereoselectivty in polymerization reactions.

The system shown in Scheme 47 could be used to control stereoselectivity, tacticity as well as activity in polymerization reactions. The structures (P-P)-*trans* **68** and (M-M)-*trans* **68** should show a low activity with no selectivity in a polymerization reaction. The structures (M-M)-*cis* **68** and (P-P)-*cis* **68** should be able to catalyze a polymerization with a cooperative effect and due to the helical chirality be selective for the chirality of the monomer upon insertion.

5 Experimental Section

5.1 Materials and Methods

5.1.1 Analytical Instrumentation

NMR spectra were recorded on a 500 MHz (125 MHz for ^{13}C, 470 MHz for ^{19}F) Bruker AVANCE II 500 spectrometer or on a 300 MHz (75 MHz for ^{13}C) Bruker AVANCE II 300 spectrometer at 25 °C using residual protonated solvent signals[266] as internal standards (^{1}H: $\delta(CDCl_3)$ = 7.26 ppm, $\delta(C_6D_6)$ = 7.16 ppm, $\delta(CD_2Cl_2)$ = 5.32 ppm, δ(DMSO-d_6) = 2.50 ppm; ^{13}C: $\delta(CDCl_3)$ = 77.16 ppm, $\delta(C_6D_6)$ = 128.06 ppm, $\delta(CD_2Cl_2)$ = 53.84 ppm, δ(DMSO-d_6) = 39.52 ppm). Ultrahigh-performance liquid chromatography / mass spectrometry (UPLC/MS) was performed on a Waters Acquity UPLC equipped with a Waters LCT Premier XE Mass detector for high-resolution MS (HR-MS, ESI^+-ionization) and with Waters Alliance systems (consisting of a Waters Separations Module 2695, a Waters Diode Array Detector 996 and a Waters Mass Detector ZQ 2000). UV/Vis spectroscopy was performed on a setup that was assembled consisting of a 500 W high pressure Hg(Xe) lamp (LOT Oriel) coupled to a monochromator (LOT Oriel MSH-300), which was equipped with an electronic shutter. The light output of the monochromator was transferred to the cell compartment of a Cary60 spectrophotometer using an optical fiber. The irradiation beam was assembled orthogonal to the measurement beam of the spectrophotometer illuminating ca. 1 cm² of the front area of a 3 mL quartz cuvette (10x10 mm), which was thermostated at 25 °C. During photokinetic measurements effective stirring of the sample was ensured. The minimal time resolution of the Cary60 spectrophotometer while scanning a wavelength range of 300 nm is 3 s. The intensity of the irradiation beam was kept low enough that no inhomogeneities due to illumination of only a part of the cuvette front area were detected and the spectral changes within the time resolution of the spectrometer could be neglected. Irradiation of polymerization reactionswere performed by employing Roithner LEDs (UVTOP335-TO18, and UVTOP365-06) driven by a GW Instek GPD-3303S linear DC powersupply.Thermogravimetric analysis was performed on a PerkinElmer Pyris 1 TGA equipped with a PerkinElmer Pyris 1 TGA autosampler and a PerkinElmer thermal analysis gas station. Fourier-transform infrared spectroscopy was carried out either on a Jasco FTIR-6600 or a Bruker Vertex 70v each equipped with a Specac Golden Gate single reflection diamond ATR sample holder. Anaytical GPC measurements in THF as the mobile phase were performed on a WGE Dr. Bures system equipped with three 300x8 mmSDV columns (50 Å, 5 µm, 500 Å, 5 µm, 1000 Å, 5 µm) in a WGE Dr.Bures TAU 2010

column oven at 60 °C and at room temperature, using a WGE Dr.Bures Q-2010 GPC pump and a Knauer Smartline 3800 autosampler. Detection was achieved using a Knauer K2301RI-detector and a Knauer Smartline 2500 UV-detector. Flow-rate was 1.0 mL/min. Columns were calibrated using a Polystyrene Calibration Kit S-L-10 LOT 79, using 2,4-Di-*tert*-butyl-4-methoxy-phenol as internal standard. TLC was performed on Merck Silica Gel 60 F254 TLC plates with a fluorescent indicator employing 254 nm UV-lamp for visualization. All calculations have been performed using the Gaussian09 (Rev. A02 and Rev. C01)[197] software package. For geometry optimizations no symmetry constraints were applied. Optimized structures were proven to correspond to minima on the potential energy surface by frequency calculatios. All energies include zero-point corrections.

5.1.2 Chemicals and Solvents

Solvents and commercial starting materials were used as supplied. The solvents were dried before use, if necessary, employing an Innovative Technologies solvent purification system (multi-unit micro series). Silica gel for chromatography (0.035–0.070 mm, 60 Å) was used for column chromatography. The petroleum ether (PE) used had a boiling range of 40–60 °C. β-Butyrolactone was rectified over CaH_2 using a 1.5m coulumn prior to use.

5.2 Synthetic procedures

5.2.1 Photoswitchable FI- and salen complexes

Unfunciontionalized Salen Ligand

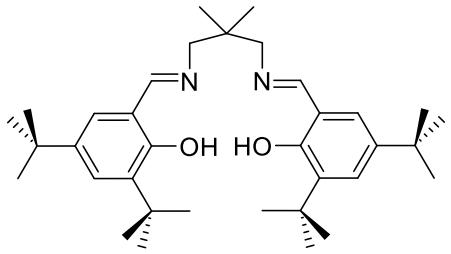

2,2-dimethylpropane-1,3-diamine (0.53 ml, 4.27 mmol) was added to a solution of 3,5-di-tert-butyl-2-hydroxybenzaldehyde (2.00 g, 8.53 mmol) in EtOH (12 ml)/DCM (4 ml) at room temperature and the mixture was stirred for several hours to afford a yellow suspension. After filtration, the product was recrystallized from EtOH/$CHCl_3$ to give the lignad (1.99 g, 3.72 mmol, 87 % yield) as a redish brown crystaline solid.

^{1}H-NMR (300 MHz, CD_2Cl_2): δ = 13.94 (s, 2H), 8.42 (s, 2H), 7.42 (d, *J* = 2.5 Hz, 2H), 7.17 (d, *J* = 2.5 Hz, 2H), 1.59 (s, 4H), 1.48 (s, 18H), 1.34 (s, 18H), 1.13 (s, 6H) ppm.

Salen-complexes for irradiaton screening

To a solution of the unfunctionalized ligand (100 mg, 0.187 mmol) in THF (6 mL) the metal reagent (1.2eq) was added, followed by trethylamine (0.6 ml, 0.5 mmol) except for Al and Cr. The mixture was stirred at ambient temperature for 3 h and then concentrated down to 2 mL and cooled in the freezer. The resulting precipitate was filtered, and then dried in vacuo. The complex was used without further purification for the irradiation screening.

4-(tert-butyl)-2-((2,6-dimethylphenyl)diazenyl)phenol

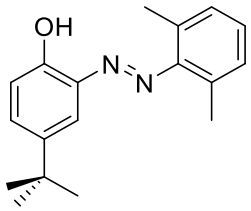

To a solution of 2,6-dimethylaniline (2.00 g, 16.5 mmol) in 1M HCl (17 ml) and Water (17 ml) at 0-5 °C was added a solution of sodium nitrite (1.14 g, 16.5 mmol) in 5 ml water and the resulting solution was stirred for 1 h to give a brown solution. 4-(tert-butyl)phenol (2.48 g, 16.5 mmol) was dissolved in the 1M NaOH (17 ml) and MeOH (17 ml). Then the solution was added dropwise to the diazononium solution. The brown reaction mixture was extracted with DCM (3x 50 ml). The organic phase was dried and the solvent was removed. The crude product was purified by column chromatography (silica gel, DCM:PE = 1:1) to afford 4-(tert-butyl)-2-((2,6-dimethylphenyl)diazenyl)phenol (3.40 g, 12.0 mmol, 73 %) as a red oil.

^{1}H-NMR (500 MHz, $CDCl_3$): δ = 12.25 (br, 1H), 7.84 (d, *J* = 2.5 Hz, 1H), 7.34 (dd, *J* = 8.7, 2.6 Hz, 1H), 7.11 – 7.03 (m, 3H), 6.92 (d, *J* = 8.7 Hz, 1H), 2.32 (s, 6H), 1.28 (s, 9H) ppm. **^{13}C-NMR (126 MHz, $CDCl_3$):** δ = 150.09, 148.68, 142.93, 137.06, 131.35, 131.12, 129.68, 129.60, 128.83, 117.85, 34.17, 31.43, 19.53 ppm. **MS (ESI-HRMS):** calculated for $C_{18}H_{23}N_2O$ (M^+): 283.1810. found: 283.1778.

4-(*tert*-butyl)-2-((2,6-diethylphenyl)diazenyl)phenol

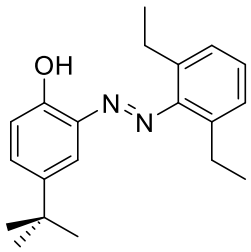

To a solution of 2,6-diethylaniline (4.48 g, 30.0 mmol) in Water (75 ml) and conc. HCl (7.5 ml), sodium nitrite (2.07 g, 30.0 mmol) in Water (150 ml) was slowly added at 0°C and stirred for 20 min. To the resulting brown solution was added a solution of 4-(tert-butyl)phenol (4.51 g, 30.0 mmol) in Ethanol (75 ml) and 1M NaOH (30 ml) and stirred for 15 h. The brown reaction mixture was extracted with DCM (3x 50 ml). The organic phase was dried and the solvent was removed. The crude product was purified by column chromatography (silica gel, DCM:PE = 1:1) to afford 4-(tert-butyl)-2-((2,6-diethylphenyl)diazenyl)phenol (3.62 g, 11.7 mmol, 39 %) as a red oil.

^{1}H-NMR (500 MHz, $CDCl_3$): δ = 12.58 (br, 1H), 8.04 (d, *J* = 2.5 Hz, 1H), 7.52 (dd, *J* = 8.7, 2.6 Hz, 1H), 7.36 – 7.22 (m, 1H), 7.10 (d, *J* = 8.7 Hz, 1H), 2.79 (q, *J* = 7.5 Hz, 1H), 1.46 (s, 1H), 1.29 (t, *J* = 7.5 Hz, 1H) ppm. **^{13}C-NMR (126 MHz, $CDCl_3$):** δ = 150.04, 148.83, 142.97, 137.12, 136.85, 131.20, 129.80, 128.89, 127.82, 117.93, 34.22, 31.49, 25.50, 15.58 ppm. **MS (ESI-HRMS):** calculated for $C_{20}H_{27}N_2O$ (M^+): 311.2123. found: 311.1889.

5-(*tert*-butyl)-3-((2,6-dimethylphenyl)diazenyl)-2-hydroxybenzaldehyde (67)[198]

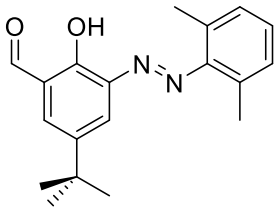

4-(tert-butyl)-2-((2,6-dimethylphenyl)diazenyl)phenol (1.90 g, 6.7 mmol) was dissolved in anhydrous trifluoroacetic acid (20 ml, 260.0 mmol) under Argon, and hexamethylenetetramine (0.94 g, 6.7 mmol) was added in one portion. The brown solution was refluxed until all the starting phenol was converted. The mixture was then cooled to r.t., 1M HCl (20 mL) was added and stirred for 15 min, the product was extracted with DCM (3x 50 mL). The combined organic extracts were dried and the solvent removed. The purple residue was purified by column

chromatography (silica gel, DCM:PE = 1:1) to afford **67** (908 mg, 2.9 mmol, 44 %) as a brown solid.

^{1}H-NMR (500 MHz, $CDCl_3$): δ = 13.54 (br, 1H), 10.54 (s, 1H), 8.19 (d, *J* = 2.7 Hz, 1H), 7.99 (d, *J* = 2.7 Hz, 1H), 7.25 – 7.16 (m, 1H), 2.47 (s, 1H), 1.40 (s, 1H) ppm. **^{13}C-NMR (126 MHz, $CDCl_3$):** δ = 189.41, 153.78, 148.25, 142.86, 137.87, 135.42, 131.90, 129.78, 129.54, 129.26, 124.55, 34.34, 31.26, 19.77 ppm. **MS (ESI-HRMS):** calculated for $C_{19}H_{23}N_2O_2$ (M^+): 311.1760. found: 311.1737.

5-(*tert*-butyl)-3-((2,6-diethylphenyl)diazenyl)-2-hydroxybenzaldehyde[198]

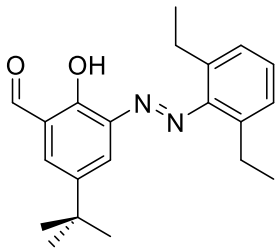

4-(tert-butyl)-2-((2,6-diethylphenyl)diazenyl)phenol (1.50 g, 4.8 mmol) was dissolved in anhydrous trifluoroacetic acid (15 ml, 195.0 mmol) under Argon, and hexamethylenetetramine (0.68 g, 4.8 mmol) was added in one portion. The brown solution was refluxed until all the starting phenol was converted. The mixture was then cooled to r.t., 1M HCl (20 mL) was added and stirred for 15 min, the product was extracted with DCM (3x 50 mL). The combined organic extracts were dried and the solvent removed. The purple residue was purified by column chromatography (silica gel, DCM:PE = 1:1) to afford 5-(tert-butyl)-3-((2,6-diethylphenyl)diazenyl)-2-hydroxybenzaldehyde (435 mg, 1.3 mmol, 27 %) as an orange solid.

^{1}H-NMR (500 MHz, $CDCl_3$): δ = 13.26 (br, 1H), 10.44 (s, 1H), 8.09 (d, *J* = 2.7 Hz, 1H), 7.91 (d, *J* = 2.7 Hz, 1H), 7.23 – 7.04 (m, 1H), 2.65 (q, *J* = 7.5 Hz, 1H), 1.30 (s, 1H), 1.13 (t, *J* = 7.5 Hz, 1H) ppm. **^{13}C-NMR (126 MHz, $CDCl_3$):** δ = 189.45, 153.80, 148.28, 142.91, 137.92, 137.25, 135.15, 129.51, 129.46, 127.95, 124.56, 34.35, 31.25, 25.60, 15.55 ppm. **MS (ESI-HRMS):** calculated for $C_{21}H_{27}N_2O_2$ (M^+): 339.2073. found: 339.2037.

Ligand 18-Me[116]

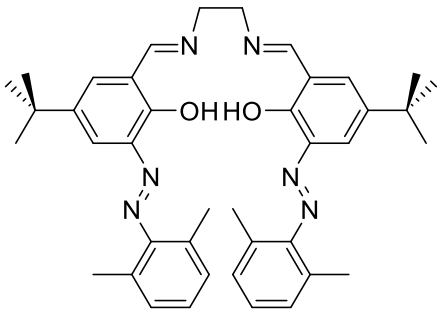

Ethane-1,2-diamine (0.06 ml, 0.95 mmol) was added to a solution of **67** (590 mg, 1.90 mmol) in Ethanol (4 ml) at room temperature and the mixture was stirred for several hours to afford an orange suspension. After filtration, the product was recrystallized from EtOH/$CHCl_3$ = 3:1 to give ligand **18-Me** (452 mg, 0.70 mmol, 74 %) as a redish brown crystalline solid.

^{1}H-NMR (500 MHz, CD_2Cl_2): δ = 13.81 (s, 1H), 8.55 (s, 1H), 7.76 (d, *J* = 2.5 Hz, 1H), 7.52 (d, *J* = 2.2 Hz, 1H), 7.18 – 7.09 (m, 3H), 4.05 (s, 2H), 2.35 (s, 6H), 1.32 (s, 9H) ppm. **^{13}C-NMR (126 MHz, CD_2Cl_2):** δ = 166.23, 156.95, 152.02, 141.82, 141.11, 131.61, 131.31, 129.58, 128.52, 121.09, 60.43, 34.66, 31.59, 19.24 ppm. **MS (ESI-HRMS):** calculated for $C_{40}H_{78}N_6O_2$ (M^-): 643.3761. found: 643.3729.

Ligand 18-Et[116]

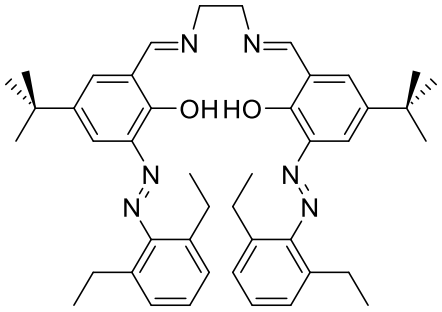

Ethane-1,2-diamine (0.04 ml, 0.64 mmol) was added to a solution of 5-(tert-butyl)-3-((2,6-diethylphenyl)diazenyl)-2-hydroxybenzaldehyde (435 mg, 1.29 mmol) in Ethanol (4 ml) at room temperature and the mixture was stirred for several hours to afford an orange suspension. After filtration, the product was recrystallized from EtOH/CHCl3 = 3:1 to give ligand **18-Et** (396 mg, 0.57 mmol, 88 % yield) as an orange, crystalline solid.

^{1}H-NMR (500 MHz, CD_2Cl_2): δ = 13.67 (s, 1H), 8.45 (s, 4H), 7.65 (d, *J* = 2.5 Hz, 1H), 7.41 (d, *J* = 2.4 Hz, 1H), 7.13 – 7.04 (m, 3H), 3.96 (s, 2H), 2.59 (q, *J* = 7.5 Hz, 4H), 1.22 (s, 9H), 1.05 (t, *J* = 7.5 Hz, 6H) ppm. **^{13}C-NMR (126 MHz, CD_2Cl_2):** δ = 166.54, 157.17, 151.89,

141.82, 141.24, 137.06, 131.79, 128.57, 127.96, 121.05, 60.41, 34.68, 31.59, 25.74, 15.95 ppm. **MS (ESI-HRMS):** calculated for $C_{44}H_{57}N_6O_2$ (M^+): 701.4543. found: 701.4539.

Ligand 19[116]

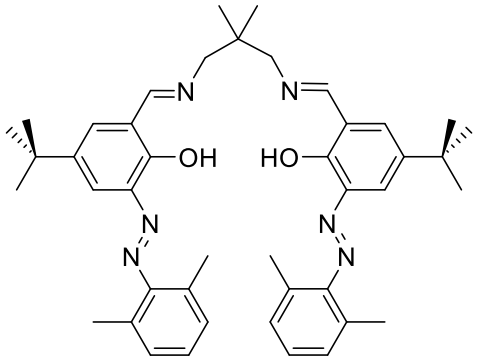

2,2-dimethylpropane-1,3-diamine (0.02 ml, 0.16 mmol) was added to a solution of **67** (100 mg, 0.32 mmol) in Ethanol (3 ml) and Chloroform (1 ml) at room temperature and the mixture was stirred for several hours to afford an orange suspension. After filtration, the product was recrystallized from EtOH/$CHCl_3$ to give ligand **19** (81 mg, 0.12 mmol, 73 %) as a red, crystalline solid.

^{1}H-NMR (500 MHz, CD_2Cl_2): δ = 14.13 (s, 2H), 8.53 (s, 2H), 7.77 (d, *J* = 2.5 Hz, 2H), 7.52 (d, *J* = 2.3 Hz, 2H), 7.18 – 7.10 (m, 6H), 3.61 (s, 6H), 2.37 (s, 12H), 1.35 (s, 18H), 1.14 (s, 6H) ppm. **^{13}C-NMR (126 MHz, CD_2Cl_2):** δ = 165.85, 157.41, 152.15, 141.49, 141.19, 131.60, 131.05, 129.35, 128.23, 120.79, 68.55, 36.72, 34.51, 31.44, 24.52, 18.98 ppm. **MS (ESI-HRMS):** calculated for $C_{43}H_{55}N_6O_2$ (M^+): 687.4387. found: 687.4366.

Ligand 20[116]

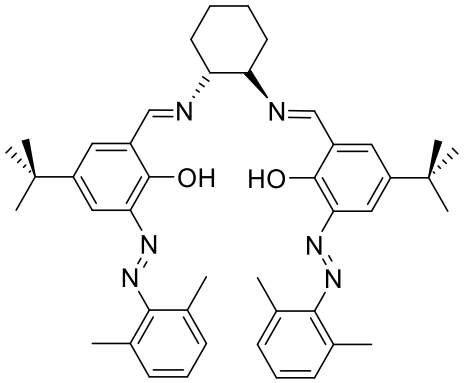

trans-cyclohexane-1,2-diamine (37 mg, 0.32 mmol) was added to a solution of **67** (200 mg, 0.64 mmol) in Ethanol (3 ml) and Chloroform (1 ml) at room temperature and the mixture was stirred for several hours to afford an orange suspension. After filtration, the product was recrystallized from EtOH/$CHCl_3$ to give ligand **20** (154 mg, 0.22 mmol, 68 % yield) as a red, crystalline solid.

^{1}H-NMR (500 MHz, CD_2Cl_2): δ = 13.89 (s, 2H), 8.45 (s, 2H), 7.68 (d, *J* = 2.5 Hz, 2H), 7.40 (d, *J* = 2.4 Hz, 2H), 7.13 (q, *J* = 4.7 Hz, 6H), 3.46 (dd, *J* = 5.8, 4.0 Hz, 2H), 2.33 (s, 12H), 2.01 (d, *J* = 14.3 Hz, 2H), 1.92 (d, *J* = 8.2 Hz, 2H), 1.81 (d, *J* = 8.6 Hz, 2H), 1.58 – 1.51 (m, 2H), 1.25 (s, 18H) ppm. **^{13}C-NMR (126 MHz, CD_2Cl_2):** δ = 164.92, 157.10, 152.03, 141.44, 141.00, 131.64, 131.07, 129.33, 128.21, 120.68, 73.28, 34.40, 33.43, 31.35, 24.61, 18.98 ppm. **MS (ESI-HRMS):** calculated for $C_{44}H_{53}N_6O_2$ (M^-): 697.4230. found: 697.4187.

Ligand 17[199]

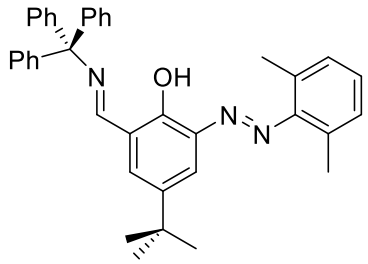

67 (1.49 g, 4.8 mmol) was dissolved in methanol (30 mL). Triphenylmethanamine (1.5 g, 5.78 mmol) and few droplets of formic acid were added to the solution. Afterwards, the mixture was heated to reflux and stirred for 3 days. The resulting red precipitate was filtered and washed with a small amount of cold methanol to yield ligand **17** as a red solid (2.41 g, 4.37 mmol, 91 %). **^{1}H-NMR (500 MHz, CD_2Cl_2)** δ = 14.49 (s, 1H), 8.18 (s, 1H), 7.81 – 7.12 (m, 20H), 2.37 (s, 6H), 1.33 (s, 9H) ppm. **^{13}C-NMR (75 MHz, CD_2Cl_2)** δ = 164.1, 156.7, 151.6, 144.6, 141.4, 140.6, 131.9, 130.7, 129.7, 129.0,

128.1, 127.9, 127.3, 120.8, 118.4, 79.1, 34.2, 31.0, 18.6 ppm. **MS (ESI-HRMS):** calculated for $C_{38}H_{38}N_3O$ (M^+): 252.3009. found: 252.3007.

5.1.2 Photoswitchable binuclear salen- complexes

2-(1,3-dioxan-2-yl)-4-nitrophenol (26)[200]

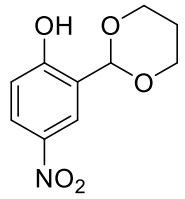

To solution of 2-hydroxy-5-nitrobenzaldehyde (5.00 g, 29.9 mmol),triethylorthoformiate (11.0 ml, 65.8 mmol) und propane-1,3-diol (25.0 ml, 346 mmol) in benzene (60 ml) tetrabutylammonium tribromid (0.29 g, 0.6 mmol) were added and stirred at ambient temperature for 12h. Water (100ml) was added to the reaction mixture and extracted with ethylacetate (2 x 100 ml) dried over anhydrous $MgSO_4$ and concentrated *in vacuo*. Recristalization of the crude from n-hexane/chloroform (3:1) afforded **26** (5.05 g, 22.42 mmol, 75%) as a white solid.

^{1}H-NMR (500 MHz, CD_2Cl_2) δ = 8.78 (s, 1H), 8.15 – 8.08 (m, 2H), 6.94 (dd, 1H), 5.73 (s, 1H), 4.35 – 4.30 (m, 2H), 4.08 – 4.02 (m, 2H), 2.38 – 2.16 (m, 1H), 1.59 – 1.50 (m, 1H) ppm. **^{13}C-NMR (126 MHz, CD_2Cl_2)** δ = 161.6, 141.2, 126.7, 125.0, 123.6, 118.2, 101.9, 68.2, 26.1 ppm. **MS (ESI-HRMS):** calculated for $C_{10}H_{10}NO_5$ (M^-): 224.0564. found: 224.0584.

(2-(1,3-dioxan-2-yl)-4-nitrophenoxy)(tert-butyl)dimethylsilane (27)

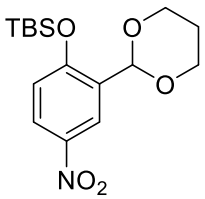

To a solution of **26** (2.79 g, 12.39 mmol) and imidazole (2.53 g, 37.20 mmol) in dry dichloromethane (10 ml), a solution of TBS-Cl (2.80 g, 18.58 mmol) in dichloromethane (10 mL) was added dropwise, and the reaction was stirred overnight at ambient temperature. Saturated NH_4Cl (300 mL) was added, the two phases were separated, and the aqueous layer was extracted with dichloromethane (3 × 100 mL). The combined organic layers were washed with brine, dried over anhydrous $MgSO_4$ and concentrated *in vacuo*. The residue was purified by chromatography on silica gel (DCM:PE = 2:1) to afford **27**(4.20 g, 12.37 mmol, 99% yield)

as a pale yellow oil.

^{1}H-NMR (300 MHz, CD_2Cl_2) δ = 8.44 (d, *J* = 3.0 Hz, 1H), 8.10 (dd, *J* = 9.0, 3.0 Hz, 1H), 6.87 (d, *J* = 9.0 Hz, 1H), 5.75 (s, 1H), 4.27 – 4.15 (m, 2H), 4.02 – 3.87 (m, 2H), 2.32 – 2.07 (m, 1H), 1.50 – 1.37 (m, 1H), 1.05 (s, 9H), 0.30 (s, 6H).ppm. **^{13}C-NMR (75 MHz, CD_2Cl_2)** δ = 159.16, 142.24, 131.23, 125.95, 124.52, 119.32, 96.67, 68.08, 26.30, 25.86, 18.70, -4.06 ppm. **MS (ESI-HRMS):** calculated for $C_{16}H_{26}NO_5Si$ (M^+): 340.1575. found: 340.1333.

4-((tert-butyldimethylsilyl)oxy)-3-(1,3-dioxan-2-yl)aniline (28)

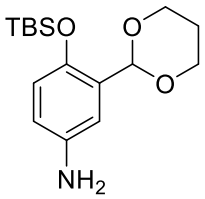

A mixture of **27** (1.00 g, 2.95 mmol) and Pd-C (0.31 g, 0.29 mmol) was stirred in Ethanol (50 ml) under hydrogen atmosphere (1atm) for 1h. After a full consumption of the starting material the mixture was filtered of a plug of celite (eluent: EA) and concentrated under reduced pressure *in vacuo*. The residue was purified by flash chromatography on silica gel (DCM:MeOH = 50:1) to afford **28** (0.91 g, 2.95 mmol, 99% yield) as a pale yellow oil.

^{1}H-NMR (300 MHz, CD_2Cl_2) δ = 6.85 (d, *J* = 2.9 Hz, 1H), 6.59 (d, *J* = 8.5 Hz, 1H), 6.52 (dd, *J* = 8.5, 2.9 Hz, 1H), 5.68 (s, 1H), 4.21 – 4.11 (m, 2H), 3.96 – 3.83 (m, 2H), 3.44 (br, 1H), 2.23 – 2.05 (m, 1H), 1.43 – 1.34 (m, 1H), 1.01 (s, 9H), 0.17 (s, 6H) ppm. **^{13}C-NMR (75 MHz, CD_2Cl_2)** δ = 145.45 (s), 141.23, 130.55, 120.09, 116.77, 114.48, 97.85, 68.03, 26.53, 26.16, 18.65, -4.11 ppm. **MS (ESI-HRMS):** calculated for $C_{15}H_{28}NO_3Si$ (M^+): 310.1833. found: 310.1480.

1,2-bis(4-((tert-butyldimethylsilyl)oxy)-3-(1,3-dioxan-2-yl)phenyl)diazene (29)[93]

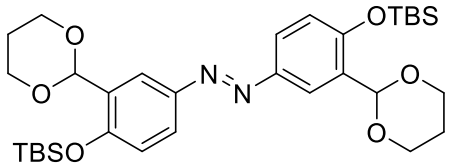

Copper (I) bromide (1.76 g, 12.28 mmol), pyridine (2.98 ml, 36.8 mmol), and **28** (3.80 g, 12.28 mmol) were mixed in dichloromethane (150 ml) under air (1 atm). The reaction mixture was stirred vigorously at ambient temperature for 20 h and concentrating under vacuum, the residue was purified by flash chromatography on a short silica gel (DCM:PE = 1:1) to afford **29** (2.93, 4.76 mmol, 78%) as a yellow solid.

^{1}H-NMR (500 MHz, $CDCl_3$) δ = 8.21 (d, *J* = 2.5 Hz, 2H), 7.84 (dd, *J* = 8.7, 2.5 Hz, 2H), 6.87 (d, *J* = 8.7 Hz, 2H), 5.83 (s, 2H), 4.30 – 4.23 (m, 4H), 4.03 – 3.91 (m, 4H), 2.36 – 2.21 (m, 2H), 1.48 – 1.39 (m, 2H), 1.05 (s, 18H), 0.28 (s, 12H) ppm. **^{13}C-NMR (126 MHz, $CDCl_3$)** δ = 155.25, 147.01, 130.10, 124.45, 122.97, 119.11, 97.32, 67.71, 29.84, 25.86, 18.43, -4.10.ppm. **MS (ESI-HRMS):** calculated for $C_{32}H_{51}N_2O_6Si_2$ (M^+): 615.3280. found: 615.3302.

Disalicylaldehyde functionalized azobenzene (30)[201]

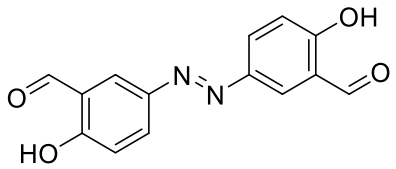

A mixture of **29** (200 mg, 0.325 mmol) and iodine (8 mg, 0.033 mmol) in acetone (20 ml) was stirred at refluxing temperature for 5 min. The product precipitated from the reaction mixture. Filtration afforded the product (59 mg, 0.218 mmol, 67%) as a yellow powder.

^{1}H-NMR (300 MHz, Acetone-d6) δ = 11.32 (s, 2H), 10.23 (s, 2H), 8.40 (d, *J* = 2.4 Hz, 2H), 8.20 (dd, *J* = 8.8, 2.5 Hz, 2H), 7.19 (d, *J* = 8.9 Hz, 2H) ppm. A ^{13}C-NMR could not be recorded due to low solubility in all common NMR-solvents. **MS (ESI-HRMS):** calculated for $C_{14}H_9N_2O_2$ (M^-): 269.0568. found: 269.0576.

2-hydroxy-5-(4,4,5,5-tetramethyl-1,3,2-dioxaborolan-2-yl)benzaldehyde (32)

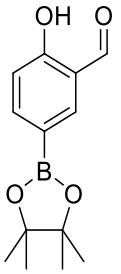

Potassium acetate (3.72 g, 37.9 mmol) and Pd(Cl_2)dppf (0.935 g, 1.313 mmol were added to a solution of bis(pinacolato)diboron (3.00 g, 14.92 mmol) in dioxane (20ml). The solution was stirred for 15 min at room temperature. 5-bromo-2-hydroxybenzaldehyde (4.62 g, 18.19 mmol) was then added, the resulting solution was heated to 85°C and stirred for 20h. The reaction was then quenched by the addition of water (200 mL). The resulting solution was extracted with ethyl acetate (4 x 50 mL), dried over anhydrous $MgSO_4$ and concentrated in vacuo to give a residue, which was purified by silica gel column chromatography eluting with (PE/DCM = 1:1) and then pure DCM to afford **32** (2.88 g, 11.62 mmol, 78%).

^{1}H-NMR (500 MHz, $CDCl_3$): δ = 11.22 (s, 1H), 9.92 (s, 1H), 8.04 (d, J = 1.6 Hz, 1H), 7.94 (dd, J = 8.4, 1.6 Hz, 1H), 6.98 (d, J = 8.4 Hz, 1H), 1.35 (s, 12H) ppm. **^{13}C-NMR (126 MHz, $CDCl_3$): δ =** 197.09, 164.15, 143.36, 141.57, 117.22, 84.22, 25.01 ppm. **MS (ESI-HRMS):** calculated for $C_{12}H_{20}BN_2O_2$ (M^+): 249.1293. found: 264.0775.

1,2-bis(3-bromophenyl)diazene (33)[202]

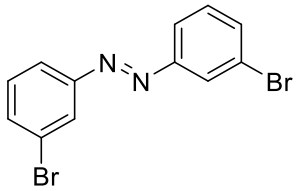

A mixture of 3-bromoaniline (6.15 ml, 56.5 mmol) and (diacetoxyiodo)benzene (17.29 g, 53.7 mmol) in CH_2Cl_2 (390 mL) was transferred to a 1-L round-bottom flask. The resulting solution was stirred at room temperature for 21 h until complete consumption of the aniline was observed by TLC. After the reaction was complete, the resulting solution was extracted from brine (2 x 500 mL), dried with $MgSO_4$, and concentrated under reduced pressure. The resulting crude product was purified through a silica-gel column (EtOAc/PE = 1:50). Azobenzene **33** (6.34 g, 66 %) was obtained as a fluffy yellow solid.

^{1}H-NMR (500 MHz, $CDCl_3$) δ = 7.99 (t, *J* = 1.9 Hz, 2H), 7.82 (ddd, *J* = 7.9, 1.8, 1.0 Hz, 2H),

7.55 (ddd, *J* = 8.0, 2.0, 1.1 Hz, 2H), 7.35 (t, *J* = 7.9 Hz, 2H) ppm. **^{13}C-NMR (126 MHz, $CDCl_3$)** δ = 153.17, 134.14, 130.53, 124.75, 123.24, 123.21 ppm. **MS (ESI-HRMS):** calculated for $C_{12}H_8Br_2N_2$ (M^-): 337.9060. found: 337.9074.

3',3'''-(diazene-1,2-diyl)bis(4-hydroxy-[1,1'-biphenyl]-3-carbaldehyde) (34)

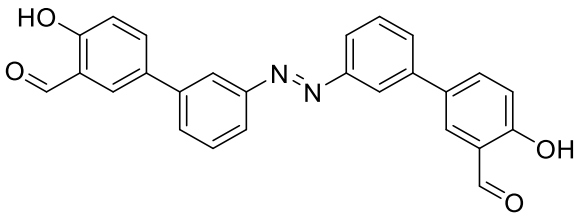

32 (889 mg, 3.58 mmol), azobenzene **33** (203 mg, 0.597 mmol), caesium carbonate (2.334 g, 7.16 mmol) and $PdCl_2$(dppf)-CH_2Cl_2 (29 mg, 0.036 mmol) were dissolved in THF (24 ml), ethanol (24 ml) und DMF (6,00 ml). The resulting solution was stirred at room temperature for 3h. The mixture was taken up in EtOAc (200 mL), washed with brine (3x 200 mL) dried over $MgSO_4$ and concentrated in vacuo to give a residue, which was purified by silica gel column chromatography eluting (DCM/PE = 1:1 then 7:3). The resulting product was recrystallized in ethanol and trichloromethane to give azobenzene **34** (0.175 g, 0.414 mmol, 69%).

^{1}H-NMR (500 MHz, DMSO-d_6): δ = 10.96 (s, 1H), 10.35 (s, 1H), 8.18 (t, J = 1.9 Hz, 1H), 8.07 (d, J = 2.8 Hz, 1H), 8.00 (dd, J = 8.7, 2.5 Hz, 1H), 7.91 (ddd, J = 7.8, 1.9, 1.0 Hz, 1H), 7.88 (ddd, J = 7.8, 2.0, 1.1 Hz, 1H), 7.70 (t, J = 7.9 Hz, 1H), 7.16 (d, J = 8.7 Hz, 1H) ppm. **^{13}C-NMR (126 MHz, DMSO-d_6):** δ = 191.87, 190.86, 161.17, 160.07, 154.44, 153.25, 151.82, 140.81, 135.09; 131.23, 122.98, 118.69 ppm. **MS (ESI-HRMS):** calculated for $C_{26}H_{19}N_2O_4$ (M^+): 423.1339. found: 423.1250.

***trans*-2-aminocyclohexan-1-aminium chloride[174]**

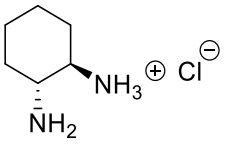

Under inert atmosphere *trans*-cyclohexyl diamine (2.1 ml, 17.5 mmol) was dissolved in dry diethylether (15 ml). A solution of HCl in dioxane (4M, 4.4ml, 17.7mmol, 1.01 eq) was added to the diamine under fast stirring. Formation of white precipitate is observed. The solution was stirred at room temperature for 20h. The resulting product was filtered and washed with diethylether to give the product (2.57 g, 17.03 mmol, 97%). The compound was directly used without further purification.

2-(((2-(l4-azanyl)cyclohexyl)imino)methyl)-4,6-di-tert-butylphenol, chloride salt (35)[174]

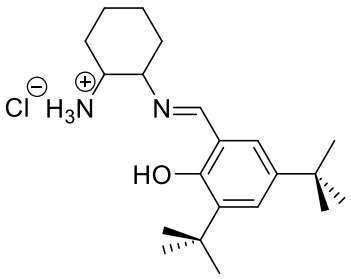

Under inert atmospheres *trans*-2-aminocyclohexan-1-aminium chloride (2.57 g, 17.03 mmol) was dissolved in a mixture (1:1) dry methanol/dry ethanol (120 ml). Then **57** (3.99 g, 17.03 mmol) was added under stirring. The solution was stirred at room temperature for 72h. The solvent was then reduced under vacuum and the product wash with DCM to give **35** (4.27 g, 11.63 mmol, 68%). The chloride salt was used without further purification.

Ligand 38

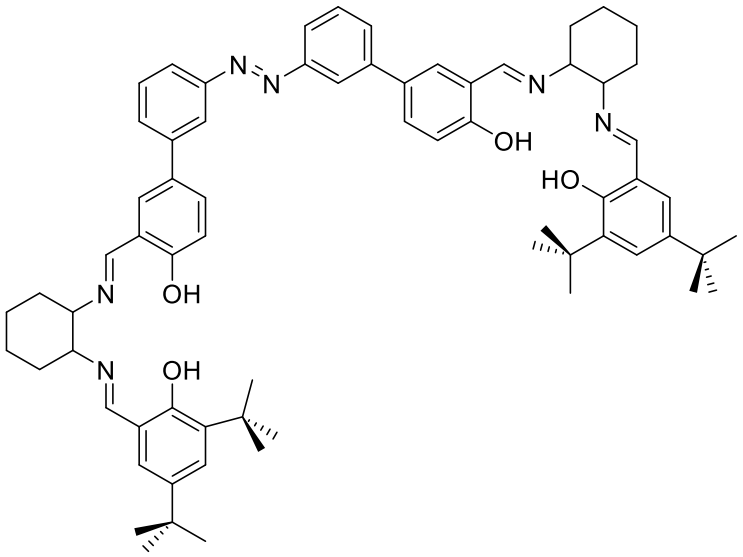

The reaction was performed under inert atmosphere. Azobenzene **34** (400 mg, 0.947 mmol) was added to a schlenk tube with 3A molecular sieves in DCM (10 ml). **35** was dropped rapidly to a second schlenk tube with triethylamine (0.63 ml, 4.55 mmol) in DCM (10 ml). The solution was added into the first schlenk tube and stirred at room temperature for 20h to give the crude product (1.1 g). 300 mg of the crude product was then purified by GPC (eluent: THF) to give **11** (87 mg, mmol, 34%).

^{1}H-NMR (500 MHz, CD_2Cl_2): δ = 13.67 (s, 2H), 13.42 (s, 2H), 8.41 (s, 2H), 8.29 (s, 2H), 8.07 (q, *J* = 1.7 Hz, 2H), 7.85 (dt, *J* = 7.8, 1.4 Hz, 2H), 7.62 – 7.60 (m, 2H), 7.59 (t, *J* = 1.9 Hz, 2H), 7.55 (t, *J* = 7.8 Hz, 2H), 7.50 (dd, *J* = 2.3, 1.4 Hz, 2H), 7.28 (d, *J* = 2.5 Hz, 2H), 7.00 (d, *J* = 2.5

Hz, 2H), 6.97 (d, *J* = 8.7 Hz, 2H), 3.47 – 3.39 (m, 2H), 3.38 – 3.29 (m, 2H), 2.06 – 1.73 (m, 18H), 1.37 (d, *J* = 9.6 Hz, 18H), 1.21 – 1.19 (m, 18H) ppm. **^{13}C-NMR (126 MHz, CD_2Cl_2):):** δ = 166.52, 165.45, 158.39, 153.64, 141.83, 140.65, 136.77, 131.31, 130.46, 130.00, 129.55, 127.37, 126.62, 121.59, 121.31, 118.37, 117.79, 108.53, 98.96, 73.34, 72.90, 68.17, 35.39, 34.49, 33.74, 33.41, 31.68, 29.66, 24.83, 24.47 ppm. **MS (ESI-HRMS):** calculated for $C_{68}H_{83}N_6O_4$ (M^+): 1047.6470. found: 1047.6464.

Co (II) Ligand 38[131]

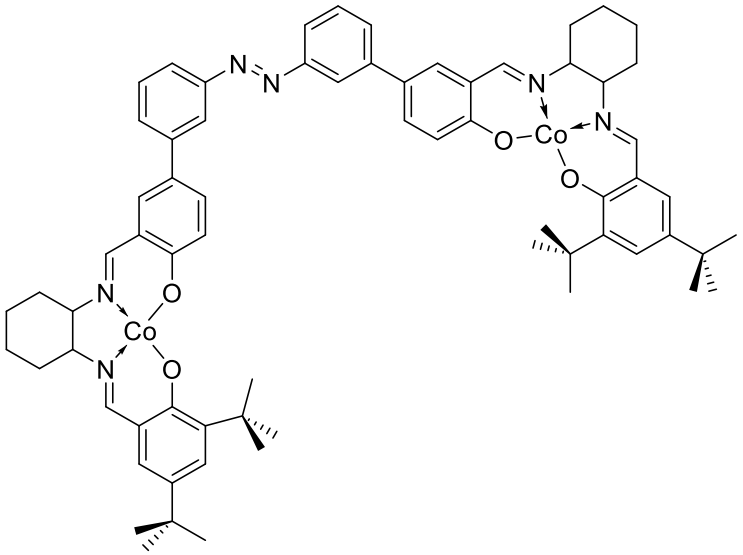

Under inert atmosphere cobalt acetate tetrahydrate (37 mg, 0.148 mmol, 2.1 eq) was put in a schlenk tube and heated under vacuo until the color changed from pink to purple. It was then dissolved in ethanol (5 ml). Ligand **38** (74 mg, 0.071 mmol, 1 eq) was dissolved in DCM (2 ml) in a second schlenk tube and added into the cobalt acetate solution. The mixture was first heated to 70°C for 1h then up to 80°C for 1h and finally slowly cooled down to room temperature. The red precipitate was then filtered and washed with ethanol (5 ml) and pentane (10 ml). Complex **12** was obtained as dark red solid (45 mg, 0.039 mmol, 55%).

MS (ESI-HRMS): calculated for $C_{68}H_{83}Co_2N_6O_4$ (M^+): 1160.4821. found: 1160.4717.

Co(III)-complex 31[131]

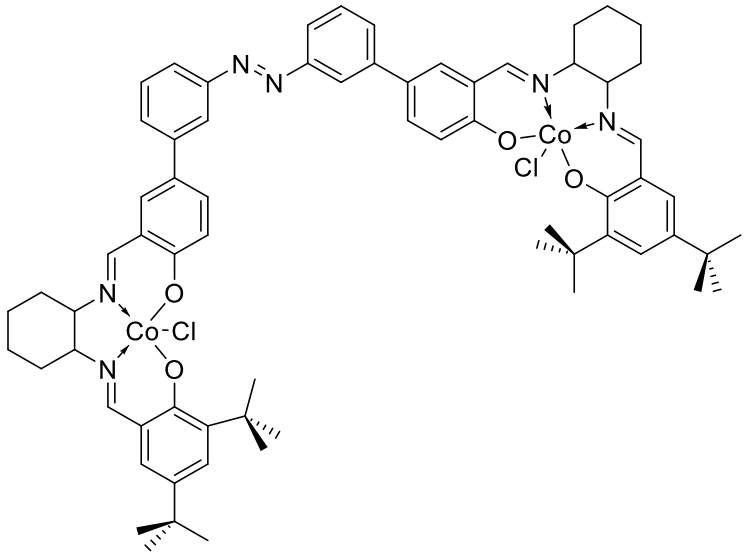

Complex **Co(II)-Ligand 38** (45 mg, 0.039 mmol) was put into a flask and dissolved in dichloromethane (10 ml). Then was *para*-toluenesulfonic acid monohydrate (16 mg, 0.084 mmol) added. The resulting solution was stirred open to air for 72h, during which all solvent evaporated. The dark solids were redissolved in dichloromethane (70 ml) and washed with brine (3x 100ml), then dried over magnesium sulfate and filtered. The solvent was removed and the dark green solid was washed with pentane (5 ml) to afford complec **31** (24 mg, 0.020 mmol, 51%).

^{1}H NMR (500 MHz, DMSO-d_6): δ = 8.25 (d, *J* = 11.9 Hz, 2H), 7.96 – 7.90 (br, 4H), 7.86 (d, *J* = 7.9 Hz, 2H), 7.72 (t, *J* = 7.5 Hz, 2H), 7.51 (d, *J* = 8.7 Hz, 2H), 7.47 – 7.42 (br, 2H), 3.70 – 3.55 (br, 2H), 3.12 – 2.99 (br, 4H), 2.06 – 1.85 (br, 4H), 1.75 (s, 18H), 1.69 – 1.53 (m, 4H), 1.30 (s, 18H). **MS (ESI-HRMS):** calculated for $C_{68}H_{83}Co_2N_6O_4$ (M^+-2Cl): 1160.4749. found: 1160.4668.

5.1.3 Photoswitchable binuclear Salphen- Complex

1,2-bis(3-bromo-4-methylphenyl)diazene (37)[93]

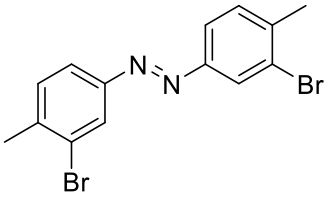

3-bromo-4-methylaniline (1.00 g, 5.37 mmol), copper (I) bromide (0.77 g, 5.37 mmol) and pyridine (1.30 ml, 16.12 mmol) were dissolved in dichloromethane (20 ml). The resulting solution was stirred at room temperature for 48h. The residue was filtered over celite and washed with dichloromethane. It was then washed with brine (3x 300 ml), dried over $MgSO_4$ and purified by silica gel column chromatography eluting (DCM/PE = 1:1) to afford **37** (797 mg, 2.16 mmol, 40%).

^{1}H-NMR (500 MHz, $CDCl_3$): δ = 8.09 (d, J = 1.9 Hz, 2H), 7.78 (dd, J = 8.0, 2.0 Hz, 2H), 7.39 (d, J = 8.1 Hz, 2H), 2.48 (s, 6H) ppm. **^{13}C-NMR (126 MHz, Chloroform-*d*):** δ = 151.54, 141.33, 131.27, 125.83, 125.63, 123.07, 23.19 ppm.

5',5'''-(diazene-1,2-diyl)bis(4-hydroxy-2'-methyl-[1,1'-biphenyl]-3-carbaldehyde) (38)

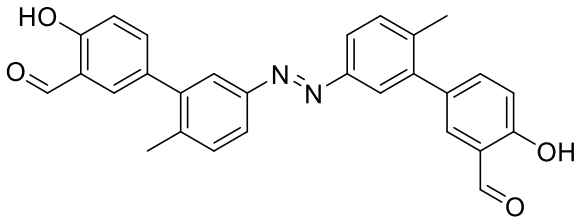

Azobenzene **37** (490 mg, 1.330 mmol), **32** (990 mg, 3.99 mmol) and caesium carbonate (5.20 g, 15.96 mmol) were dissolved in THF (40 ml), Ethanol (40 ml) and DMF (10 ml). The solution was degassed and $PdCl_2$(dppf) (58 mg, 0,080 mmol) was added. The resulting solution was stirred at room temperature for 20h. The mixture was dissolved in EtOAc (300 ml) and washed with brine (3x 200 ml) and dried over $MgSO_4$. The crude product was purified through column chromatography with (DCM/PE = 1:1) as eluent. The solid was then recrystallized in ethanol and chloroform to yield **38** (270 mg, 0.599 mmol, 45%).

^{1}H-NMR (500 MHz, $CDCl_3$): δ = 11.05 (s, 2H), 9.94 (s, 2H), 7.84 (dd, J = 8.1, 2.2 Hz, 2H), 7.79 (d, J = 1.9 Hz, 2H), 7.58 (q, J = 2.5, 2.0 Hz, 2H), 7.56 (d, J = 2.5 Hz, 2H), 7.43 (d, J = 8.7 Hz, 2H), 7.08 (d, J = 8.1 Hz, 2H), 2.35 (s, 6H) ppm. **^{13}C NMR (126 MHz, $CDCl_3$):** δ = 196.69, 160.96 , 151.15, 140.88, 139.05, 138.01, 134.09, 133.20, 131.49, 123.93 , 122.42, 120.55,

117.77, 20.72 ppm. **MS (ESI-HRMS):** calculated for $C_{28}H_{23}N_2O_4$ (M^+): 451.1652. found: 451.1652.

2-(*tert*-butyl)-4-((triisopropylsilyl)oxy)phenol[203]

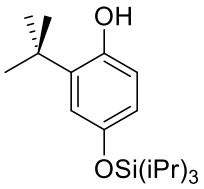

To a solution of *tert*-butylhydroquinone (5.00 g, 30.1 mmol) in DCM (300 mL) was added imidazole (2.66 g, 39.1 mmol) and DMAP (1.84 g, 15.1 mmol). To the resulting solution was added triisopropylsilyl chloride (6.96 g. 36.1 mmol) in 25 mL DCM in a dropwise manner, and the mixture was then stirred for 15 h at ambient temperature. The mixture filtered and the solution was concentrated under vacuum. The residue was purified by chromatography (DCM/PE = 1:10) to yield the product as a clear liquid (8.02 g, 2,5 mmol, 88%).

^{1}H NMR (300 MHz. $CDCI_3$): δ = 6.81 (s, 1 H). 6.64-6.54 (m, 2H). 3.12(s. 1 H), 1.46 (s.9H). 1.33-1.21 (m. 3H). 1.16 (m, 18H) ppm.

3-(*tert*-butyl)-2-hydroxy-5-((triisopropylsilyl)oxy)benzaldehyde[203]

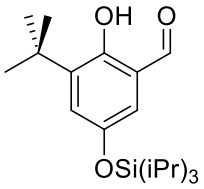

Triethylamine (1.85 ml, 2.0 mmol) was added dropwise to a solution of 4-(tert-butyl)phenol (3.22 g, 10.0 mmol), magnesium chloride (19,01 g, 200 mmol) and paraformaldehyde (660 mg, 22.0 mmol) in dry THF (50 ml) under a nitrogen atmosphere. After heating at reflux for 24 h, diluted HCl was added at RT until the precipitate dissolved. Most of the THF was removed by rotary evaporation, then the aqueous phase was extracted with CH_2Cl_2 (3x 25 mL). The combined organic phases were dried over $MgSO_4$, filtered, and concentrated under reduced pressure. Silica gel flash column chromatography (DCM/PE = 1:20) of the residue gave the product (3.12 g, 8.9 mmol, 89%)

^{1}H NMR (400 MHz, $CDCI_3$,): δ = 9.78 (s. 1 H). 7.14 (d, *J* = 2.9 Hz. 1 H). 6.86 (d, J=2.9Hz. IH). 1.28-1.22 (m, 3H), 1.15 (d, J=7.2Hz. 18H) ppm.

3-(tert-butyl)-2,5-dihydroxybenzaldehyde[176]

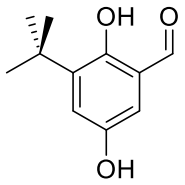

A tetrabutylammonium flouride solution (1.0 M in THF, 10 mL, 10 mmol) was added dropwide to a solution 3-(*tert*-butyl)-2-hydroxy-5-((triisopropylsilyl)oxy)benzaldehyde (3.0 g, 8.5 mmol) in 60 mL THF at-78 'C and allowed to warm to room temperature over 3 h. The reaction mixture was poured into 100 mL water and extracted (100mL x 3) with DCM. The organic layers were combined, washed with saturated aqueous ammonium chloride (100 mL x 2), dried over magnesium sulfate and concentrated. The product was purified by silica gel chromatography (DCM/PE = 1:5) to give 1.1 g (5.4 mmol, 63%) product as a yellow solid. Mp

1H-NMR (300 MHz, CDC1$_3$): δ = 10.12 (s, 1H), 7.25 (d, J = 1.6 Hz, 1H), 7.10(d, J = 1.4 Hz, 1H), 1.48 (s, 9H) ppm.

Ligand 41[176]

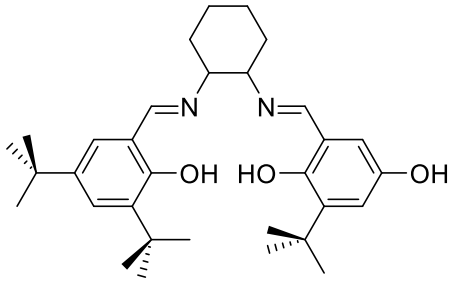

The reaction was performed under inert atmosphere. 3-(tert-butyl)-2,5-dihydroxybenzaldehyde 5 (1.00, 1.90 mmol) was added to a schlenk tube with 3 Å molecular sieves in DCM (10 ml). **35** (0.69 g, 1.90 mmol) was added to a second schlenk tube with triethylamine (1.3 ml, 9.1 mmol) in DCM (10 ml). The solution was added into the first schlenk tube and stirred at room temperature for 20 h to give the crude product (0.76 g). 300 mg of the crude product was then purified by GPC (eluent: THF) to give **41** (60 mg, mmol, 25%).

^{1}H-NMR (300 MHz, CD_2Cl_2): δ = 8.35 (s, 1H), 8.12 (s, 1H), 7.42 (d, J 2.3, 1H), 7.05 (d, J=2.3, 1H), 6.87 (d, J= 2.3, 1H), 6.44 (d, J= 2.3, 1H), 3.29 (m, 2H), 1.89 (m, 4H), 1.71 (m,4H), 1.52 (s, 9H), 1.42 (s, 9H), 1.32 (s, 9H) ppm.

4,4'-(diazene-1,2-diyl)dibenzoic acid (42)[204]

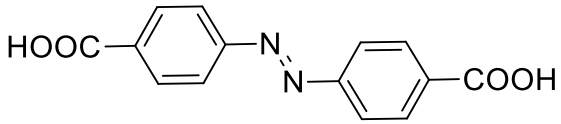

5.0 g (30 mmol) 4-nitrobenzoic acid and 16.6 g (92 mmol) NaOH were dissolved in 75 mL water and the solution was stirred at 60 °C. In a beaker, 33.0 g (183 mmol) glucos was dissolved in 50 mL water at 70 °C. The glucose solution was added dropwise over one hour to the solution of nitrobenzoic acid. After the addition was complete, the solution was left to stir at 60 °C for 1 hour, after it cooled to room temperature the solution was stir for 18 hours. The precipitate was filtered on a fritted funnel to yield a crude orange powder. The solid was dissolved in 375 mL water, then acidified to pH ~ 3. The pink precipitate was filtered, washed with water and to dried to yield 3.1 g (23.4 mmol, 78%)

^{1}H NMR (300 MHz, DMSO-d_6): δ = 13.17 (br. s., 1 H), 8.15 (d, *J*=8.78 Hz, 4 H), 8.00 (d, *J*=8.78 Hz, 4 H) ppm.

3-bromo-2,6-difluoroanilin (44)

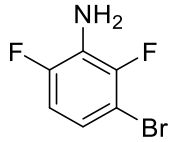

To 2,6-difluoroaniline (20.00 g, 155 mmol) in acetic acid (90 ml), Ac_2O (17.54 ml, 186 mmol) were added and stirred at 90°C for 1h. After cooling to room temperature the solution was extracted with DCM (3 x 30 mL). The organic phases were then evaporated. The crude N-(2,6-difluorophenyl)acetamide (25.50 g, 149 mmol) was disolved in TFA (120 ml) and conc. H_2SO_4 (160 ml) and NBS (26.50 g, 149 mmol) was added in small portions. The Reaction mixture was stirred at room temperature overnight. The reaction mixture was extracted three times with DCM (30 mL). Most of the solvent was removed and then taken-up in Ethanol (100 ml) and conc. HCl (100 ml). The mixture was stirred at 70°C for 18 h. After cooling to room temperature Ethanol was evaporated and **44** (19.10 g, 92 mmol, 69 % yield) precipitated.

^{1}H-NMR (300 MHz, $CDCl_3$): δ = 6.78 (dddd, J = 10.7, 10.0, 8.1, 3.7 Hz, 2H), 3.83 (s, 2H) ppm. **^{13}C-NMR (75 MHz, $CDCl_3$):** δ = 119.75, 119.64, 111.93, 111.67 ppm.

1-bromo-2,4-difluoro-3-nitrosobenzene

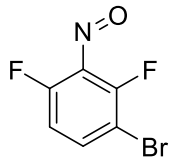

To **44** (0.25 g, 1.20 mmol) was added DCM (20 mL), Water (12 mL), and OXONE (1.48 g, 2.40 mmol) and stirred vigorously for 44 h. The organic phase was removed, washed with 1 M HCl (2 x 10 mL), saturated $NaHCO_3$ (2 x 10 mL), water (10 mL) and then brine (10 mL). The organic player was dried over $MgSO_4$, filtered and 5 mL toluene was added to prevent the product (**4b**) (1.07 g, 4.81 mmol, 100%) from dryness and then evaporated. The nitrose compound was used without further purification.

1,2-bis(3-bromo-2,6-difluorophenyl)diazene (45)

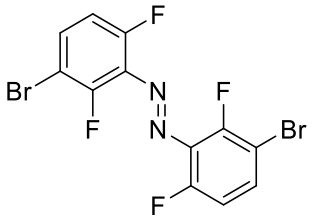

3-bromo-2,6-difluoroaniline (**4**) (208 mg, 1.00 mmol), Acetic Acid (10 ml) and TFA (1.7 ml) were added to 1-bromo-2,4-difluoro-3-nitrosobenzene (0.27 g, 1.20 mmol) in the toluene residue. The soution was left to stir at room temperature overnight. The reaction mixture was quenched with saturated $NaHCO_3$ and ethylacetate was added and dried over $MgSO_4$. The crude product was purified by column chromatography (DCM/PE; 5:95) to (DCM/PE; 10:90) to give the azobenzene (1.51 g, 3.67 mmol, 49%). The product was not stable enough to measure an NMR spectrum.

MS (ESI-HRMS): calculated for $C_{12}H_4N_2F_4Br_2$ (M^+): 457.8452. found: 457.6742.

Azobenzene (47)

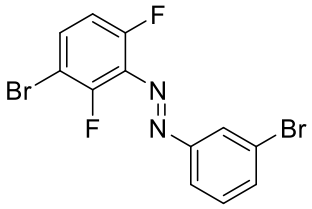

To **44** (1.00 g, 4.81 mmol) DCM (100 ml), Water (60 ml), and OXONE (5.91 g, 9.62 mmol) were added and stir vigorously overnight at room temperature. The organic phase was removed, washed with 1 M HCl, saturated $NaHCO_3$, water and brine, dried over $MgSO_4$ and 20 mL toluene was added to prevent the 1-bromo-2,4-difluoro-3-nitrosobenzene from dryness and was then evaporated. To the toluene residue 3-bromoaniline (0.44 ml, 4.01 mmol), acetic acid (50 ml) and TFA (8,33 ml) were added, and left to stir at room temperature overnight. The solution was quenched with saturated $NaHCO_3$ and ethylacetate. The organic layer was dried over $MgSO_4$ and purified with column chromatography to (DCM/PE = 1:9) to give **47** (0.22 g, 0.59 mmol, 15 % yield).

^{1}H-NMR (500 MHz, $CDCl_3$): δ = 8.05 (t, J = 1.9 Hz, 1H), 7.90 (ddd, J = 8.0, 1.7, 1.2 Hz, 1H), 7.66 (ddd, J = 7.9, 1.8, 1.0 Hz, 1H), 7.56 (ddd, J = 9.0, 7.2, 5.4 Hz, 1H), 7.42 (t, J = 7.9 Hz, 1H), 7.03 – 6.97 (m, 1H) ppm. **^{13}C-NMR (126 MHz, $CDCl_3$):** δ = 156.19, 154.14, 153.24, 151.20, 135.09, 133.63, 131.92, 130.70, 124.98, 123.32, 113.48, 105.57 ppm.

4-(4,4,5,5-tetramethyl-1,3,2-dioxaborolan-2-yl)benzene-1,2-diamine (50)[205]

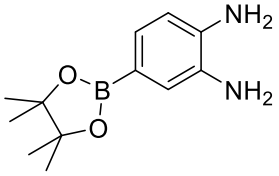

Dioxane (24.0 mL) was added via syringe to a flame-dried Schlenk tube equipped with a stir bar and subjected to three freeze-pump-thaw cycles. Then dichlorobis(tricyclohexylphosphine)palladium(II) (0.34 g, 0.46 mmol), bis(pinacolato)diboron (3.26 g, 12.83 mmol), 4-bromobenzene-1,2-diamine (2.00 g, 10.69 mmol), and potassium acetate (1.57 g, 16.04 mmol) were quickly added under argon. The solution was then stirred at 80 °C for 42 h. After the completion of the reaction was confirmed by UPLC, it was diluted with EtOAc (400 mL) and extracted from brine (2 x 400 mL). The resulting crude product was dried with $MgSO_4$, concentrated under reduced pressure, and purified through column

chromatography (DCM/MeOH = 50:1). **50** (1.80 g, 72 %) was isolated as an off-white solid.

^{1}H-NMR (300 MHz, $CDCl_3$): δ = 7.10 (dd, J = 7.5 Hz, 1.0 Hz, 1H), 7.08 (d, J = 1.0 Hz, 1H), 6.66 (d, J = 7.5 Hz, 1H), 3.9-3.3 (s, broad, 4H), 1.29 (s, 12H) ppm. **^{13}C-NMR (75 MHz, $CDCl_3$):** δ = 139.2, 133.8, 128.2, 123.5, 115.7, 83.8, 25.2 ppm. **MS (ESI-HRMS):** calculated for $C_{12}H_{20}BN_2O_2$ (M^+): 235.1612. found: 235.1096.

(E)-3',3'''-(diazene-1,2-diyl)bis(([1,1'-biphenyl]-3,4-diamine)) (56)[205]

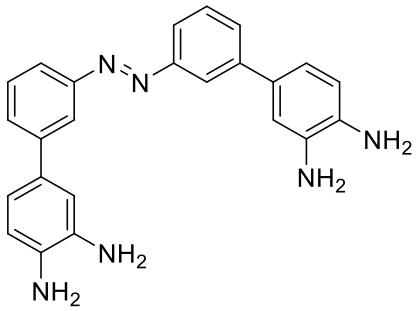

To a flame-dried Schlenk tube was added a mixture of dioxane (27.0 ml) and water (2.67 ml). The solution was subjected to three freeze-pump-thaw cycles and left under argon atmosphere. Then $Pd(dppf)Cl_2$ (0.11 g, 0.15 mmol), azobenzene **33** (1 g, 2.94 mmol), diamine **50** (1.65 g, 7.06 mmol), and potassium carbonate (2.03 g, 14.71 mmol) were added to the Schlenk tube. The sealed reaction mixture was refluxed at 110 °C for 21 h. At the conclusion of the reaction, the mixture was diluted with ethyl acetate (300 mL) and washed with brine (2 x 400 mL). The crude product was dried with $MgSO_4$, concentrated, and purified by column chromatography (CH_2Cl_2/MeOH = 50:1). Azobenzene **56** (800 mg, 69 %) was concentrated to dryness, resulting in a red solid.

^{1}H-NMR (500 MHz, DMSO-D_6): δ = 8.02 (dd, *J* = 1.8 Hz, 2H), 7.76 (ddd, *J* = 7.8, 1.8, 1.0 Hz, 2H), 7.71 (ddd, *J* = 7.7, 1.6, 1.1 Hz, 2H), 7.59 (dd, *J* = 7.8 Hz, 2H), 7.00 (d, *J* = 2.1 Hz, 2H), 6.87 (dd, *J* = 8.0, 2.1 Hz, 2H), 6.63 (d, *J* = 8.0 Hz, 2H), 4.68 (d, *J* = 36.6 Hz, 2H) ppm. **^{13}C-NMR (126 MHz, DMSO-D_6):** δ = 152.43, 142.51, 135.56, 135.29, 129.71, 128.30, 127.71, 119.81, 119.10, 115.85, 114.61, 112.45 ppm. **MS (ESI-HRMS):** calculated for $C_{24}H_{23}N_6$ (M^+): 395.1979. found: 395.1979.

Ligand 58

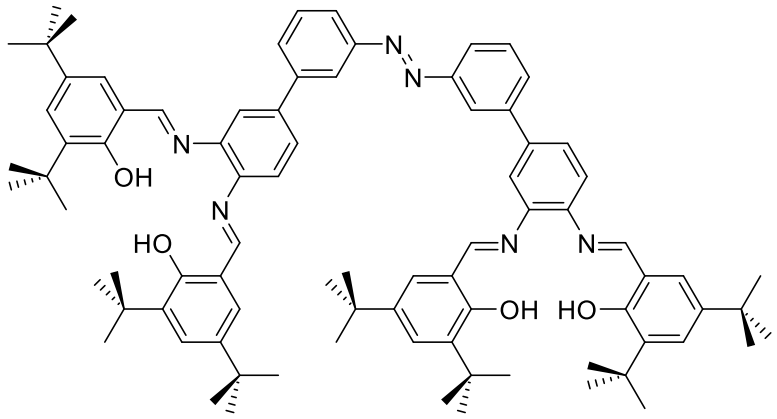

A solution of azobenzene **56** (300 mg, 0.76 mmol), **57** (1.07 g, 4.56 mmol), and 4-methylbenzenesulfonic acid hydrate (0.72 mg, 3.80 µmol) in toluene (5 mL) was refluxed in a Dean-Stark apparatus at 130 °C for 18 h. The reaction mixture was cooled to room temperature, and volatiles were removed under vacuum. The resulting solid residue was then recrystallized in ethanol. Ligand **58** (750 mg, 78%) was dried under high vacuum, resulting in a powdery yellow solid.

^{1}H-NMR (300 MHz, CD_2Cl_2): δ =: 13.66 (s, 2H), 13.62 (s, 2H), 8.87 (s, 2H), 8.82 (s, 2H), 8.36 (dd, *J* = 1.8 Hz, 2H), 8.04 (ddd, *J* = 7.9, 1.8, 1.1 Hz, 2H), 7.90 (ddd, *J* = 7.7, 1.7, 1.1 Hz, 2H), 7.80 – 7.64 (m, 6H), 7.55 – 7.49 (m, 4H), 7.49 (s, 2H), 7.46 (s, 2H), 7.34 (t, *J* = 2.6 Hz, 4H), 1.48 (s, 18H), 1.48 (s, 18H), 1.37 (s, 18H), 1.36 (s, 18H) ppm. **^{13}C-NMR (126 MHz, CD_2Cl_2):** δ = 165.68, 165.08, 158.86, 153.57, 143.72, 142.46, 141.57, 141.06, 139.88, 137.38, 130.20, 129.94, 128.83, 127.51, 127.42, 126.40, 122.25, 121.94, 120.49, 118.90, 118.87, 118.81, 35.41, 34.48, 31.56, 29.57 ppm. **MS (ESI-HRMS):** calculated for $C_{84}H_{101}N_6O_4$ (M^-): 1257.7890. found: 1257.7913. **FT-IR:** $\tilde{\nu}$ = 2955.33, 2907.74, 2869.25, 2778.85, 2742.91, 2706.34, 3655.53, 1615.06, 1580.94, 1502.17, 1472.43, 1437.13, 1392.32, 1361.66, 1319.95, 1272.96, 1250.87, 1228.59, 1201.18, 1171.10, 1122.48, 1027.90, 980.52, 954.69, 931.96, 909.33, 878.72, 853.81, 823.40, 799.29, 772.37, 731.88, 689.93, 644.02, 536.44 cm^{-1}.

Complex 51[128]

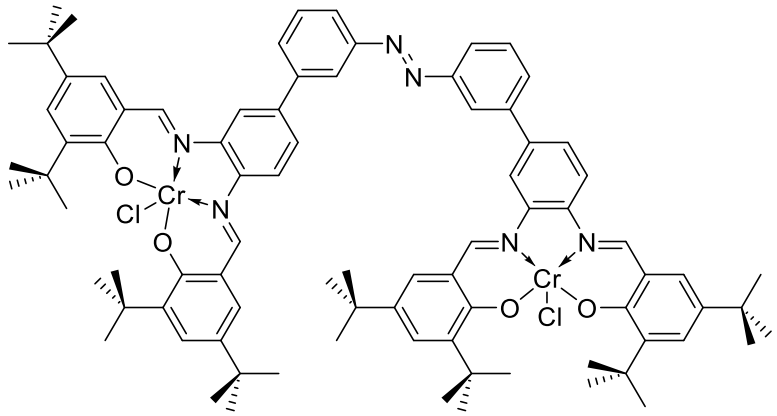

Ligand **58** (500 mg, 0.40 mmol) was transferred to a 10-mL Schlenk tube under argon atmosphere. Then $CrCl_2$ (127 mg, 1.03 mmol) was added to the tube, and the mixture was dissolved in dry, anhydrous THF (8.0 mL). The resulting solution was stirred under argon for 3 h at room temperature, and then it was exposed to air and stirred overnight. Following the addition of 2,6-lutidine (239 µl, 2.06 mmol), the solution was stirred under air for another 4.5 h at room temperature. Once the reaction was complete, the solution was diluted with CH_2Cl_2 (500 mL) and extracted from NaCl (500 mL x 3) and NH_4Cl (500 mL x 3). Then it was dried with $MgSO_4$ and concentrated under reduced pressure, resulting in complex **51** (450 mg, 79 %), which was used without further purification.

MS (ESI-HRMS): calculated for $C_{84}H_{98}Cl_2Cr_2N_6O_4$ (M^-): 1428.5837. found: 1428.5996. **FT-IR:** $\tilde{\nu}$ = 3600 – 2400 broad signal, 2953.81, 2908.04, 2866.36, 1607.11, 1580.41, 1524.27, 1460.45, 1425.45, 1425.95, 1384.57, 1326.02, 1252.59, 1196.97, 1168.77, 1133.39, 1024.35, 868.00, 837.37, 780.14, 654.82, 538.29 cm^{-1}. **Elemental Analysis**: calculated for $C_{84}H_{108}Cl_2Cr_2N_6O_9$: C = 66.35%, H = 7.16%, N = 5.53 %. found: C = 65.96%, H = 7.59%, N = 5.68%.

Di-tert-butyl (4-bromo-1,2-phenylene)dicarbamate (59)[206]

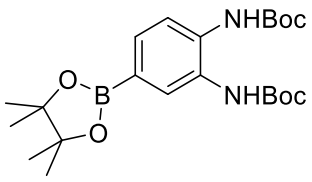

To a 100-mL round-bottom flask were added di-*tert*-butyl dicarbonate (5.46 ml, 23.52 mmol) and sulfamic acid (0.052 g, 0.54 mmol). To the mixture was added 4-bromobenzene-1,2-diamine **54** (2.00 g, 10.69 mmol). Without the addition of solvent, the reaction was sonicated for 30 min at room temperature. Once the reaction was complete, EtOAc was added to the reaction mixture. The organic layer was washed with water (3 × 200 ml) and brine (2 × 200 ml)

and dried with $MgSO_4$. The product was purified on a silica column using dichloromethane as eluent. Diamine **59** (3.90 g, 94 %) was afforded as an off-white solid.

^{1}H-NMR (500 MHz, CD_2Cl_2): δ = 7.68 (d, *J* = 3.3 Hz, 1H), 7.26 (d, *J* = 7.2 Hz, 1H), 7.14 (dd, *J* = 8.6, 2.3 Hz, 1H), 6.73 (s, 1H), 6.53 (s, 1H), 1.43 (s, 18H) ppm. **MS (ESI-HRMS):** calculated for $C_{16}H_{23}BN_2O_6$ (M^+): 434.2588. found: 234.2625.

Di-tert-butyl (4-((3-aminophenyl)ethynyl)-1,2-phenylene)dicarbamate (60)

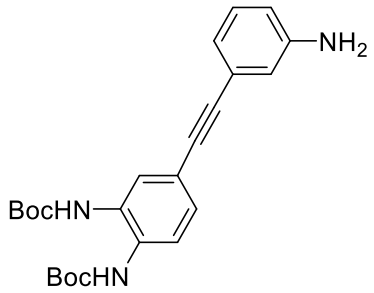

Anhydrous toluene (60 ml) and Et_3N (19.4 ml) were added to an over-dried Schlenk flask under argon, followed by the addition of diamine **59** (3.00 g, 7.75 mmol). The solution was thoroughly degassed through three freeze-pump-thaw cycles. Then 3-ethynylaniline (0.89 mL, 8.52 mmol) and $Pd(PPh_3)_4$ (895 mg, 0.76 mmol) were added to the flask under argon. The resulting mixture was heated to 80 °C and stirred for 24 h. For the first three hours, an addition equivalent of 3-ethynylaniline was added to the reaction. After the reaction was complete, it was diluted with DCM and washed with brine (500 mL x 3). The crude product was purified on a silica column (EtOAc/PE = 1:3). Alkyne **60** (1.95 g, 57 %) was isolated as an off-white oil that solidified upon concentration under reduced pressure.

^{1}H-NMR (500 MHz, CD_2Cl_2): δ = 7.53 (s, 1H), 7.47 (d, *J* = 6.7 Hz, 1H), 7.19 (dd, *J* = 8.4, 1.9 Hz, 1H), 7.03 (t, *J* = 11.7, 4.0 Hz, 1H), 6.81 (dt, 2H), 6.74 (t, 1H), 6.65 (s, 1H), 6.57 (ddd, *J* = 8.1, 2.4, 1.0 Hz, 1H), 3.69 (s, 2H), 1.42 (s, 18H) ppm. **MS (ESI-HRMS):** calculated for $C_{24}H_{30}N_3O_4$ (M^+): 424.2231. found: 424.2091.

Di-tert-butyl (4-(3-aminophenethyl)-1,2-phenylene)dicarbamate (61)[207]

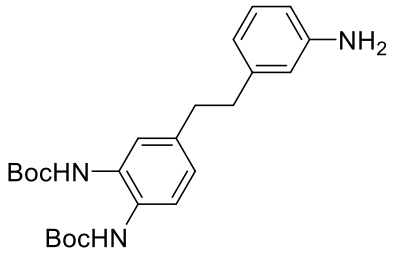

An oven-dried round-bottom flask was evacuated and refilled with argon. Then alkyne **60** (2.19 g, 5.16 mmol) and 5 % palladium on charcoal (1.31 g, 12.34 mmol) were added to the flask. Slowly MeOH (44.0 mL) was added to the flask, followed by the addition of Et_3N (2.88 mL, 20.65 mmol). The atmosphere in the flask was replaced with hydrogen gas, and the reaction was allowed to proceed with stirring for 3 h at room temperature. Once the reaction was complete, the solution was filtered through celite, eluting with EtOAc. The crude material was purified on a silica column (EtOAc/PE = 1:3). Amine **61** (2.16 g, 98 %) was isolated as an off-yellow oil.

^{1}H-NMR (500 MHz, CD_2Cl_2): δ = 7.29 (s, 1H), 7.24 (d, *J* = 7.6 Hz, 1H), 6.95 (dd, *J* = 7.7 Hz, 1H), 6.87 (dd, *J* = 8.2, 1.8 Hz, 1H), 6.70 (s, 1H), 6.59 (s, 1H), 6.49 (d, *J* = 7.6 Hz, 1H), 6.44 (dd, *J* = 1.7 Hz, 1H), 6.41 (dd, *J* = 7.5, 1.9 Hz, 1H), 3.58 (s, 2H), 2.87 – 2.51 (m, 4H), 1.41 (s, 18H) ppm. **^{13}C-NMR (126 MHz, CD_2Cl_2):** δ = 154.38, 154.11, 147.21, 143.32, 129.50, 129.36, 128.55, 125.62, 118.78, 115.41, 112.91, 80.88, 38.06, 37.57, 28.38, 28.36, 21.53 ppm. **MS (ESI-HRMS):** calculated for $C_{24}H_{34}N_3O_4$ (M^+): 428.2544. found: 248.2427.

Tetra-*tert*-butyl (((diazene-1,2-diylbis(3,1-phenylene))bis(ethane-2,1-diyl))bis(benzene-4,1,2-triyl))tetracarbamate (62)[208]

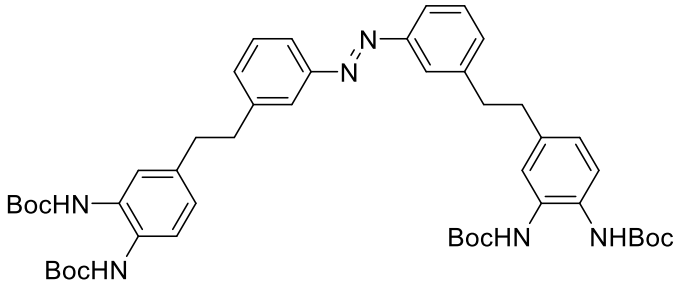

Amine **61** (2.16 g, 5.05 mmol) and copper (I) bromide (0.73 g, 5.05 mmol) were added to a 100-mL roundbottom flask. The reagents were dissolved in CH_2Cl_2 (35 mL) followed by the addition of pyridine (1.22 mL, 15.16 mmol). The reaction was stirred for 6 h at room temperature. Once the reaction was complete, the solution was filtered through celite and

washed with brine. The resulting crude product was purified on silica column (EtOAc/PE = 1:4). Azobenzene **62** (1.10 g, 1.29 mmol, 51 %) was isolated as an orange solid.

^{1}H-NMR (400 MHz, CD_2Cl_2): δ = 7.81 (dd, *J* = 1.6 Hz, 2H), 7.77 – 7.74 (m, 2H), 7.53 – 7.40 (m, 4H), 7.40 – 7.23 (m, 4H), 6.99 (dd, *J* = 9.4, 4.7 Hz, 2H), 6.81 (s, 2H), 6.67 (s, 2H), 3.16 – 2.87 (m, 8H), 1.51 (s, 36H) ppm. **MS (ESI-HRMS):** calculated for $C_{48}H_{63}N_6O_8$ (M^+): 851.4702. found: 851.4727.

4,4'-((diazene-1,2-diylbis(3,1-phenylene))bis(ethane-2,1-diyl))bis(benzene-1,2-diamine) (62a)[209]

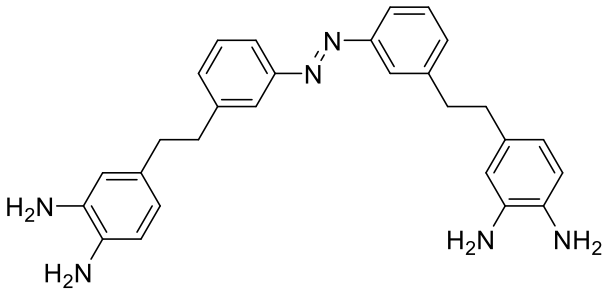

To a 100-ml round-bottom flask was added azobenzene **92** (1.05 g, 1.23 mmol). The compound was dissolved in CH_2Cl_2 (12 ml), and then 2,2,2-trifluoroacetic acid (10 ml) was added to the solution. The reaction was stirred for 2 h at room temperature. Once it was complete, the resulting solution was diluted with CH_2Cl_2 (400 ml) and extracted from $NaHCO_3$ (400 ml x 3) and brine (400 ml x 3). The solution was dried with $MgSO_4$ and concentrated under reduced pressure. The resulting product **62a** (530 mg, 95 %) was used without further purification.

MS (ESI-HRMS): calculated for $C_{28}H_{31}N_6$ (M^+): 451.2605. found: 451.2544.

Ligand 63

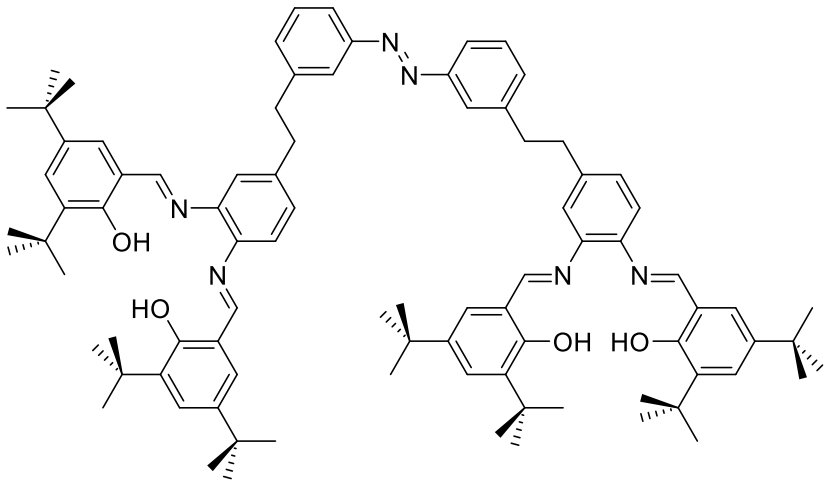

A solution of azobenzene **62a** (230 mg, 0.51 mmol), **57** (718 mg, 3.06 mmol), and 4-toluenesulfonic acid hydrate (0.485 mg, 2.55 µmol) in toluene (15 mL) was refluxed in a Dean-Stark apparatus at 130 °C for 40 h. The reaction mixture was cooled to room temperature, and volatiles were removed under vacuum. The resulting solid residue was then recrystallized in chloroform/ethanol; 50:1. Ligand **63** (517 mg, 77%) was dried under vacuum, resulting in a powdery yellow solid.

^{1}H-NMR (400 MHz, CD_2Cl_2): δ = 13.60 (s, 2H), 13.51 (s, 2H), 8.61 (s, 2H), 8.49 (s, 2H), 7.76 – 7.67 (m, 4H), 7.42 – 7.32 (m, 6H), 7.28 – 7.20 (m, 2H), 7.18 – 7.07 (m, 8H), 6.95 (d, *J* = 1.7 Hz, 2H), 3.00 (m, 8H), 1.34 (m, 36H), 1.24 (m, 36H). **MS (ESI-HRMS):** calculated for $C_{88}H_{111}N_6O_4$ (M^+): 1315.8661. found: 1315.8656. **FT-IR:** $\tilde{\nu}$ = 2957.07, 2911.02, 2868.50, 2777.75, 2743.51, 2704.26, 2655.20, 1616.07, 1588.57, 1568.25, 1467.14, 1436.11, 1393.24, 1361.18, 1324.82, 1270.35, 1249.09, 1200.58, 1172.96, 1134.69, 1114.17, 1082.11, 1024.72, 987.01, 926.88, 872.01, 851.46, 822.01, 796.52, 771.75, 729.18, 693.84, 648.85, 518.08, 494.51 cm^{-1}.

Complex 52

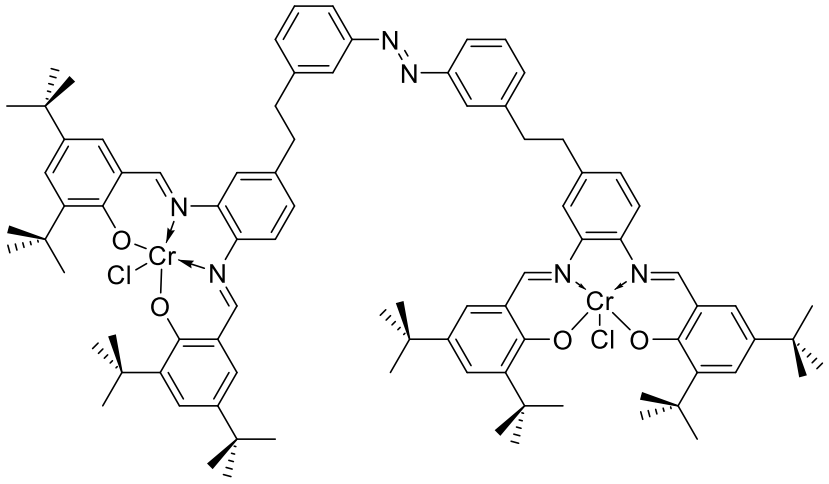

Ligand **63** (100 mg, 0.076 mmol) was transferred to a 10-mL Schlenk tube under argon atmosphere. Then $CrCl_2$ (24.3 mg, 0.20 mmol) was added to the tube, and the mixture was dissolved in dry, anhydrous THF (3.0 mL). The resulting solution was stirred under argon for 18 h at room temperature, and then it was exposed to air and stirred for another 3 h. Following the addition of 2,6-lutidine (46 µl, 0.40 mmol), the solution was stirred under air for another 3 h at room temperature. Once the reaction was complete, the solution was diluted with CH_2Cl_2 (100 mL), extracted from NaCl (100 mL x 3) and NH_4Cl (100 mL x 3). Then it was dried with $MgSO_4$ and concentrated under reduced pressure, resulting in complex **12** (80 mg, 71 %), which was used without further purification.

MS (ESI-HRMS): calculated for $C_{88}H_{106}Cl_2Cr_2N_6O_4$ (M^-): 1484.6463. found: 1484.6234. **FT-IR:** $\tilde{\nu}$ = 3600 – 2400 broad signal, 2953.59, 2921.26, 2853.55, 1610.45, 1583.63, 1525.30, 1461.02, 1429.38, 1385.57, 1359.56, 1326.47, 1252.75, 1198.31, 1170.21, 1133.92, 1026.03, 872.58, 810.91, 780.74, 749.14, 696.38, 569.04, 540.67 cm^{-1}. **Elemental Analysis**: calculated for $C_{88}H_{116}Cl_2Cr_2N_6O_9$: C = 67.03%, H = 7.42%, N = 5.31 %. found: C = 66.67%, H = 7.60%, N = 5.63%.

Tetra-*tert*-butyl(((diazene-1,2-diylbis(3,1-phenylene))bis(ethyne-2,1-diyl))bis(benzene-4,1,2-triyl)) (*E*)-tetracarbamate (64).

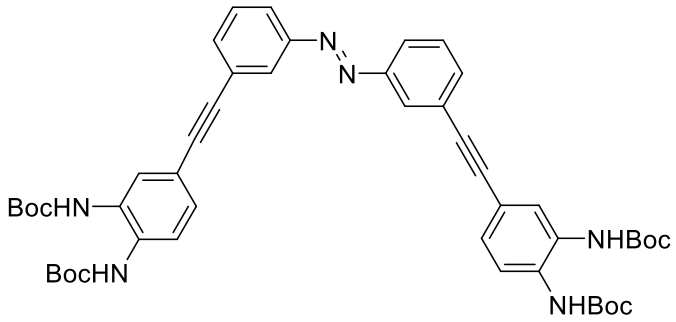

60 (1.50 g, 3.54 mmol) was dissolved in DCM (15 ml) and (diacetoxyiodo)benzene (1.08 g, 3.36 mmol) was added. The mixture was stirred at RT for 24 h. Once the reaction was completed, the mixture was diluted with DCM and washed 3 x with brine. The organic phase was dried with $MgSO_4$ and then purified on a silica column (DCM/MeOH = 50:1). Azobenzene **64** (945 mg, 1.12 mmol, 63 %) was isolated as an orange solid.

^{1}H-NMR (500 MHz, CD_2Cl_2) δ = 8.07 (t, *J* = 2.5 Hz, 2H), 7.91 (ddd, *J* = 1.2, 2.5, 7.9 Hz, 2H), 7.68 (d, *J* = 1.9 Hz, 2H), 7.65 (ddd, *J* = 1.2, 2.5, 7.9 Hz, 2H), 7.59 (d, *J* = 8.4 Hz, 2H), 7.53 (t, *J* = 7.9 Hz, 2H), 7.34 (dd, *J* = 1.9, 8.4 Hz, 2H), 6.92 (s, 2H), 6.77 (s, 2H), 1.52 (s, 18H, CH_3), 1.52 (s, 18H) ppm. **^{13}C-NMR (75 MHz, CD_2Cl_2)** δ = 153.58, 153.22, 152.38, 134.00, 130.42, 129.28, 128.85, 128.69, 127.44, 125.53, 124.27, 123.61, 123.16, 109.99, 89.49, 88.24, 80.98, 27.93 ppm. **MS (ESI-HRMS):** calculated for $C_{48}H_{54}N_6NaO_8$ (M^+): 865.3901. found: 8653975.

(E)-4,4'-((Diazene-1,2-diylbis(3,1-phenylene))bis(ethyne-2,1-diyl))bis(benzene-1,3-diamine) (65).

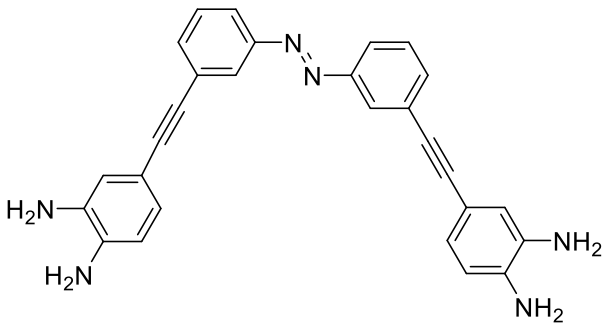

64 (945 mg, 1.12 mmol) was dissolved in DCM (10 ml). Trifluoroacetic acid (8.6 ml, 12.814 g, 112 mmol) was added dropwise and the mixture was stirred at room temperature for 3 h. The

mixture was diluted with EtOAc, washed 2 x with $NaHCO_3$, 1 x with NaOH and 2x with Brine. The organic phase was dried with $MgSO_4$ and evaporated. Tetraamine **65** (450 mg, 1.02 mmol, 91 %) was isolated as an orange solid.

^{1}H-NMR (500 MHz, DMSO-d6) δ = 7.92 (m, 2H), 7.90 (dt, *J* = 7.6, 1.7 Hz, 2H), 7.66 (dt, *J* = 7.6, 1.6 Hz, 2H), 7.63 (dt, *J* = 7.6, 1.6 Hz, 2H), 6.74 (d, *J* = 1.9 Hz, 2H), 6.69 (dd, *J* = 7.9, 1.9 Hz, 2H), 6.52 (d, *J* = 7.9 Hz, 2H), 4.96 (s, 2H) ppm. **MS (ESI-HRMS):** calculated for $C_{28}H_{23}N_6$ (M^+): 443.1984. found: 443.1890. ^{13}C-NMR could not be recorded due to low solubility in all standard NMR solvents.

Ligand 66

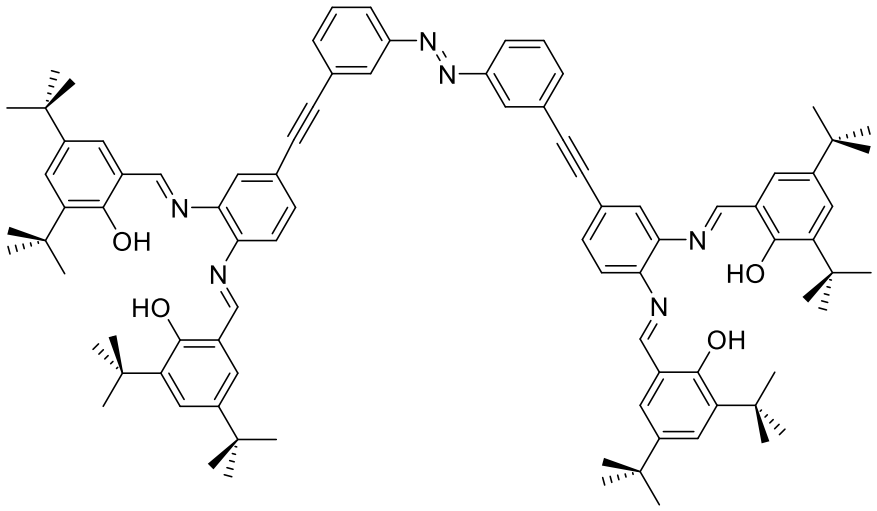

65 (66 mg, 0.15 mmol), 4-toluenesulfonic acid (0.1 mg, 0,6 µmol) and triethoxymethane (0.1 ml, 90 mg, 0.6 mmol) were suspended in Toluene (15 ml). **57** (210 mg, 0.895 mmol) was added and the mixture was stirred at reflux for 48 hours. Once the reaction was completed, it was evaporated and the residue was recrystallized from EtOH and chloroform. Ligand **66** (11 mg, 8.42 µmol, 6 %) was isolated as a yellow solid.

^{1}H-NMR (500 MHz, CD_2Cl_2) δ = 13.50 (s, 2H), 13.49 (s, 2H), 8.75 (s, 2H), 8.73 (s, 2H), 8.14 (t, *J* = 1.2 Hz, 2H), 7.97 (ddd, *J* = 7.9, 1.6, 1.2 Hz, 2H), 7.72 (ddd, *J* = 7.9, 1.6, 1.2 Hz, 2H), 7.59 (t, *J* = 7.9 Hz, 2H), 7.57 (dd, *J* = 8.2, 1.9 Hz, 2H), 7.51 (d, *J* = 1.9 Hz, 2H), 7.47 (d, *J* = 2.4 Hz, 4H), 7.31 (d, *J* = 8.2 Hz, 2H), 7.30 (d, *J* = 2.4 Hz, 2H), 7.28 (d, *J* = 2.4 Hz, 2H), 1.43 (s, 18H), 1.43 (s, 18H), 1.33 (s, 18H), 1.32 (s, 18H) ppm. **^{13}C NMR (126 MHz, CD_2Cl_2)** δ = 165.88, 165.17, 159.00, 143.42, 141.35, 137.82, 133.84, 131.32, 130.39, 129.55, 128.53, 127.10, 125.53, 123.12, 122.83, 120.98, 119.89, 119.17, 90.10, 80.17, 35.57, 34.64, 31.54,

29.54 ppm. **MS (ESI-HRMS):** calculated for $C_{88}H_{102}N_6O_4$ (M^+): 1308.8300. found: 1308.8943.

Typical procedure for polymerization reactions

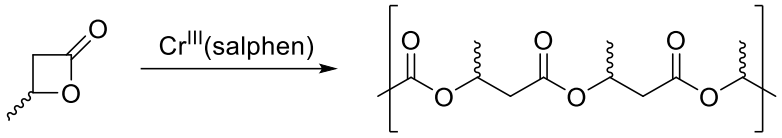

In the glovebox the catalyst (0.1 mol%) and β-Butyrolactone were transferred into an oven-dried vial and stirred until all of the catalyst was dissolved. The mixture was then split up into two batches and transferred into inert Schlenk-tubes. The Schlenk-tubes were then transferred into a pre-heated oil bath (100°C) under vigorous stirring. In regular intervals a sample was taken and quenched with $CDCl_3$ for NMR-analysis. After the polymerization was completed the polymer was precipitated by EtO_2/*n*-hexane (1/3). The liquid was decanted, the polymer washed with EtO_2/*n*-hexane (1/3) and then dried in vacuo until constant weight.

For irradiation experiments the Schlenk-tube was wrapped with 3 LEDs in aluminum foil and then completely immerged into the oil bath.

Literature

(1) Sakakura, T.; Choi, J.-C.; Yasuda, H. *Chem. Rev.* **2007**, *107*, 2365.
(2) Dalko, P. I.; Moisan, L. *Angew. Chem. Int. Ed.* **2004**, *43*, 5138.
(3) Giannerini, M.; Fañanás-Mastral, M.; Feringa, B. L. *Nat Chem* **2013**, *5*, 667.
(4) Hawker, C. J.; Wooley, K. L. *Science* **2005**, *309*, 1200.
(5) Yoon, T. P.; Jacobsen, E. N. *Science* **2003**, *299*, 1691.
(6) White, C.; Burnett, J. *Journal of Chromatography A* **2005**, *1074*, 175.
(7) Dri, C.; Peters, M. V.; Schwarz, J.; Hecht, S.; Grill, L. *Nat. Nanotechnol.* **2008**, *3*, 649.
(8) Hla, S.-W.; Bartels, L.; Meyer, G.; Rieder, K.-H. *Phys. Rev. Lett.* **2000**, *85*, 2777.
(9) Ho, W. *J. Phys. Chem.* **2002**, *117*, 11033.
(10) Okawa, Y.; Aono, M. *Nature* **2001**, *409*, 683.
(11) Stoll, R. S.; Hecht, S. *Angew. Chem. Int. Ed.* **2010**, *49*, 5054.
(12) Hell, S. W. *Science* **2007**, *316*, 1153.
(13) LaFratta, C. N.; Fourkas, J. T.; Baldacchini, T.; Farrer, R. A. *Angew. Chem. Int. Ed.* **2007**, *46*, 6238.
(14) Zhou, W.; Kuebler, S. M.; Braun, K. L.; Yu, T.; Cammack, J. K.; Ober, C. K.; Perry, J. W.; Marder, S. R. *Science* **2002**, *296*, 1106.
(15) Kamber, N. E.; Jeong, W.; Waymouth, R. M.; Pratt, R. C.; Lohmeijer, B. G. G.; Hedrick, J. L. *Chem. Rev.* **2007**, *107*, 5813.
(16) Domski, G. J.; Rose, J. M.; Coates, G. W.; Bolig, A. D.; Brookhart, M. *Prog. Polym. Sci.* **2007**, *32*, 30.
(17) Bielawski, C. W.; Grubbs, R. H. *Prog. Polym. Sci.* **2007**, *32*, 1.
(18) Iha, R. K.; Wooley, K. L.; Nyström, A. M.; Burke, D. J.; Kade, M. J.; Hawker, C. J. *Chem. Rev.* **2009**, *109*, 5620.
(19) Pollard, T. D.; Cooper, J. A. *Science* **2009**, *326*, 1208.
(20) Yoon, H. J.; Kuwabara, J.; Kim, J.-H.; Mirkin, C. A. *Science* **2010**, *330*, 66.
(21) Gregson, C. K. A.; Gibson, V. C.; Long, N. J.; Marshall, E. L.; Oxford, P. J.; White, A. J. P. *J. Am. Chem. Soc.* **2006**, *128*, 7410.
(22) Broderick, E. M.; Guo, N.; Vogel, C. S.; Xu, C.; Sutter, J.; Miller, J. T.; Meyer, K.; Mehrkhodavandi, P.; Diaconescu, P. L. *J. Am. Chem. Soc.* **2011**, *133*, 9278.
(23) Magenau, A. J. D.; Strandwitz, N. C.; Gennaro, A.; Matyjaszewski, K. *Science* **2011**, *332*, 81.
(24) Fors, B. P.; Hawker, C. J. *Angew. Chem.* **2012**, *124*, 8980.
(25) Tanabe, M.; Manners, I. *J. Am. Chem. Soc.* **2004**, *126*, 11434.
(26) Tanabe, M.; Vandermeulen, G. W. M.; Chan, W. Y.; Cyr, P. W.; Vanderark, L.; Rider, D. A.; Manners, I. *Nat. Mater.* **2006**, *5*, 467.
(27) Zheng, X.; Yue, M.; Yang, P.; Li, Q.; Yang, W. *Polymer Chemistry* **2012**, *3*, 1982.
(28) Hartley, G. S. *Nature* **1937**, 281.
(29) Henzl, J.; Mehlhorn, M.; Gawronski, H.; Rieder, K.-H.; Morgenstern, K. *Angew. Chem. Int. Ed.* **2006**, *45*, 603.
(30) Tong, X.; Pelletier, M.; Lasia, A.; Zhao, Y. *Angew. Chem. Int. Ed.* **2008**, *47*, 3596.
(31) Turansky, R.; Konopka, M.; Doltsinis, N. L.; Stich, I.; Marx, D. *Phys. Chem. Chem. Phys.* **2010**, *12*, 13922.
(32) García-Amorós, J.; Velasco, D. *Beilstein J. Org. Chem.* **2012**, *8*, 1003.
(33) Bléger, D.; Schwarz, J.; Brouwer, A. M.; Hecht, S. *J. Am. Chem. Soc.* **2012**, *134*, 20597.
(34) Bang, C.-U.; Shishido, A.; Ikeda, T. *Macromol. Rapid Commun.* **2007**, *28*, 1040.

(35) Parker, R. M.; Gates, J. C.; Rogers, H. L.; Smith, P. G. R.; Grossel, M. C. *J. Mater. Chem.* **2010**, *20*, 9118.
(36) Ferri, V.; Elbing, M.; Pace, G.; Dickey, M. D.; Zharnikov, M.; Samorì, P.; Mayor, M.; Rampi, M. A. *Angew. Chem. Int. Ed.* **2008**, *47*, 3407.
(37) Frank, J. A.; Moroni, M.; Moshourab, R.; Sumser, M.; Lewin, G. R.; Trauner, D. *Nat Commun* **2015**, *6*.
(38) Velema, W. A.; van der Berg, J. P.; Hansen, M. J.; Szymanski, W.; Driessen, A. J. M.; Feringa, B. L. *Nat Chem* **2013**, *5*, 924.
(39) Velema, W. A.; Szymanski, W.; Feringa, B. L. *J. Am. Chem. Soc.* **2014**, *136*, 2178.
(40) Norikane, Y.; Tamaoki, N. *Org. Lett.* **2004**, *6*, 2595.
(41) Muraoka, T.; Kinbara, K.; Aida, T. *Nature* **2006**, *440*, 512.
(42) Murakami, H.; Kawabuchi, A.; Kotoo, K.; Kunitake, M.; Nakashima, N. *J. Am. Chem. Soc.* **1997**, *119*, 7605.
(43) Guo, S.; Matsukawa, K.; Miyata, T.; Okubo, T.; Kuroda, K.; Shimojima, A. *J. Am. Chem. Soc.* **2015**.
(44) Peters, M. V.; Stoll, R. S.; Kühn, A.; Hecht, S. *Angew. Chem. Int. Ed.* **2008**, *47*, 5968.
(45) Imahori, T.; Yamaguchi, R.; Kurihara, S. *Chem. Eur. J.* **2012**, *18*, 10802.
(46) Cacciapaglia, R.; Di Stefano, S.; Mandolini, L. *J. Am. Chem. Soc.* **2003**, *125*, 2224.
(47) Stoll, R. S.; Hecht, S. *Org. Lett.* **2009**, *11*, 4790.
(48) Rau, H. *Angewandte Chemie International Edition in English* **1973**, *12*, 224.
(49) Wegner, H. A. *Angew. Chem. Int. Ed.* **2012**, *51*, 4787.
(50) Beharry, A. A.; Sadovski, O.; Woolley, G. A. *J. Am. Chem. Soc.* **2011**, *133*, 19684.
(51) Hampson, G. C.; Robertson, J. M. *J. Chem. Soc.* **1941**, 409.
(52) Mostad, A.; Romming, C. *Acta Chem. Scand.* **1971**, 3561.
(53) Bandara, H. M. D.; Burdette, S. C. *Chem. Soc. Rev.* **2012**, *41*, 1809.
(54) Fischer, E. *J. Am. Chem. Soc.* **1960**, *82*, 3249.
(55) Bortolus, P.; Monti, S. *J. Phys. Chem.* **1979**, *83*, 648.
(56) Wang, L.; Xu, W.; Yi, C.; Wang, X. *Journal of Molecular Graphics and Modelling* **2009**, *27*, 792.
(57) Schultz, T.; Quenneville, J.; Levine, B.; Toniolo, A.; Martínez, T. J.; Lochbrunner, S.; Schmitt, M.; Shaffer, J. P.; Zgierski, M. Z.; Stolow, A. *J. Am. Chem. Soc.* **2003**, *125*, 8098.
(58) Malkin, S.; Fischer, E. *J. Phys. Chem.* **1962**, *66*, 2482.
(59) Siampiringue, N.; Guyot, G.; Monti, S.; Bortolus, P. *Journal of Photochemistry* **1987**, *37*, 185.
(60) Magee, J. L.; Shand, W.; Eyring, H. *J. Am. Chem. Soc.* **1941**, *63*, 677.
(61) Rau, H.; Lueddecke, E. *J. Am. Chem. Soc.* **1982**, *104*, 1616.
(62) Fujino, T.; Arzhantsev, S. Y.; Tahara, T. *J. Phys. Chem. A* **2001**, *105*, 8123.
(63) Dokić, J.; Gothe, M.; Wirth, J.; Peters, M. V.; Schwarz, J.; Hecht, S.; Saalfrank, P. *J. Phys. Chem. A* **2009**, *113*, 6763.
(64) Blevins, A. A.; Blanchard, G. J. *The Journal of Physical Chemistry B* **2004**, *108*, 4962.
(65) Whitten, D. G.; Wildes, P. D.; Pacifici, J. G.; Irick, G. *J. Am. Chem. Soc.* **1971**, *93*, 2004.
(66) Dunn, N. J.; Humphries, W. H.; Offenbacher, A. R.; King, T. L.; Gray, J. A. *J. Phys. Chem. A* **2009**, *113*, 13144.
(67) Serra, F.; Terentjev, E. M. *Macromolecules* **2008**, *41*, 981.
(68) Emond, M.; Le Saux, T.; Maurin, S.; Baudin, J.-B.; Plasson, R.; Jullien, L. *Chem. Eur. J.* **2010**, *16*, 8822.
(69) Brode, W. R.; Gould, J. H.; Wyman, G. M. *J. Am. Chem. Soc.* **1952**, *74*, 4641.
(70) Douhal, A.; Sanz, M.; Tormo, L. *Proc. Natl. Acad. Sci. U. S. A.* **2005**, *102*, 18807.

(71) Bandara, H. M. D.; Friss, T. R.; Enriquez, M. M.; Isley, W.; Incarvito, C.; Frank, H. A.; Gascon, J.; Burdette, S. C. *J. Org. Chem.* **2010**, *75*, 4817.
(72) Ruslim, C.; Ichimura, K. *J. Mater. Chem.* **2000**, *10*, 2704.
(73) Gabor, G.; Frei, Y. F.; Fischer, E. *J. Phys. Chem.* **1968**, *72*, 3266.
(74) Sierocki, P.; Maas, H.; Dragut, P.; Richardt, G.; Vögtle, F.; De Cola, L.; Brouwer, F.; Zink, J. I. *The Journal of Physical Chemistry B* **2006**, *110*, 24390.
(75) Kojima, M.; Nebashi, S.; Ogawa, K.; Kurita, N. *J. Phys. Org. Chem.* **2005**, *18*, 994.
(76) Buncel, E.; Lawton, B. T. *Can. J. Chem.* **1965**, *43*, 862.
(77) Sawicki, E. *J. Org. Chem.* **1957**, *22*, 743.
(78) Kurita, N.; Nebashi, S.; Kojima, M. *Chem. Phys. Lett.* **2005**, *408*, 197.
(79) Han, M.; Ishikawa, D.; Muto, E.; Hara, M. *J. Lumin.* **2009**, *129*, 1163.
(80) Toro, C.; Thibert, A.; De Boni, L.; Masunov, A. E.; Hernández, F. E. *The Journal of Physical Chemistry B* **2008**, *112*, 929.
(81) Brzozowski, L.; Sargent, E. H. *J. Mater. Sci.: Mater. Electron.* **2001**, *12*, 483.
(82) Marder, S. R.; Kippelen, B.; Jen, A. K. Y.; Peyghambarian, N. *Nature* **1997**, *388*, 845.
(83) Meerholz, K.; Volodin, B. L.; Sandalphon; Kippelen, B.; Peyghambarian, N. *Nature* **1994**, *371*, 497.
(84) Tsutsumi, N.; Yoshizaki, S.; Sakai, W.; Kiyotsukuri, T. *Macromolecules* **1995**, *28*, 6437.
(85) Berg, R. H.; Hvilsted, S.; Ramanujam, P. S. *Nature* **1996**, *383*, 505.
(86) Kawano, K.; Ishii, T.; Minabe, J.; Niitsu, T.; Nishikata, Y.; Baba, K. *Opt. Lett.* **1999**, *24*, 1269.
(87) Yesodha, S. K.; Sadashiva Pillai, C. K.; Tsutsumi, N. *Prog. Polym. Sci.* **2004**, *29*, 45.
(88) Merino, E. *Chem. Soc. Rev.* **2011**, *40*, 3835.
(89) Nystrom, R. F.; Brown, W. G. *J. Am. Chem. Soc.* **1948**, *70*, 3738.
(90) Hutchins, R. O.; Lamson, D. W.; Rua, L.; Milewski, C.; Maryanoff, B. *J. Org. Chem.* **1971**, *36*, 803.
(91) Wei, W.-h.; Tomohiro, T.; Kodaka, M.; Okuno, H. *J. Org. Chem.* **2000**, *65*, 8979.
(92) Khan, A.; Hecht, S. *Chem. Eur. J.* **2006**, *12*, 4764.
(93) Zhang, C.; Jiao, N. *Angew. Chem. Int. Ed.* **2010**, *49*, 6174.
(94) Monir, K.; Ghosh, M.; Mishra, S.; Majee, A.; Hajra, A. *Eur. J. Org. Chem.* **2014**, *2014*, 1096.
(95) Haghbeen, K.; Tan, E. W. *J. Org. Chem.* **1998**, *63*, 4503.
(96) Hegarty, A. F., Ed.; Wiley: New York, 1978.
(97) Zollinger, H. *Diazo Chemistry I. Aromatic and Heteroaromatic Compounds*; VCH: New York, 1994.
(98) Zollinger, H. *Azo and Diazo Chemistry Aliphatic and Aromatic Compounds*; Interscience: New York, 1961.
(99) Davey, M. H.; Lee, V. Y.; Miller, R. D.; Marks, T. J. *J. Org. Chem.* **1999**, *64*, 4976.
(100) Entwistle, I. D.; Gilkerson, T.; Johnstone, R. A. W.; Telford, R. P. *Tetrahedron* **1978**, *34*, 213.
(101) Caro, H. *Angew. Chem.* **1898**, *11*, 845.
(102) Gowenlock, B. G.; Richter-Addo, G. B. *Chem. Rev.* **2004**, *104*, 3315.
(103) Yu, B.-C.; Shirai, Y.; Tour, J. M. *Tetrahedron* **2006**, *62*, 10303.
(104) Kang, H.-M.; Jung, J.-W.; Cho, C.-G. *J. Org. Chem.* **2006**, *72*, 679.
(105) Lim, Y.-K.; Lee, K.-S.; Cho, C.-G. *Org. Lett.* **2003**, *5*, 979.
(106) Kim, K.-Y.; Shin, J.-T.; Lee, K.-S.; Cho, C.-G. *Tetrahedron Lett.* **2004**, *45*, 117.
(107) Schiff, H. *Ann. Suppl.* **1864**, *3*, 343.
(108) Makio, H.; Fujita, T. *Acc. Chem. Res.* **2009**, *42*, 1532.

(109) Makio, H.; Terao, H.; Iwashita, A.; Fujita, T. *Chem. Rev.* **2011**, *111*, 2363.
(110) Darensbourg, D.; Rieger, B., Künkel, A., Coates, G. W., Reichardt, R., Dinjus, E., Zevaco, T. A., Eds.; Springer Berlin / Heidelberg: 2012; Vol. 245, p 1.
(111) Cozzi, P. G. *Chem. Soc. Rev.* **2004**, *33*, 410.
(112) Whiteoak, C. J.; Salassa, G.; Kleij, A. W. *Chem. Soc. Rev.* **2012**, *41*, 622.
(113) Gennari, C.; Piarulli, U. *Chem. Rev.* **2003**, *103*, 3071.
(114) Cole, B. M.; Shimizu, K. D.; Krueger, C. A.; Harrity, J. P. A.; Snapper, M. L.; Hoveyda, A. H. *Angewandte Chemie International Edition in English* **1996**, *35*, 1668.
(115) Childers, M. I.; Longo, J. M.; Van Zee, N. J.; LaPointe, A. M.; Coates, G. W. *Chem. Rev.* **2014**, *114*, 8129.
(116) Nomura, N.; Ishii, R.; Yamamoto, Y.; Kondo, T. *Chem. Eur. J.* **2007**, *13*, 4433.
(117) Breteler, M. R. T.; Zhong, Z.; Dijkstra, P. J.; Palmans, A. R. A.; Peeters, J.; Feijen, J. *J. Polym. Sci., Part A: Polym. Chem.* **2007**, *45*, 429.
(118) Normand, M.; Kirillov, E.; Roisnel, T.; Carpentier, J.-F. *Organometallics* **2011**, *31*, 1448.
(119) Terao, H.; Iwashita, A.; Matsukawa, N.; Ishii, S.; Mitani, M.; Tanaka, H.; Nakano, T.; Fujita, T. *ACS Catalysis* **2011**, *1*, 254.
(120) Mitani, M.; Furuyama, R.; Mohri, J.-i.; Saito, J.; Ishii, S.; Terao, H.; Kashiwa, N.; Fujita, T. *J. Am. Chem. Soc.* **2002**, *124*, 7888.
(121) Tanaka, R.; Viehmann, P.; Hecht, S. *Organometallics* **2012**, *31*, 4216.
(122) Hormnirun, P.; Marshall, E. L.; Gibson, V. C.; Pugh, R. I.; White, A. J. P. *Proc. Natl. Acad. Sci. USA* **2006**, *103*, 15343.
(123) Jacobsen, E. N. *Acc. Chem. Res.* **2000**, *33*, 421.
(124) Wezenberg, S. J.; Kleij, A. W. *Angew. Chem. Int. Ed.* **2008**, *47*, 2354.
(125) Zhang, W.; Loebach, J. L.; Wilson, S. R.; Jacobsen, E. N. *J. Am. Chem. Soc.* **1990**, *112*, 2801.
(126) Melov, S.; Ravenscroft, J.; Malik, S.; Gill, M. S.; Walker, D. W.; Clayton, P. E.; Wallace, D. C.; Malfroy, B.; Doctrow, S. R.; Lithgow, G. J. *Science* **2000**, *289*, 1567.
(127) Zelder, F. H.; Rebek Jr, J. *Chem. Commun.* **2006**, 753.
(128) Vagin, S. I.; Reichardt, R.; Klaus, S.; Rieger, B. *J. Am. Chem. Soc.* **2010**, *132*, 14367.
(129) Zintl, M.; Molnar, F.; Urban, T.; Bernhart, V.; Preishuber-Pflügl, P.; Rieger, B. *Angew. Chem. Int. Ed.* **2008**, *47*, 3458.
(130) Eberhardt, R.; Allmendinger, M.; Rieger, B. *Macromol. Rapid Commun.* **2003**, *24*, 194.
(131) Hirahata, W.; Thomas, R. M.; Lobkovsky, E. B.; Coates, G. W. *J. Am. Chem. Soc.* **2008**, *130*, 17658.
(132) Ikada, Y.; Jamshidi, K.; Tsuji, H.; Hyon, S. H. *Macromolecules* **1987**, *20*, 904.
(133) Tsuji, H.; Horii, F.; Hyon, S. H.; Ikada, Y. *Macromolecules* **1991**, *24*, 2719.
(134) Drumright, R. E.; Gruber, P. R.; Henton, D. E. *Adv. Mater.* **2000**, *12*, 1841.
(135) Dubois, P.; Jacobs, C.; Jerome, R.; Teyssie, P. *Macromolecules* **1991**, *24*, 2266.
(136) Spassky, N.; Wisniewski, M.; Pluta, C.; Le Borgne, A. *Macromol. Chem. Phys.* **1996**, *197*, 2627.
(137) Nomura, N.; Ishii, R.; Akakura, M.; Aoi, K. *J. Am. Chem. Soc.* **2002**, *124*, 5938.
(138) Cheng, M.; Attygalle, A. B.; Lobkovsky, E. B.; Coates, G. W. *J. Am. Chem. Soc.* **1999**, *121*, 11583.
(139) Chisholm, M. H.; Patmore, N. J.; Zhou, Z. *Chem. Commun.* **2005**, *0*, 127.
(140) Marshall, E. L.; Gibson, V. C.; Rzepa, H. S. *J. Am. Chem. Soc.* **2005**, *127*, 6048.
(141) Ovitt, T. M.; Coates, G. W. *J. Am. Chem. Soc.* **2002**, *124*, 1316.
(142) Neilson, B. M.; Bielawski, C. W. *ACS Catalysis* **2013**, 1874.

(143) Stoll, R. S.; Peters, M. V.; Kuhn, A.; Heiles, S.; Goddard, R.; Bühl, M.; Thiele, C. M.; Hecht, S. *J. Am. Chem. Soc.* **2008**, *131*, 357.
(144) Neilson, B. M.; Bielawski, C. W. *J. Am. Chem. Soc.* **2012**, *134*, 12693.
(145) Neilson, B. M.; Bielawski, C. W. *Chem. Commun.* **2013**, *49*, 5453.
(146) Neilson, B. M.; Bielawski, C. W. *Organometallics* **2013**, *32*, 3121.
(147) Sud, D.; Norsten, T. B.; Branda, N. R. *Angew. Chem.* **2005**, *117*, 2055.
(148) Wang, J.; Feringa, B. L. *Science* **2011**, *331*, 1429.
(149) Zhao, D.; Neubauer, T. M.; Feringa, B. L. *Nat Commun* **2015**, *6*.
(150) Grignard, V. *C. R. Acad. Sci.* **1900**, *130*, 1322.
(151) Wu, G.; Huang, M. *Chem. Rev.* **2006**, *106*, 2596.
(152) Posner, G. H. *An introduction to synthesis using organocopper reagents*; Wiley: New York, 1980.
(153) Knowles, W. S. *Angew. Chem. Int. Ed.* **2002**, *41*, 1998.
(154) Noyori, R. *Angew. Chem. Int. Ed.* **2002**, *41*, 2008.
(155) Sharpless, K. B. *Angew. Chem. Int. Ed.* **2002**, *41*, 2024.
(156) Chauvin, Y. *Angew. Chem. Int. Ed.* **2006**, *45*, 3740.
(157) Grubbs, R. H. *Angew. Chem. Int. Ed.* **2006**, *45*, 3760.
(158) Schrock, R. R. *Angew. Chem. Int. Ed.* **2006**, *45*, 3748.
(159) Johansson Seechurn, C. C. C.; Kitching, M. O.; Colacot, T. J.; Snieckus, V. *Angew. Chem. Int. Ed.* **2012**, *51*, 5062.
(160) Negishi, E.-i. *Angew. Chem. Int. Ed.* **2011**, *50*, 6738.
(161) Suzuki, A. *Angew. Chem. Int. Ed.* **2011**, *50*, 6722.
(162) Coates, G. W.; Waymouth, R. M. *Science* **1995**, *267*, 217.
(163) Prier, C. K.; Rankic, D. A.; MacMillan, D. W. C. *Chem. Rev.* **2013**, *113*, 5322.
(164) Kurihara, M.; Hirooka, A.; Kume, S.; Sugimoto, M.; Nishihara, H. *J. Am. Chem. Soc.* **2002**, *124*, 8800.
(165) Yamaguchi, K.; Kume, S.; Namiki, K.; Murata, M.; Tamai, N.; Nishihara, H. *Inorg. Chem.* **2005**, *44*, 9056.
(166) Marquis, S.; Ferrer, B.; Alvaro, M.; Garcia, H. *J. Phys. Chem. A* **2007**, *111*, 6034.
(167) Baleizao, C.; Gigante, B.; Ramoa Ribeiro, F.; Ferrer, B.; Palomares, E.; Garcia, H. *Photochem. Photobiol. Sci.* **2003**, *2*, 386.
(168) de Castro, B.; Ferreira, R.; Freire, C.; Garcia, H.; Palomares, E. J.; Sabater, M. J. *New J. Chem.* **2002**, *26*, 405.
(169) Sabater, M. J.; Álvaro, M.; García, H.; Palomares, E.; Scaiano, J. C. *J. Am. Chem. Soc.* **2001**, *123*, 7074.
(170) Formentin, P.; Alvaro, M.; Garcia, H.; Palomares, E.; Sabater, M. J. *New J. Chem.* **2002**, *26*, 1646.
(171) Peretti, K. L.; Ajiro, H.; Cohen, C. T.; Lobkovsky, E. B.; Coates, G. W. *J. Am. Chem. Soc.* **2005**, *127*, 11566.
(172) Ajiro, H.; Peretti, K. L.; Lobkovsky, E. B.; Coates, G. W. *Dalton Trans.* **2009**, 8828.
(173) Ahmed, S. M.; Poater, A.; Childers, M. I.; Widger, P. C. B.; LaPointe, A. M.; Lobkovsky, E. B.; Coates, G. W.; Cavallo, L. *J. Am. Chem. Soc.* **2013**, *135*, 18901.
(174) Campbell, E. J.; Nguyen, S. T. *Tetrahedron Lett.* **2001**, *42*, 1221.
(175) Fischer, E. *J. Phys. Chem.* **1967**, *71*, 3704.
(176) Konsler, R. G.; Karl, J.; Jacobsen, E. N. *J. Am. Chem. Soc.* **1998**, *120*, 10780.
(177) Coppinger, G. M.; Bell, E. R. *J. Phys. Chem.* **1966**, *70*, 3479.
(178) Reichardt, R.; Vagin, S.; Reithmeier, R.; Ott, A. K.; Rieger, B. *Macromolecules* **2010**, *43*, 9311.

(179) Bloembergen, S.; Holden, D. A.; Bluhm, T. L.; Hamer, G. K.; Marchessault, R. H. *Macromolecules* **1989**, *22*, 1656.
(180) Hmamouchi, M.; Lavellee, C.; Prud'homme, R. E.; Leborgne, A.; Spassky, N. *Macromolecules* **1989**, *22*, 130.
(181) Roy, N.; Bruchmann, B.; Lehn, J.-M. *Chem. Soc. Rev.* **2015**, *44*, 3786.
(182) Cordier, P.; Tournilhac, F.; Soulie-Ziakovic, C.; Leibler, L. *Nature* **2008**, *451*, 977.
(183) Bergman, S. D.; Wudl, F. *J. Mater. Chem.* **2008**, *18*, 41.
(184) Wang, Q.; Mynar, J. L.; Yoshida, M.; Lee, E.; Lee, M.; Okuro, K.; Kinbara, K.; Aida, T. *Nature* **2010**, *463*, 339.
(185) Syrett, J. A.; Becer, C. R.; Haddleton, D. M. *Polymer Chemistry* **2010**, *1*, 978.
(186) Belowich, M. E.; Stoddart, J. F. *Chem. Soc. Rev.* **2012**, *41*, 2003.
(187) Herrmann, A. *Chem. Soc. Rev.* **2014**, *43*, 1899.
(188) Cordes, E. H.; Jencks, W. P. *J. Am. Chem. Soc.* **1962**, *84*, 832.
(189) Sander, E. G.; Jencks, W. P. *J. Am. Chem. Soc.* **1968**, *90*, 6154.
(190) Burnworth, M.; Tang, L.; Kumpfer, J. R.; Duncan, A. J.; Beyer, F. L.; Fiore, G. L.; Rowan, S. J.; Weder, C. *Nature* **2011**, *472*, 334.
(191) Wilson, D.; Branda, N. R. *Angew. Chem. Int. Ed.* **2012**, *51*, 5431.
(192) Gostl, R.; Senf, A.; Hecht, S. *Chem. Soc. Rev.* **2014**, *43*, 1982.
(193) Kovaříček, P.; Lehn, J.-M. *J. Am. Chem. Soc.* **2012**, *134*, 9446.
(194) Ciaccia, M.; Cacciapaglia, R.; Mencarelli, P.; Mandolini, L.; Di Stefano, S. *Chemical Science* **2013**, *4*, 2253.
(195) Brode, W. R.; Pearson, E. G.; Wyman, G. M. *J. Am. Chem. Soc.* **1954**, *76*, 1034.
(196) Weinstein, J.; Wyman, G. M. *J. Am. Chem. Soc.* **1956**, *78*, 4007.
(197) M.J.T. Frisch, G. W. S., H. B.; Scuseria, G. E.; Robb, M. A.; Cheeseman, J. R.; Scalmani, G.; Barone, V.; Mennucci, B.; Petersson, G. A.; Nakatsuji, H.; Caricato, M.; Li, X.; Hratchian, H. P.; Izmaylov, A. F.; Bloino, J.; Zheng, G.; Sonnenberg, J. L.; Hada, M.; Ehara, M.; Toyota, K.; Fukuda, R.; Hasegawa, J.; Ishida, M.; Nakajima, T.; Honda, Y.; Kitao, O.; Nakai, H.; Vreven, T.; Montgomery, Jr., J. A.; Peralta, J. E.; Ogliaro, F.; Bearpark, M.; Heyd, J. J.; Brothers, E.; Kudin, K. N.; Staroverov, V. N.; Kobayashi, R.; Normand, J.; Raghavachari, K.; Rendell, A.; Burant, J. C.; Iyengar, S. S.; Tomasi, J.; Cossi, M.; Rega, N.; Millam, J. M.; Klene, M.; Knox, J. E.; Cross, J. B.; Bakken, V.; Adamo, C.; Jaramillo, J.; Gomperts, R.; Stratmann, R. E.; Yazyev, O.; Austin, A. J.; Cammi, R.; Pomelli, C.; Ochterski, J. W.; Martin, R. L.; Morokuma, K.; Zakrzewski, V. G.; Voth, G. A.; Salvador, P.; Dannenberg, J. J.; Dapprich, S.; Daniels, A. D.; Farkas, Ö.; Foresman, J. B.; Ortiz, J. V.; Cioslowski, J.; Fox, D. J. *Gaussian 09 Rev. A.02, Gaussian Inc.*; Wallingford CT, 2009.
(198) Lindoy, L. F.; Meehan, G. V.; Svenstrup, N. *Synthesis* **1998**, *1998*, 1029.
(199) Normand, M.; Dorcet, V.; Kirillov, E.; Carpentier, J.-F. *Organometallics* **2013**, *32*, 1694.
(200) Karimi, B.; Ebrahimian, G. R.; Seradj, H. *Org. Lett.* **1999**, *1*, 1737.
(201) Sun, J.; Dong, Y.; Cao, L.; Wang, X.; Wang, S.; Hu, Y. *J. Org. Chem.* **2004**, *69*, 8932.
(202) Ma, H.; Li, W.; Wang, J.; Xiao, G.; Gong, Y.; Qi, C.; Feng, Y.; Li, X.; Bao, Z.; Cao, W.; Sun, Q.; Veaceslav, C.; Wang, F.; Lei, Z. *Tetrahedron* **2012**, *68*, 8358.
(203) Pospisil, P. J.; Carsten, D. H.; Jacobsen, E. N. *Chem. Eur. J.* **1996**, *2*, 974.
(204) Liu, D.; Xie, Y.; Shao, H.; Jiang, X. *Angew. Chem. Int. Ed.* **2009**, *48*, 4406.
(205) Liu, S.-Y.; Nocera, D. G. *J. Am. Chem. Soc.* **2005**, *127*, 5278.
(206) Upadhyaya, D. J.; Barge, A.; Stefania, R.; Cravotto, G. *Tetrahedron Letters* **2007**, *48*, 8318.
(207) Coquerel, Y.; Rodriguez, J. *Arkivoc* **2008**, *xi*, 227.
(208) Zhang, C.; Jiao, N. *Angew Chem Int Ed Engl* **2010**, *49*, 6174.
(209) Hartwig, S.; Nguyen, M. M.; Hecht, S. *Polymer Chemistry* **2010**, *1*, 69.

List of abbreveations

AB	azobenzene
Boc	*tert*-butyloxycarbonyl
DAE	diarylethene
DCC	dynaic combinatorial chemistry
DCM	dichloromethane
DFT	discrete Fourier transform
DMAP	4-dimethylaminopyridine
DMSO	dimethylsulfoxide
ESI	electronspray ionization
FTIR	Fourier transform infrared
GPC	gel permeation chromatography
HOMO	highest occupied molecular orbital
LED	light emitting diode
LMCT	ligand-to-metal charge transfer
LUMO	lowest unoccupied molecular orbital
MS	mass spectrometry
NMR	nuclear magnetic resonance
PE	petrolether, polyethylene
PHB	polyhydroxybutyrate
PIDA	(diacetoxyiodo)benzene
PLA	polylactide
PP	polypropylene
PS	polystyrene
PSS	photostationary state
ROMP	ring-opening metathesis polymerization
ROP	ring-opening polymerization
rt	room temperature
STM	
TBS	
TEA	triethylamine
TFA	trifluoroacetic acid
THF	tetrahydrofurane

TGA	thermogravimetric analysis
TLC	thin layer chromatography
UPLC	ultra-high performance liquid chromatography
UV	ultraviolett
Vis	visible

Selbstständigkeitserklärung

Ich erkläre, dass ich die Dissertation selbständig und nur unter Verwendung der von mir gemäß § 7 Abs. 3 der Promotionsordnung der Mathematisch-Naturwissenschaftlichen Fakultät, veröffentlicht im Amtlichen Mitteilungsblatt der Humboldt-Universität zu Berlin Nr. 126/2014 am 18.11.2014 angegebenen Hilfsmittel angefertigt habe.

Berlin, den 23.02.2016

Antti Alexander Senf